

Investigating the Association Between Enhancements in Perceptual Sensitivity to Object Form and Reach to Grasp Performance

by

Michael Cao

A thesis

presented to the University of Waterloo

in fulfillment of the

thesis requirement for the degree of

Master of Science

in

Kinesiology

Waterloo, Ontario, Canada, 2017

© Michael Cao 2017

Author's Declaration

I hereby declare that I am the sole author of this thesis. This is a true copy of the thesis, including any required final revisions, as accepted by my examiners.

I understand that my thesis may be made electronically available to the public.

Abstract

The act of reaching to grasp an object serves as a primary method of interaction with the surrounding environment. Therefore, it is important to understand the association between perceptual sensitivity to object form and the corresponding movement kinematics. As such, the objective of this study was to examine the association between the enhancement in perceptual sensitivity to object form and reach to grasp performance. Thirty visually healthy participants were tested in two experimental tests: a psychophysical test to establish perceptual sensitivity to object form, and a motor task to measure the kinematics of a reach to grasp movement. A method of constant stimuli was used to assess perceptual sensitivity for two shape perception tasks: radial frequency (RF) and motion defined form (MDF). The main outcome measures were the perceptual threshold (i.e., accuracy) and just noticeable difference (JND). The motor task consisted of a reach to grasp task where movement kinematics were quantified using 3 measures: maximum grip aperture (MGA), time in deceleration (TID), and time grasping (TIG). Both perceptual tasks, and the kinematic task were performed during binocular and monocular viewing. It was hypothesised that the magnitude of binocular advantage (i.e., the improvement in performance during binocular compared to monocular viewing) found for the perceptual tasks will be positively associated with a binocular advantage during the reach to grasp task. Results showed a significant binocular advantage for both perceptual tasks, as well as the kinematic measures of the reach to grasp task, which is consistent with previous literature. In contrast to the hypothesis, there were no significant associations between the magnitude of binocular advantage found in the perceptual tasks and reach to grasp performance. These findings indicate that binocular information appears to be processed independently for shape perception and movement execution. This is consistent with the notion of separate ventral and dorsal streams being involved in processing binocular signals for the purpose of perception and action. However, it is important to note that limitations of this study may contribute to the lack of perceptual-reach to grasp association.

Acknowledgement

I would like to thank Dr. Ewa Niechwiej-Szwedo of the Faculty of Applied Health Sciences for her continuous support and guidance throughout the thesis process. The door to Prof. Niechwiej-Szwedo was always open to providing me advice, education, and opportunities for growth. I would also like to thank my thesis committee members, Dr. Michael Barnett Cowan and Dr. Bill McIlroy for their expertise and recommendations in elevating the quality of my research.

Lastly, I would like to give a special thanks to the graduate students, lab assistants, and volunteers within the Developmental Visuomotor Neuroscience Lab for their help throughout the research process.

Table of contents

List of Figures	vii
List of Tables	ix
1.0 Literature Review	1
1.1 Introduction	1
1.2 Object Form Perception	4
1.2.1 Neural structures in object form perception	4
1.2.2 Quantifying object form perception	4
1.2.2.1 Radial Frequencies (RF) stimulus	5
1.2.2.2 Effect of viewing condition on RF form perception	6
1.2.2.3 Motion Defined Form (MDF) stimulus	7
1.2.2.4 Effect of viewing condition of MDF perception	8
1.2.3 Neural mechanism for enhanced binocular object form perception	9
1.3 Contribution of Vision to Reach to Grasp Performance	9
1.3.1 Neural substrates	9
1.3.2 Effects of object intrinsic and extrinsic properties on reach to grasp.....	11
1.3.3 Reach to grasp as a function of movement planning and control	12
1.3.4 Movement control model: impulse and limb target control	14
1.3.5 Effects of viewing condition on reach to grasp performance	15
1.3.6 Neural mechanisms for enhanced binocular reach to grasp	17
1.4 Interaction Between Perceptual and Motor Performance	18
1.4.1 Neural interaction between ventral and dorsal streams	18
1.4.2 Physiological and behavioural support for ventral-dorsal interaction	19
1.4.3 Link between object form perception and reach to grasp	21
1.5 Gap in Literature and Rationale for Research	23
1.6 Research Objectives	23
1.7 Research Question	24
1.8 Hypotheses	24

2.0 Investigating the Association Between Enhancements in Perceptual Sensitivity to Object Form and Reach to Grasp Performance	25
2.1 Methods	25
2.1.1 Participants	25
2.1.2 Experimental Design	25
2.1.3 Materials and Procedures	26
2.2 Results	34
2.2.1 Binocular advantage in perceptual measures	35
2.2.2 Binocular advantage in kinematic measures	38
2.2.3 Perceptual – Kinematic Correlation	44
2.3 Discussion	47
2.3.1 Methodological considerations – perceptual and reach to grasp tasks	48
2.3.2 Binocular advantage as a probe for ventral-dorsal interaction	51
2.3.3 Behavioural explanations for findings	53
2.3.4 Neurological/physiological explanation of findings	54
2.3.5 Interpretation of unexpected findings	55
2.3.6 Alternative conclusions for lack of perceptual-reach to grasp association	57
2.3.7 Auxiliary findings	58
2.3.8 Limitations	58
2.3.9 Future research direction	59
2.4 Conclusion	60
References	62
Appendices	74

List of Figures

Framework: components of a visually guided reach to grasp movement	1
Highlighting properties of radial frequency shape	5
RF stimulus presentation	27
MDF stimulus presentation	28
Typical data from staircase protocol with threshold (line) and reversals (arrows) highlighted ...	29
Optorak Camera (Left) and Marker placement (right)	31
Experimental set up of reach to grasp task	32
Psychometric functions of participant demonstrating binocular advantage for RF stimulus	36
Psychometric functions of participant not demonstrating binocular advantage for RF stimulus	36
Boxplot outlining RF binocular advantage ratios for threshold and JND	36
Psychometric functions of participant demonstrating binocular advantage for MDF stimulus	37
Psychometric functions of participant not demonstrating binocular advantage for MDF stimulus	37
Boxplot outlining MDF binocular advantage ratios for threshold and JND	38
Position, velocity, and grasp aperture graphs for a typical reach to grasp trial	39
Distribution of binocular and monocular SGA values for single participant	40
Distribution of binocular and monocular mean SGA values for entire sample	40
Distribution of binocular and monocular MGA values for single participant	41
Distribution of binocular and monocular mean MGA values for entire sample	41
Distribution of binocular and monocular TID values for single participant	42
Distribution of binocular and monocular mean TID values for entire sample	42
Distribution of binocular and monocular TIG values for single participant	43
Distribution of binocular and monocular mean TIG values for entire sample	43
Association between RF Threshold and MGA binocular advantage ratio	45
Association between RF JND and MGA binocular advantage ratio	45

Association between MDF Threshold and SGA binocular advantage ratio 46
Association between MDF JND and SGA binocular advantage ratio 46

List of Tables

RF properties	27
MDF properties	28
Pearson correlation coefficients of binocular advantage of RF- kinematic measures	46
Pearson correlation coefficients of binocular advantage of MDF- kinematic measures ..	47

1.0 Literature Review

1.1 Introduction

Reaching to grasp an object is a common goal directed movement in everyday life. On average, we handle approximately 142 objects per day, excluding structural items such as handles, taps, and light switches (Zucotti, 2015). The number of reach to grasp actions drastically increases if structural items, multiple handling of the same objects, and a more reliable method than self-reporting were included. The quantity of reach to grasp actions performed on any given day demonstrate its importance in everyday function. In addition, the quality of reach to grasp movements is also important in the successful completion of everyday tasks. The quality of this movement refers to the accuracy, precision, and efficiency of the movement. For example, a shaky and hesitant reach towards a coffee mug followed by a mis-grasp causing the contents to spill is unfavorable. In certain occupations, accurate and precise reach to grasp movements are absolute requirements as in the case of a surgeon whereby the allowable margin of error is low and the consequences of mistakes are high. For example, laparoscopic surgeries are usually performed through small incisions of 0.5 – 1.5 cm, far away from the site of surgery, yielding a demand for highly precise and controlled reach to grasp movements (Mir et al., 2011). Although reach to grasp movements are diverse in terms of amplitude, speed, and goal, they can all be described by similar phases of movement (Elliot et al., 2010). Figure 1 is a framework that outlines the sensorimotor processing stages during the performance of a visually guided reach to grasp movement, which will form the focus of this literature review.

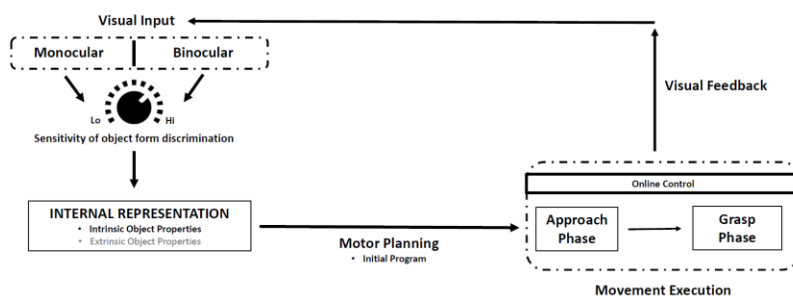


Figure 1. Framework: components of a visually guided reach to grasp movement

Prior to the beginning of any visually guided reach to grasp movement, vision captures information regarding the object's intrinsic and extrinsic properties (Goodale et al, 1994; Monaco et al., 2015). Intrinsic properties are those that are native to the object itself, namely shape/form, size, texture, and mass. Extrinsic properties of the object include spatial location and orientation. Different viewing conditions such as binocular and monocular viewing have been shown to elicit differences in the perception of object features, such that an advantage can be associated with the former viewing condition (Blake and Fox, 1973; Servos and Goodale, 1994; Melmoth and Grant, 2006). This perceptual advantage is captured and quantified through higher sensitivity to changes in object features during discrimination tasks. For example, binocular viewing conditions elicit a lower threshold for object form discrimination, suggesting that binocular observers are able to accurately perceive smaller changes in object form (Steeves et al., 2004; Hayward et al., 2011). This binocular advantage is found consistently amongst the visually healthy population, but the magnitude varies between individuals (Loftus, Servos, and Goodale, 2004).

The internal representation of the visual scene is modulated by the sensitivity of the visual system in detecting object features (Intraub, Morelli, and Gagnier, 2015). This internal representation, consisting of intrinsic and extrinsic properties of the object, provides information for motor planning (Bootsma et al., 1994; Korneev, Kurganskii, 2014). Information from different modalities is integrated to obtain a complete representation of environment (Sober and Sabes, 2003). Proprioceptive information regarding the location and configuration of the limbs along with the previously mentioned visual input all contribute to this process (Hansen et al., 2006).

The motor plan is carried out by sending efference signals to the appropriate motor units. A forward internal model in the CNS uses a copy of the efference to predict the expected sensory consequences, and the next state of the limb (Miall and Wolpert, 1996; Wolpert, 2005). Therefore, the forward internal model can be used to adjust movements prior to receiving sensory feedback from the environment. Upon the availability of actual sensory feedback, the predicted sensory feedback is compared to that of the actual, and adjustments are made during movement execution to minimize error. This is known as the closed loop online control, which

utilizes sensory feedback from both the visual and somatosensory systems to adjust the kinematics of the limb in motion (Proteau and Masson, 1997; Saunders and Knill, 2003; Hansen et al., 2007). This adjustment is done continuously online to enhance movement accuracy and precision, while adhering to movement goals. The availability and quality of visual input has been shown to modulate the characteristics of this closed loop of online control, ultimately affecting the performance of the reach to grasp task (Mendoza et al., 2006; Grierson and Elliot, 2009). More accurate information available from the visual system, during binocular viewing compared to monocular viewing, has been shown to improve the planning and execution of movements via higher peak acceleration and peak velocity, decreased variability of limb trajectory, decreased time spent in grasp phase, lower end point variability, and quicker overall movement time (Servos and Goodale, 1994; Jackson et al., 2010; Melmoth and Grant, 2006; Read et al., 2012).

To summarize, separate studies have shown that perceptual sensitivity to object form is greater during binocular viewing (Steeves et al., 2004; Hayward et al., 2011), and that visually guided movements are performed more efficiently (Servos and Goodale, 1994; Melmoth and Grant, 2006). However, it is currently unknown whether increased sensitivity to object features is directly associated with improved motor planning and execution. Therefore, this thesis will address this gap in current knowledge and assess the relationship between visual sensitivity to object form and the performance of reach to grasp. To do so, the manipulation of viewing condition will be introduced to the perceptual and motor tasks. The elicited binocular advantage will provide an opportunity to assess the relationship of the degree of enhancements between the perceptual and tasks. Given the importance and regularity of reach to grasp in both leisure and professional aspects of life, understanding factors that modulate its performance can benefit the approach to completing these tasks optimally. The following literature review will provide a comprehensive synthesis of the current knowledge on 3 topics: 1) Object form perception, 2) Contribution of vision on reach to grasp movement 3) Interaction between perception and action.

1.2 Object Form Perception

1.2.1 Neural structures in object form perception

Visually encoding an object's intrinsic and extrinsic features has been proposed to occur through two pathways: the ventral "what" and dorsal "how" pathways (Goodale and Milner, 1992; Goodale et al., 1994; Whitwell, Milner, and Goodale, 2014). The ventral stream is responsible for perceptual identification of objects. As such, the perception of object form projects through the ventral pathway in the absence of a subsequent goal directed movement (Goodale et al., 1994). Object feature encoding begins at the retina as the light initiates the transduction process at the photoreceptors and undergoes primary processing in the primary visual cortex (V1) to decode spatial features, such as spatial frequency, orientation, disparity and color. This information is further processed in the extra-striate cortex where neurons respond to increasingly complex shapes to extract a more global organization of the scene (Lamme and Roelfsema, 2000). V2 cells are tuned to similar properties as V1, but are modulated by more complex properties such as illusory contours and figure/background segregation. Area V3 has been suggested to have a role in global motion processing and projects dorsally to the posterior parietal cortex (PPC) and ventrally to the inferotemporal cortex (TE). Area V4 receives strong feedforward input from V2, and is tuned to intermediately complex object features such as shape and form, but not faces and tools as those are processed in the TE. Entry to the ventral stream begins at region V4, and projects along the temporal lobe to multiple regions including inferior temporal areas TEO and TE, and temporal polar area TG. Additionally, the lateral occipital area (LO) located within the ventral stream has shown to be involved with object recognition (Grill-Spector, 2003). fMRI studies further showed LO activation for object form irrespective of how they are defined (motion, texture, or luminance contrast) (Grill-Spector et al., 1998). Moreover, LO appeared to code for overall object form, rather than local features (Kourzi and Kanwisher, 2001). In summary, structures in the ventral stream play a fundamental role in the perception of object form.

1.2.2 Quantifying object form perception

The sensitivity to object form perception can be measured quantitatively using

psychophysical methods. Two types of stimuli, radial frequencies (RF) and motion defined form (MDF), have been used to study the sensitivity of the visual system to object form (Giaschi et al., 1997; Wilkinson et al., 1998). RF form is perceived as a function of contour contrast while MDF utilizes motion contrast. By manipulating the contour (RF) and motion (MDF) of the object under different viewing conditions (binocular/monocular) and measuring the changes in sensitivity (threshold and just noticeable difference (JND)), a relationship can be established between the viewing condition and perceptual performance. This information can provide insight about the contribution of binocular vision to the perception of object shape.

1.2.2.1 Radial Frequency (RF) stimulus

Radial frequencies are circular shapes with systematic deformations. These deformations are defined by sinusoidal modulations of the radius. Deformations can be changed based on phase, amplitude, and frequency. Figure 3 is an example of a radial frequency with amplitude and radial frequency properties labelled.

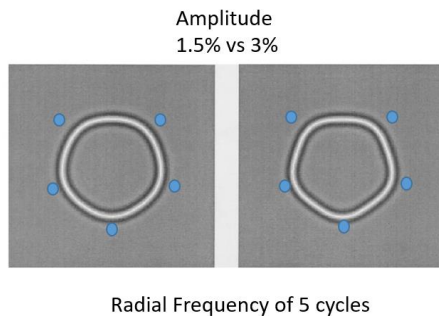


Figure 2. Highlighting properties of radial frequency shape (*Altered Based on Wilkinson, Wilson, and Habak, 1997*)

A study that recorded responses from 103 neurons in area V4 of anesthetized primates demonstrated that RF shapes activate a subset of these neurons (Gallant et al., 1993). These V4 neurons project directly to neurons in the TE cortex, making the perception of radial frequencies predominantly a function of the ventral stream of visual processing (Wang et al., 1999). Given this, RF shapes have been used to measure sensitivity to global object form under various conditions: curvature, luminance, and contour contrast (Wilkinson, Wilson, and Habak, 1997; Steeves et al., 2003; Bell et al., 2006). Determining the perceptual sensitivity towards

changes in these properties provides insight into the neural mechanisms involved in encoding of object shape. For example, manipulating the amplitude provides a measure of the sensitivity of the visual system to curvature, and studies have shown that RF shapes elicit reproducible thresholds between individuals. The RF stimulus provides insight into global feature perception by manipulating local features. It has been shown that discrimination of object curvature based on changes in amplitude is within the hyperacuity range. Differences as low as 2-4 sec of arc in radial deformation can be detected while viewing binocularly (Wilkinson, Wilson, and Habak, 1997). Further studies have found that observers are sensitive to slight RFs deformations (approx. 1% of radius) with accuracy up to 90% within just 167 ms (Wilkinson et al., 1998). One explanation for the high sensitivity to RF shapes may be evolutionary in nature. The development of the ventral stream is thought to be biased towards naturally occurring objects such that they are perceived with higher sensitivity. Since curves are commonly found in natural objects, the perceptual system might be finely tuned to discriminating them (Biederman, 1987). Therefore, the RF stimulus provides a useful probe for studying the mechanisms involved in object form perception.

1.2.2.2 Effect of viewing condition on RF form perception

Separate studies have used the RF shapes to assess object form discrimination under different viewing conditions and contrast levels. Monocular viewing conditions elicited higher thresholds (i.e., lower sensitivity) for form perception as compared to binocular viewing conditions. This was consistent under different contrast conditions (6.25%, 12.5%, 25%, 100%) (Steeves et al., 2003); however, the binocular advantage was largest at lower contrast levels. For example, during the monocular viewing condition the amplitude threshold was approximately 20% higher in comparison to binocular viewing. At 100% contrast, the difference in threshold between viewing conditions was only ~5% (Steeves et al., 2003). It appears that binocular advantage is more apparent when the visual system is challenged during lower contrast.

The number of cycles within the RF shape does not affect the sensitivity to form perception. Similar sensitivity to changes in deformations of RFs shapes with 3 – 24 cycles was

found for both binocular and monocular viewing conditions (Wilkinson et al., 1998). Previous studies using RF shapes have provided insight about the potential effects of shape properties on behavioural performance. Thus, the RF could be an ideal stimulus to be implemented in related studies as experimenters are able to adjust its properties to test different hypotheses.

1.2.2.3 Motion Defined Form (MDF) stimulus

Motion defined form is a stimulus used to determine the sensitivity to global shape perception through motion of dots. Stimuli are composed of an array of dots whereby the target form is defined by dots moving in one coherent direction. The dots outside of the target form move in the opposite direction. Under circumstances where 100% of the dots in the target and background are moving in opposite direction, the form of the object can be easily perceived. As this condition is not challenging to the visual system enough to test for perceptual thresholds, the dot coherence is often adjusted, such that a previous experiment found binocular thresholds to be approximately 10-15% among participants aged 18-31 (Hayward et al., 2011). Dot coherence represents the percentage of dots in the stimulus target moving in a coherent direction. For example, a dot coherence of 50% means that 50% of the dots in the target form are moving to the right while the remaining dots are moving randomly. Movement speed of the dots can also be manipulated to obtain different effects. Developmental studies have found object form perception for slow velocities to mature later in life, suggesting that it is more challenging to the visual system to process slowly moving stimuli (Hayward et al., 2011). Increased thresholds were also found in healthy observers as well as those with abnormal binocular vision for stimuli presented at slow velocities (Giaschi et al., 1992).

Neurons that are sensitive to direction of motion have been found as early as areas V1, V2, and V3 in primate studies (Deo Yeo and Van Essen, 1985; Hawken et al., 1988). The middle temporal area (MT), a region of the extrastriate cortex receives input from the early visual areas and is largely tuned to the speed and direction of moving stimuli (Dubner and Zeki, 1971; Maunsell and Van Essen, 1983). Within MT, local visual motion signals are integrated into global motion of complex objects (Movshon et al., 1985). Furthermore, presentation of MDF stimulus

has also shown to activate neurons in the medial superior temporal area (MST), which receives input from MT and then projects into the parietal area 7a (Allman et al., 1985). With lower dot coherence, increased activation of these areas would be expected as they facilitate the perception of contrasting motion. In humans, MT neurons respond to motion defined shapes, and it is thought that MT is a major structure involved in the processing of the MDF stimulus (Alleman et al., 1985; Saito et al., 1986; Tanaka et al., 1986).

Motion perception has been associated with dorsal stream function, but recent research has found more complex interactions between the two pathways (Freud et al., 2016). fMRI studies have determined parallel activations in both ventral and dorsal streams with the presentation of MDF stimuli (Wang et al., 1999). Dorsal motion specific middle temporal area (MT)/V5, as well as ventral fusiform gyrus (FG) and inferior temporal gyrus (TG) are simultaneously activated with the motion defined form stimulus. As motion stimulus alone activates only the MT/V5 areas, it appears the addition of form perception with a motion detection task requires interaction between the ventral and dorsal streams (Rainville and Wilson, 2003).

1.2.2.4 Effect of viewing condition on MDF perception

Although MDF has not been used in previous literature to specifically assess differences in performance between binocular/monocular viewing conditions, there are studies that demonstrate enhanced binocular performance compared to other conditions. For example, a binocular advantage for the perception of object form as a function of dot coherence was found for dot velocity of 0.1 deg/s in a group of visually healthy participants compared to amblyopic group (Hayward et al., 2011). A separate study found MDF thresholds to be lower in healthy binocular control subjects as compared to a group of patients with parieto-temporal lesions (Regan et al., 1992). Monocular performance on the MDF task has not been directly compared to binocular performance in visually normal subjects, although the binocular advantage compared to visually affected groups indicates that binocular vision is important for the performance of this task. As such, decreased sensitivity to MDF would be expected for monocular viewing compared to binocular viewing.

1.2.3 Neural mechanism for enhanced binocular performance in object form perception

Previous studies have demonstrated binocular viewing of RF and MDF stimuli to result in greater perceptual sensitivity to object form. Additionally, the combination of information from both eyes has been shown to enhance visual acuity, contrast sensitivity, brightness perception, pattern recognition, and depth perception (Steinman and Garzia, 2000). As the process in which this binocular summation occurs is still an active area of research, concepts such as probability and neural summation can provide some insight (Frisen and Lindblom, 1987). Probability summation explains the binocular enhancement in perceptual performance to be due to greater probability of detection, having two independent sets of information (Steinman and Garzia, 2000). Further experiments demonstrated that optimal summation occurred when corresponding points on the two retinas were stimulated with the same target and when presentation occurred simultaneously (or within 100ms) (Matin, 1960). This neural summation combines input from the two eyes to strengthen neural signal (Campbell and Green, 1965). Binocular neurons (neurons activated by stimuli presented in either eye) are found in striate cortex (V1), extrastriate cortex (V2), ventral extrastriate cortex (V4), dorsal extrastriate area (V5/MT), medial superior temporal area (MST), anterior intraparietal area (AIP), and a collection of areas in the anterior inferotemporal cortex (IT) (Steinman and Garzia, 2000). As these neurons are found in structures of both the ventral and dorsal streams, a contribution of binocular vision to both perception and action is expected.

1.3 Contribution of Vision to Reach to Grasp Performance

1.3.1 Neural substrates

Visual information about object properties and environmental context is extracted to formulate a motor plan according to one's behavioural goals. Vision is an essential modality to connect the external features of the environment with the internal plans to interact with it. A separate pathway in the dorsal stream of visual processing was shown to be involved in processing of object features that undergo sensorimotor transformations for visually guided actions (Goodale et al., 1994). The dorsal stream shares a common pathway with the ventral pathway in the visual cortex, but branches out at area V5/MT (middle temporal area) to project

to various surrounding areas. Connective pathways have been identified with V3A, MST (medial superior temporal area), FST (fundus of the superior temporal area), and multiple parietal regions. Some parietal regions include the lateral, medial, and anterior intraparietal areas LIP, MIP, and AIP. These pathways ultimately terminate in dorsal lateral regions of the prefrontal cortex (DLPFC).

Physiological evidence demonstrates the role of dorsal stream neurons in transforming visual information into appropriate motor movements. Primate neuroimaging studies have shown lateral intraparietal areas (LIP) to play a primary role in visual control of saccadic eye movements, anterior intraparietal areas (AIP) to be involved with visual control of grasping movements, and medial intraparietal areas (MIP) and parietal-occipital sulcus (V6A) to be engaged during visual control of reaching (Anderson and Buneo, 2003; Sakata, 2003). These different areas have been also shown to interact during the performance of different visuomotor tasks; for example, V6A is involved in the visual control of both reaching and grasping. Human fMRI studies have found AIP to also be activated for both reaching and grasping (Culham et al., 2003). More specifically, this AIP activation was found to be smaller when removing the grasping component from the movement (Culham et al., 2003). This demonstrates a particular role of AIP in controlling grasping.

Recent findings have demonstrated heterogeneity of the dorsal pathway in terms of neural representations (Kravitz et al., 2011). During visually guided tasks, posterior areas of the dorsal stream are more sensitive to gaze-centered representations of objects location and features (Roth and Zohary, 2015), while anterior areas, which are closer to motor cortex, are more sensitive to movement related information (Gallivan et al., 2013). In addition to this anterior-posterior gradient, the dorsal stream may also be mapped in the medial-lateral axis. More posterior-medial areas (V7, IPS1-2) are strongly connected to early visual cortex (Stepniewska et al., 2016) and ventral structures (Kravitz et al., 2011), representing more perceptual properties of the input. Conversely, the anterior-lateral part of the dorsal pathway (AIP) is connected to the sensorimotor system and coupled to motor regions, contributing to visuomotor behaviors (Roth and Zohary, 2015). These findings support the contribution of the dorsal stream in transforming visual representations into motor representations.

1.3.2 Effects of object intrinsic and extrinsic properties on reach to grasp

Object intrinsic and extrinsic properties directly influence motor planning of reach to grasp movements (Monaco et al., 2015). The reach and grasp phases are affected differently by intrinsic and extrinsic properties (Paulignan et al., 1997; Frey, McCarty, and Keen, 2004; Seegelke and Hughes, 2015). The reach phase is most affected by the extrinsic features of the object. Varying the distance and orientation of the object would cause changes in the speed and direction of the trajectory in the reach phase, respectively. Object intrinsic features modulate the grasping phase (Marteniuk et al., 1990; Bootsma et al, 1994; Paulignan et al., 1997). For example, grasp aperture and finger closing kinematics also been shown to be affected by movement goals and texture/mass respectively (Flatters et al., 2012).

Grasp aperture, a vector between the thumb and index finger, proportionally mirrors the circumference or form of the object such that a larger object elicit a larger grip aperture (Paulignan et al., 1991). Although grasp aperture to object circumference ratios vary between participants, the general finding of larger grasp apertures for larger objects remains consistent. This effect is diminished with monocular viewing as larger grasp apertures have been demonstrated (Melmoth and Grant, 2006). The size and shape of the object is also modulated by grasp type. Interestingly, modulation of grasp type also alters the reach component (Marteniuk et al., 1990; Jakobson and Goodale, 1991; Bootsma et al, 1994), and vice versa (Jakobson and Goodale 1991; Chieffi and Gentilucci, 1993); suggesting interaction between the 2 components of the reach to grasp movement.

Extrinsic properties such as location of the target object in depth influence the reach phase kinematics. Objects located further in depth elicit higher acceleration, such that the entire movement time remains approximately consistent when compared to a closer located object (Paulignan et al., 1997; Bae, Choi, Armstrong, 2008). Object location along the azimuth also influences the reach phase by modulating the trajectory direction towards the object. The orientation of the object has been also shown to influence the spatial configuration of the index finger and thumb during grasp, as well as time spent grasping and transport duration (Paulun, Gegenfurtner, and Goodale, 2016). Finally, wrist postures are influenced by object orientation (Bae, Choi, Armstrong, 2008). To summarize, experimental findings provide evidence to show

that object intrinsic and extrinsic features significantly affect movement kinematics; however, reach to grasp performance can also be influenced by movement goals, which is discussed next.

Beyond the intrinsic and extrinsic properties of the object, goal of the movement also influences reach to grasp kinematics. The goal of movement has been shown to influence reach to grasp strategies (Rosenbaum et al., 2012). A phenomenon called end state comfort has been widely supported (Rosenbaum et al., 1990, 1992, 1993, 1996), whereby performers utilize grasping strategies that facilitate a comfortable end position at the end of object manipulation while forfeiting comfort in grasping the object at the beginning of the manipulation. Studies that involve the grasping of glasses (cups) have been used to demonstrate the human tendency for end state comfort (Cohen and Rosenbaum, 2004). In situations where the risk of error is heightened as in the case of a more fragile or precious target object, performers utilize a more conservative reach to grasp strategy (Flatters et al., 2011). Longer time is spent in deceleration during the reach phase, and grasping time is longer. When participants were instructed to not drop the target object following transport to a different location, an increase in force applied by the grasp was demonstrated (Flatters et al., 2011). This suggests that movement goals and motivations also modulate reach to grasp performance in addition to the physical intrinsic and extrinsic properties of the target object.

1.3.3 Reach to grasp movement planning and control

The reach to grasp movement is characterized by two phases (Woodworth, 1899; Jeannerod, 1984; Elliot et al., 2001; Elliot et al., 2010). The reach phase is defined between the onset of the hand movement towards the object to when the hand is within the vicinity of the target. The grasp phase is defined from the end of the reach phase to contact with the object. These two phases are thought to be independent, but do interact. For example, the performance of reaching has been shown to be influenced by the grasping phase, such that an unexpected shift of grasping strategy during the movement elicited modifications to reaching (Castiello, Bennett, and Paulignan, 1992). These online corrections to the reach and grasp movement occur continuously and contribute to the overall performance of the task.

The quality of the initial motor plan and the ability to engage in online control processes both contribute to the overall accuracy and precision of the reach to grasp task. Research has shown that optimal outcomes are embedded into the motor plan. These optimal outcomes include considerations for safety, energy expenditure, as well as time available for corrections. Previous studies have shown that end-point distribution of the primary reaching movement typically undershoots the target object (Worringham, 1991; Engelbrecht, Berthier, and O'Sullivan, 2003; Elliot et al., 2004). With practice, the amount of deviation decreases towards the location of the target object, minimizing the spatial gap (Pratt and Abrams, 1996; Khan, Frank, and Goodman, 1998; Elliot et al., 2004). This is thought to occur because overshooting the target is costly in terms of energy and time, as the limb is required to overcome inertia and reverse movement direction (Elliot et al., 2004; Elliot, Hansen, and Grierson, 2009). In contrast, undershooting takes up less time and energy, while also being a safer strategy, as in the case of reaching for a potentially dangerous target (i.e., a hot pot). Similar findings have been found for maximum grasp aperture measure (MGA). Participants tend to employ an aperture 2-3 times the width of the target object to optimize the outcome (Paulignan et al., 1991). Approaching the object with a grasp aperture larger rather than smaller relative to the target object is both energetically and temporally more favorable in terms of adjustment. Should a grasp aperture be smaller than required by the object, additional time and energy would be required to open the grasp aperture to make the proper adjustments. As such, kinematic measures, such as the initial reach trajectory and maximum grasp aperture, can be used as proxy measures for the initial motor plan.

During reach to grasp trials where vision is available, performers exhibit an asymmetrical velocity profile in which more time is spent after peak velocity (Hansen et al., 2006). This type of velocity profile is associated with the utilization of visual feedback for limb control (Elliot et al., 2001). With practice, performers achieve peak velocity earlier, and thus spend more time in the deceleration phase near the target object (Elliot et al., 1995; Khan and Franks, 2000). This suggests more time is available to make corrective adjustments near the object. During trials where the availability of vision is unexpected by the subject, a kinematic profile that is more symmetrical is employed such that equal time is spent before and after

peak velocity (Elliot and Allard, 1985; Hansen et al., 2006). This strategy is thought to resemble reaching without visual feedback and it is associated with longer response times. The kinematic changes due to the manipulation of visual input suggest that movement planning and control are dependent on availability of visual feedback (Elliot et al., 2010).

1.3.4 Movement control model: impulse and limb target control

Up to this point, the primary movement has been described to have very limited online control, but it is important to note that this segment of the movement is not entirely ballistic in nature. There is evidence for early online control within the primary movement (Proteau and Masson, 1997; Hansen et al., 2007; Saunders and Kill, 2003). A model of goal directed aiming suggests 2 main types of feedback-based regulation: impulse and limb-target control (Grierson and Elliot 2008; Grierson, Gonzalez, and Elliot, 2009; Elliot et al., 2010). Impulse control refers to the control that occurs early during the primary movement. Limb-target control refers to the control that fine tunes the transport of the hand as it is approaching the target object.

Impulse control occurs very early after the onset of movement. An internal feedforward model in which an efference copy simulates the movement in the CNS is activated with the generation of efference signals (Elliot et al., 2010). This process allows for corrections to be made to the initial motor plan prior to the availability of sensory feedback. Following movement onset, impulse control can be demonstrated through corrective movements made based on visual and somatosensory feedback. Perturbations induced prior to peak velocity using visually elicited illusions of movement velocity have demonstrated that subjects modulate their velocity to account for the misperception (Proteau and Masson, 1997). These corrections were made to the primary movement that has previously been thought to be completely ballistic approximately 100ms following the perturbation. (Saunders and Knill, 2003; Hansen et al., 2007). Corrections to these early perturbations demonstrate an example of impulse control based on visual and proprioceptive sensory feedback.

As the hand approaches the object following peak deceleration, limb-target control is thought to occur (Saunders and Knill, 2003). Increased processing time and available sensory information during late target control allows corrections to be made more accurately and

precisely. As such, limb- target control works to fine tune the trajectory and velocity of the hand to the target object based on location, form, and orientation.

Movement control during reach to grasp is a continuous process such that impulse and limb- target control are closely related; for example, adjustments made early in the movement influence those made later (Elliot et al., 2010). A related study has shown early visual feedback well in advance of limb peak velocity enhances later online control (Trembley et al., 2016). In addition, the provision of visual feedback as soon as peak velocity or at 25% of the movement time is adequate for online corrections to be made in the deceleration phase. These findings provide evidence for a strong contribution of vision to early online control. Given this, it is possible that the quality of the visual feedback plays a role in the quality of this impulse control. As monocular viewing lacks binocular summation and disparity, visual information regarding object features and its location becomes less certain. By consequence, it should be expected that corrections will be less efficient during monocular viewing, which will elicit goal directed aiming movements with more symmetrical velocity profile and greater endpoint variability.

In summary, goal directed aiming movements are controlled by multiple processes to ensure that accuracy and precision are achieved. The primary movement transports the hand within close proximity of the object whereby more time is spent in deceleration to undergo limb-target adjustments. Online control occurs continuously from the onset to the end of movement. The planning and online control processes are sensitive to manipulations of both the object intrinsic and extrinsic properties as well as viewing conditions, which will be reviewed in the next section.

1.3.5 Effect of viewing condition on reach to grasp performance

As vision is critical for the planning and control of reach to grasp, the binocular advantage seen in perceptual tasks also exists for the performance of upper limb movements. Endpoint variability, time spent in various phases, and accuracy to target have all been used as measures to quantify the performance of reach to grasp performance (Servos, Goodale, and Jakobson, 1991; Servos and Goodale, 1994; Melmoth and Grant, 2006; Jackson et al., 2010).

This section will discuss the kinematic differences between binocular and monocular viewing conditions.

Time to movement onset is a measure of the reaction time of a reach to grasp movement. Reaction times are quicker under binocular viewing and highlights binocular advantage for movement planning (Servos et al., 1992; Wakayama et al., 2010). The binocular advantage in reaction time may be related to the increased quality of the visual input for perception of reach distance, direction, and object features. Movement duration is the time between movement onset and movement completion, which provides insight as to the efficiency of the reach to grasp task. A longer movement time during monocular viewing for the same reach to grasp task may be a result of increased uncertainty of the initial motor plan and the application of online adjustments (Melmoth and Grant, 2006; Jackson et al., 2010).

Peak velocity and time to peak velocity can further explain the increased movement time as monocular viewing conditions are associated with lower peak velocity and acceleration. Peak velocity is achieved approximately at 30-40% of the movement during the reach phase. A slower reach to the object during monocular viewing may suggest hesitancy that allows for more time to correct for errors in trajectory (Servos, Goodale, and Jakobson, 1991). This increased uncertainty in the reach phase under monocular condition is also associated with a larger maximum grasp aperture measure (Melmoth and Grant, 2006). The lack of visual cues such as disparity and summation during monocular viewing causes a less accurate and precise internal representation, in which the motor plan is derived. As such, larger margin of error is embedded into the movement for online corrections upon the availability of more visual and somatosensory information.

Time in deceleration of the reach to grasp movement is an indicator of online adjustments when approaching the target object. Peak deceleration occurs at approximately 75-80 % of movement time and is found to be lower during monocular as compared to binocular viewing (Servos, Goodale, and Jakobson, 1991). A lower peak deceleration and longer time spent in deceleration indicates a more gradual approach to the target, providing the performer with more time to make adjustments. This increased time in deceleration can be interpreted as a more conservative strategy (Servos and Goodale, 1994). This strategy provides

the performer with more time for adjustments to movement trajectory due to the increased error in the visual perception of object intrinsic and extrinsic features (Servos, Goodale, and Jakobson, 1991; Jackson et al., 1997).

The grasping component is the time in which the fingers are closing around the object. A longer grasping phase has been demonstrated during monocular viewing. A longer grasp application allows for more adjustment opportunities, which could be due to a less accurate encoding of object features because of lack of disparity during monocular viewing. Upon contact, performers tend to be asked to manipulate the object in a certain manner. The quality of this manipulation can be measured quantitatively using the time spent in contact with the object. Again, this measure has been shown to be higher in monocular viewing conditions with the possible explanation that upon contact, more adjustments to finger contact location and force application/control are required to ensure optimal object transport. As end point variability of finger contact location on the object has shown to be greater in monocular reach to grasp, more adjustments are required to obtain a reliable grasp (Read et al., 2012).

In summary, the most drastic differences in kinematics between binocular and monocular conditions occur later in the movement during deceleration and grasping (Servos and Goodale, 1994; Watt and Bradshaw, 2000). Longer movement time during monocular viewing is due to lower peak velocities and longer time spent in deceleration, and this contributes to the increase in movement time (Watt and Bradshaw, 2000). During this time, the fingers and hand are adjusted within the proximity of the object to make an appropriate grasp. As both the hand and object are located in central foveal vision, this phase is highly modulated by the quality and availability of visual feedback (Watt and Bradshaw, 2000).

1.3.6 Neural mechanisms for enhanced binocular reach to grasp

Dorsal stream structures were found to be involved in the perception of disparity through random dot stereogram. The perception of disparity has been shown to elicit activation of dorsal areas V7, MT, dorsal intraparietal sulcus anterior (DIPSA) and medial (DIPSM (Minini, Parker, Bridge, 2010). When comparing the neural responses to disparity in the ventral stream, dorsal stream, and early visual areas, it was found the neural activity in the dorsal structures

(V3A, V7, MT) was significantly greater (Minini, Parker, Bridge, 2010). Ventral structures (V4, LO1, LO2) were found to be activated throughout various disparities (0.1 - 0.7° visual angle), however showed no differences in BOLD response. These studies suggest that the dorsal stream, along its occipital and parietal branches contribute to the perception of disparity. Given the role of the dorsal stream in reach to grasp, it would be expected that the availability of disparity during binocular viewing to contribute to the enhanced kinematic performance.

The detriments in reach to grasp performance during monocular viewing could result from the lack of binocular cues such as vergence and disparity (Marrota et al., 1995). Computation of reaching distance was shown to be dependent on vergence (Melmoth et al., 2007). In contrast, scaling of grasp and the finger configuration were shown to be dependent on disparity (Mon-Williams and Dijkerman, 1999). As both of these cues are unavailable during monocular viewing, the visual system increasingly relies on monocular pictorial cues and motion parallax to compute reach distance (Marrota, Kruyer, and Goodale, 1998). The increased reliance on pictorial cues elicits an increased activation of ventral stream structures such as LO (Verhagen et al., 2008). Pictorial cues such as height in the visual scene and familiar size have been shown to be used in the planning and control of grasping, but only during monocular conditions (Marotta and Goodale, 1999). For optimal performance in movement planning and execution, however, the availability of both binocular and monocular cues is required.

1.4 Interaction Between Perceptual and Motor Performance

1.4.1 Neural interaction between ventral and dorsal streams

Historically, the two streams of visual processing have been described as separate, but new research suggests more complex interactions during object form perception and during visually-guided reach to grasp (Freud, Plaut, and Behrmann, 2016). The ventral and dorsal streams have been identified based on neuroanatomy (Ungerleider and Mishkin, 1982); however, it is important to note the interaction between the streams. The dorsal and ventral streams have been found to project to shared regions within the superior temporal sulcus (STS) and prefrontal cortex (Baizer et al., 1991; Distler et al., 1993). Regions such as areas IPa and TEa

in the rostral STS, MT, and prefrontal cortex have been identified to receive converging inputs from both streams (Distler et al., 1993). Projections to these common regions suggest communication between the two visual processing streams. As such, the segregation of the input between the two pathways is not as clear as previously thought (Cloutman, 2013).

Research has shown numerous anatomical cross-connections to be mapped between the two pathways; most notably, between inferior parietal and inferior temporal areas. For example, ventral TE has been found to have direct projections with dorsal stream areas V3A, MT, MST, FST, and LIP (Baizer et al., 1991; Distler et al., 1993; Webster et al., 1994). Retrograde tracer fluids have detected a connection between TE with intraparietal sulcus and prefrontal cortex in a primate study (Borra et al., 2010). Diffusion imaging studies have revealed white matter tracts between the MT gyrus (MTG) and supramarginal gyrus in the context of tool use (Ramayya et al., 2010). Alternatively, projections from ventral V4 have been mapped to dorsal stream region MT, as well as FST and LIP (Felleman and Van Essen, 1991; Ungerleider, Galkin, Desimone, & Gattass, 2008). The inter-connectivity between the dorsal and ventral streams have also been found to be reciprocal (Lamme, Super, and Spekreijse, 1990; Felleman and Van Essen, 1991; Distler et al., 1993; Nassi and Callaway, 2009; Rosa et al., 2009; Pollen, 2011). For example, transcranial magnetic stimulation applied to parietal areas (dorsal stream) has elicited responses in MTG and fusiform gyri (ventral stream), and vice versa (Zanon et al., 2010). Together, these findings demonstrate the connections between the two streams of visual processing, and suggest bidirectional communication is available and active. Despite this, the functional roles of the cross-connection between the two streams during movement tasks are still unclear.

1.4.2 Physiological and behavioural support for ventral-dorsal interaction

Along with the communication between the ventral and dorsal streams, object perception, thought to be a ventral process, has been shown to elicit dorsal activity (Freud et al., 2016). Object representations within the dorsal stream have been shown to be dissociable in terms of neural response time from those generated in the ventral stream. Primate studies have demonstrated that presentation of 3D objects generates neural responses in the dorsal

stream with shorter latencies as compared to the ventral stream (Srivastava et al., 2009). Similar event related potential (ERP) studies in humans have shown early responses in parietal regions (dorsal stream) within 120ms of 3D stimuli presentation followed by ventral activation at 380 ms (Sim et al., 2015). These findings undermine the possibility of dorsal object representations are a result of the cascade projections from the ventral stream, but instead a parallel process.

Dorsal stream activity has been shown to contribute to the performance of object form perception. Lesion studies have shown patients with affected ventral stream retain some perceptual sensitivity to 3D structural object representation, as reflected by similar behavioural sensitivity as healthy controls. This finding was paired with blood-oxygen level-dependent (BOLD) responses in the dorsal stream in the absence of a ventral response in the patient group (Freud et al., 2015). Moreover, residual sensitivity to structural information was found in a patient with extensive bilateral ventral lesions who was perceptually impaired (James, 2003). Additionally, the fMRI profile of patient DF, a patient with extensive ventral damage, reveals dorsal object-selectivity in response to natural objects compared with scrambled versions of object (James, 2003). These findings suggest that a dorsal stream representation of objects can contribute to behavioural performance in object form perception, in the absence of an intact ventral stream.

Similar effect has also been demonstrated by dorsal lesion studies that tested performance of global form perception, in both humans and primates (Lestou et al., 2014; Gillebert et al., 2015; Murphy et al., 2016). Patients with posterior parietal lesions exhibit reduced sensitivity towards 3D objects that were defined by monocular cues (ventral process) (Valna, 1989). Furthermore, deactivation of the dorsal areas led to perceptual impairments related to 3D binocular disparity perception, as well as decreased ventral inferotemporal activation (Van Dromme, et al., 2016). These studies provide insight about the contributions of the dorsal stream to object perception, with a particular significance in the perception of 3D structure under binocular and monocular conditions.

To summarize, both visual processing streams can contribute to object form perception. The ventral stream has an established functional role in object perception and recognition while the dorsal stream is also involved, in addition to its established role in spatial and visuomotor control. This is supported by ventral lesion studies where dorsal stream activation has been linked to the retention of perceptual sensitivity to object features. Direct and indirect neural connections between the two streams further highlight an interaction. Object form perception appears to be a complex process, such that more research is required to establish insight into the functional role of the interaction between the two visual streams on behavioural performance.

1.4.3 Link between object form perception and reach to grasp

Visually guided reach to grasp involves both streams of visual processing, but relies more on the dorsal stream (Goodale and Milner, 1992; Culham et al., 2003). However, object form perception in the ventral stream works in conjunction to benefit reach to grasp performance. Although lesion studies provide evidence for separate pathways, there are interactions between the two streams (Wang et al., 1999; Goodale and Milner, 1992; Cloutman, 2012; Zachariou, Klatzky, and Behrmann, 2013). As previously discussed, fMRI studies have shown the grasping component to elicit higher activations in the anterior intraparietal cortex (AIP) than reaching (Culham et al., 2003). As grasping relies heavily on visual processing of object features, the increase in AIP activation suggests that it has a role in object form computations required for pre-shaping of the hand. When depth information from pictorial cues becomes more important during monocular viewing, ventral stream area LO activation was found to be coupled with dorsal area AIP and ventral premotor area (PMv) (Verhagen et al., 2008). This suggests a ventral contribution to the dorsal stream in movement planning and execution, when reach to grasp relies on pictorial information. These results support the notion that computation of object properties for grasping occurs in both ventral and dorsal stream

Although the dorsal stream is able to process and execute relatively simple visuomotor tasks independently, as demonstrated by lesion studies, the integration of the ventral stream is

required for completing more complex behavioural responses (Creem and Proffitt, 2001). Experimental scenarios are often limited to simple reach to grasp tasks towards standardized objects and therefore, elicit a greater dorsal stream response due to the lack of semantic demand. For reach to grasp tasks toward objects of meaning (tools, valuable, etc), dorsal stream provides information regarding object location and orientation in relation to the performer, while the ventral stream processes information related object recognition and semantics (Cloutman, 2012). Ultimately, the interaction between both streams of processing allows the object to be picked up and used more efficiently. The interaction between the two streams during movement execution is highlighted in a study that overloaded the ventral semantic or dorsal visuospatial system alternately and assessed reach to grasp performance towards familiar tools (Creem and Proffitt, 2001). Tools such as toothbrush, hammer, and forks were presented with the handles away from the performer. When neither stream was overloaded, performers were able to accurately grasp and pick up the tools in a congruent manner to which they are typically used, despite assuming an awkward positioning of the hand: a phenomenon coined end state comfort. When the ventral stream was overloaded with a concurrent semantic task, performers were still able to accurately grasp the objects, but not in a manner appropriate for their use. This suggests the interaction of the ventral and dorsal stream to not only accurately grasp the object (dorsal visuospatial), but also consider semantics (ventral recognition) to optimize performance after the grasp. According to this logic, more complex reach to grasp tasks whereby a goal exists following reaching and grasping the object will rely on both, the dorsal and ventral streams.

The interaction between the two visual processing streams can also be studied by looking at relative improvements in perceptual and reach to grasp task performance. In other words, does greater performance in object form perception, a function of the ventral stream, lead to improved reach to grasp performance, a function of the dorsal stream? Although this effect has not been studied directly, separate studies in perception and reach to grasp under binocular/monocular viewing conditions may provide some insight (Loftus, Servos, and Goodale, 2004; Jackson et al, 2010; Keefe, Hibbard, and Watt, 2010). Reach to grasp performance is more accurate and precise under binocular conditions. Similarly, perceptual

object recognition tasks also are improved under binocular viewing as compared with monocular. This highlights a gap in literature and warrants further inquiry to directly study the association between perception and action.

1.5 Gap in Literature and Rationale for Research

Vision has an important role in the planning and controlling of reach to grasp movements. It has been established that reach to grasp performance is influenced by the quality of visual input in both the planning and online control stage. More specifically, binocular viewing elicits less variability, faster speeds, and greater accuracy in reach to grasp performance. Separate research has examined the visual system's sensitivity to perceiving object form and found a binocular advantage (Steeves et al., 2003). It is possible that the improved performance of reach to grasp under binocular vision is linked to the enhanced ability to perceive object features. Previously discussed evidence of the interaction between the perceptual ventral and action oriented dorsal streams provides further support that a perceptual-kinematic relationship is possible. Manipulation of viewing condition has been shown to elicit a reliable and significant binocular advantage in both perceptual and reach to grasp tasks. Therefore, the manipulation of viewing condition allows the assessment of the relationship between improvements in object shape perception and reach to grasp performance during binocular viewing. The findings of this association would further probe the ventral-dorsal interaction and potentially demonstrate a relationship between perception and action. This research study will implement a two-part experiment whereby part one will assess the binocular advantage in object form perception, and part two will assess that of the reach to grasp task.

1.6 Research Objective

The main objective of the proposed research is to assess the association between the enhancements in observer's perceptual sensitivity to object form and reach to grasp performance.

1.7 Research Question

Is enhanced sensitivity (i.e., lower perceptual threshold and JND) to object form perception during binocular viewing positively associated with enhanced kinematic performance of a precision reach to grasp task?

1.8 Hypothesis

Binocular advantage in object form perception (demonstrated by lower threshold and JND) will be positively associated with binocular advantage in reach to grasp performance, as demonstrated by the following kinematic outcome measures:

- 1) Maximum grasp aperture
- 2) Time in deceleration
- 3) Time in grasping

2.0 Investigating the Association Between Enhancements in Perceptual Sensitivity to Object Form and Reach to Grasp Performance

2.1 Methods

2.1.1 Participants

Thirty visually healthy participants (16 females, 14 males, mean age 21.3 SD= 2.3) were included in the study. Participants had 20/20 visual acuity and a stereoacuity of 40 seconds of arc or better. Hand dominance was self reported by the participant, all were right hand dominant. Eye dominance was assessed using the Miles test in which participants are asked to look at a small object 5 meters away. Twenty-six participants were right eye dominant and 4 were left eye dominant. The study's protocol was approved by the University of Waterloo Research Ethics Committee. Participants signed a written consent prior to participating.

2.1.2 Experimental design

This study consisted of two sections: two psychophysical tests to measure sensitivity to object form perception, and a reach to grasp task to measure movement kinematics. Each test was performed under binocular and monocular viewing conditions. Monocular viewing conditions were implemented by covering the non-dominant eye with a translucent eye patch. A translucent material was selected over an opaque one to minimize binocular rivalry effects. Binocular rivalry can affect perceptual performance that involves identifying small changes to target objects/shapes, especially given the short duration of stimulus presentation in the psychophysical approach (Steeves et al., 2004).

During the initial assessment portion of the study, visual acuity was measured using Bailey's vision chart. Stereoacuity was measured using a "Stereogram" App on the Apple I-pod Touch. This App requires participants to wear red-cyan 3D glasses to identify which of two circles (consisting of random dots) that appear to be protruding from the screen. Using a staircase protocol, a perceptual threshold in terms of seconds of arc was determined. An additional standard clinical test was also used to measure stereoacuity (Preschool Randot Stereo Test). A brief questionnaire consisting of standard demographic questions (age, sex,

hand dominance), brief health history (visual/ physical/ neurological impairments) was also administered.

Following the assessment, participants performed the psychophysical tests. A method of constant stimulus (MOCS) protocol was used to determine the thresholds and just noticeable difference (JND) for two perceptual tasks: radial frequency (RF) and motion defined form (MDF). The kinematics section of the study was implemented next whereby participants performed a reach to grasp task in various experimental conditions (described in the next section). All tasks were performed binocularly and monocularly with the dominant eye. Figure A1 in the appendix outlines the entire experimental design. These tasks were performed in this order for all participants, while the order of viewing condition for each task was randomized.

2.1.3 Materials and procedures

Psychophysical tests to assess sensitivity to object form

All psychophysical measurements were completed using the VPixx system. Stimuli were presented on the 27" VPixx monitor with resolution of 1920x1080p and refresh rate of 120 Hz. A chin rest was used to ensure that stimuli were presented at eye level. The viewing distance was 90cm and 250cm for the RF and MDF stimuli, respectively. For monocular viewing conditions, the non-dominant eye was covered using a clear filter eye patch that allows input of light, but not form.

A staircase method and a method of constant stimuli were the two psychophysical tests used to assess the accuracy and precision of perceptual judgements using two tasks: 1) RF, and 2) MDF. Each task was first performed using the staircase method to find the approximate perceptual threshold. Then, a method of constant stimuli (MOCS) was used with test values of stimulus intensity centered around the threshold obtained from the method of limits.

Radial Frequency Stimulus

As illustrated in Figure 3, every trial began with a fixation on a crosshair ($0.5 \times 0.5^\circ$), which was presented for 0.3 seconds, and followed by the RF stimulus (radius of 0.5°) presented for 0.158 seconds. Using a two-alternative forced choice paradigm, participants were

instructed to identify if the presented stimulus is a perfect circle. Participants selected between two possible responses (yes/no) by pressing keys on the keyboard. The same stimulus and sequence were used for both staircase and MOCS protocols.

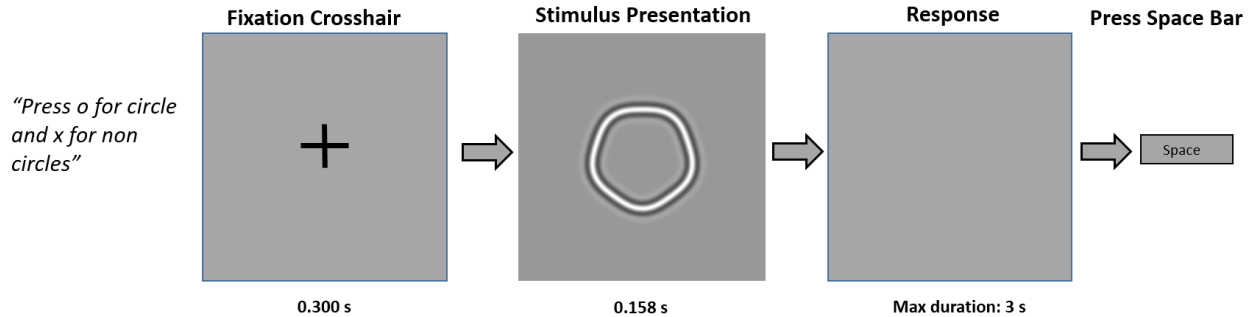


Figure 3. RF stimulus presentation

The properties of the RF stimulus are summarized in Table 1. The parameters remained constant between trials except for the amplitude (experimental manipulation) and phase. A phase manipulation involves rotating the RF shape about a certain angle, which was done to reduce learning effects from viewing similar shapes across 240 trials.

Table 1. RF properties

Property	Value
Frequency	5
Amplitude	Manipulated
Phase	0, 30, 60, 90°
Radius	0.5°
Band sigma	0.056

Motion Defined Form Stimulus

The sequence of stimulus presentation is outlined in figure 4. Upon pressing the space key on a keyboard to initiate the trial, a fixation crosshair (0.5°X0.5°) was presented for 0.150 s followed by the MDF stimulus for 0.642 s. The object was a vertical or horizontal rectangle (size 1°x 2° of visual angle). The object form was defined using a contrast of motion between the

dots in the background and foreground. Both vertical and horizontal rectangles were presented randomly, such that half of the total trials consisted of each.

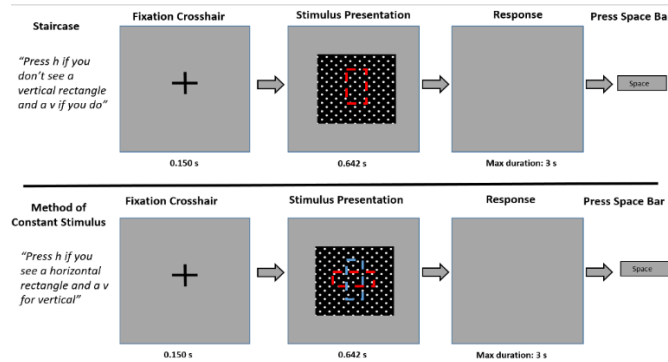


Figure 4. MDF stimulus presentation

Specific to the MDF stimulus is the change in the instructions between the staircase and MOCS protocols. In the staircase protocol participants were asked to respond whether or not they perceived a vertical rectangle. In the MDF protocol, participants were asked if they perceived a horizontal or vertical rectangle. There is a possibility that the change in the instructions for perceptual task may alter the perceptual threshold. This is especially true if there is a difference in the threshold between perceiving vertical and horizontal rectangles. As previous studies have not specifically looked into in this, a brief pilot study consisting of 3 participants was implemented. The findings suggest that the mean threshold (i.e. % dot coherence) for perceiving vertical rectangles was comparable to that of horizontal rectangle. The difference in instructions was implemented to maintain the up/down single presentation design of the staircase protocol. The following table 2 highlights the properties of the MDF stimulus.

Table 2. MDF properties

Properties	Values
Dot density	170 dots/°
Dot coherence	Manipulated (%)
Size of dots	0.022° diameter
Background dot velocity	+/- 0.1°/s
Foreground dot velocity	-/+ 0.1°/s (opposing background direction)
Orientation of Form	Vertical (2°x1°) & Horizontal (1°x2°)
Dot life time	77 frames

Staircase Protocol for RF and MDF

An identical up/down single presentation staircase test was used to approximate the mean threshold for both RF and MDF stimuli. For this protocol, a single stimulus was presented and participants made a yes/no perceptual judgement by pressing one of two keys on a keyboard. With every 2 correct responses, the manipulated variable or stimulus intensity decreased eliciting a more difficult perceptual judgement in the following trial. After a single incorrect response, the stimulus intensity increased which elicits an easier perceptual judgement. The maximum value of amplitude for the RF stimulus was set to a value of 0.05 (5% of the radius). At this value, RF shapes are easily perceivable under both viewing conditions. The maximum value of coherence for the MDF stimulus was set to 100%. The step sizes for changing stimulus intensity were set to 0.1 in a logarithmic scale for both RF and MDF staircase protocols. The staircase protocol was terminated either after 6 reversals or the completion of 100 trials. The mean threshold was defined as the average stimulus intensity from the final 4 reversals. The data from the staircase were visually inspected following each test to ensure the quality of the staircase psychometric curve.

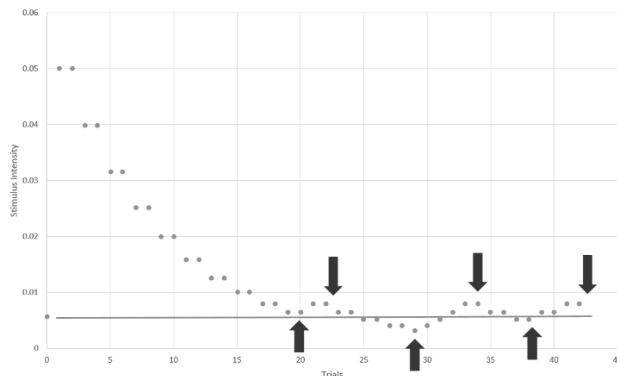


Figure 5. Typical data from staircase protocol with threshold (line) and reversals (arrows) highlighted

MOCS Protocol for RF and MDF

The mean threshold value from the staircase protocol was used to estimate the perceptual threshold of the observer to changes in amplitude (RF) and motion coherence (MDF). A more accurate measurement of this threshold can be obtained using a method of constant stimulus. As such, the threshold from the staircase was taken as a middle stimulus

intensity for the subsequent 2AFC MOCS protocol. The 4 other stimulus intensities during the MOCS protocol were determined based on the standard deviation (SD), such that the stimulus intensities were ± 0.5 and ± 1 SD. Figure A2 in the appendix outlines the sampling scheme that were implemented for the MOCS protocol. The red dot indicates the threshold value from the staircase protocol and the blue dots represent the calculated test values. The location of the estimated threshold as well as JND are highlighted.

The MOCS protocol for both RF and MDF stimuli consisted of 5 test values where each was presented 48 times in a fully randomized method for a total 240 trials. It has been shown that a total trial of 240 provides a reliable estimate of thresholds and slopes for this sampling scheme where test values are concentrated about the threshold (Wichmann and Hill, 2001). A logistic function was used to fit the psychometric curve. The fit of the curve was analyzed with the Chi-Square Goodness of Fit test. The threshold was defined as the stimulus intensity at which 75% of responses were correct. The precision of the perceptual measurement is assessed by the just noticeable difference (JND), which is the minimal perceivable change in intensity of the participant. This value will be taken as the difference in stimulus intensity between the threshold and at the 50% correct point (25% away from the threshold). The 50% correct point represents an approximate chance perception, or a guess, while the threshold represents the minimal perceivable stimulus intensity. The difference between these two values provides a measure of the smallest perceivable change in stimulus intensity that can be reliably detected/discriminated. Both the threshold and JND value together provide a description of the overall perceptual accuracy and precision of the participant.

Reach to Grasp Experimental Design

Participants were instrumented with two small infrared markers placed on the index finger and thumb of the dominant hand. The Optotrak system was calibrated using a standardized calibration probe to define the coordinate system as follows: x-axis (azimuth), y-axis (elevation), z-axis (depth). Participants performed a reach to grasp while upper limb kinematics were recorded using the Optotrak system at a sampling frequency of 500 Hz.



Figure 6. Optotrak Camera (Left) and Marker placement (right)

Reach to Grasp Task Procedure

Participants performed one practice trial for each of the 9 reaching conditions, prior to the beginning the experimental trials. This practice was included to familiarize participants to the task. Objects included in this study were cylinders with a fixed height of 3 cm and a diameter of 0.5 cm, 1 cm, and 1.5 cm. Objects were placed at the participant's midline at 3 different distances in depth: 40cm, 42cm, and 44cm. Three reaching distances and object sizes were implemented to control for the learning effects that come with repetition of the same movement. Each of the 9 reaching conditions (3 x 3 experimental design) was repeated 10 times per viewing condition for a total of 180 trials. The order of viewing conditions was randomized among participants.

Participants were seated with their head supported by a chin rest when performing the task. Participants began the trial with their eyes closed, and their index and thumb at a standardized start position located 10 cm directly in front of the participants. The cylinder was placed on a curved surface to increase the demand for accuracy and precision. A verbal cue was used as a go signal, and participants were asked to open their eyes and complete the reach to grasp task (i.e. grasp the cylinder and transport it to a different location on a platform located closer to the body (Figure 7) as fast as possible while maintaining accuracy. Specifically, after grasping, the object was transported and placed into 1 of 3 stencils that outlined the circumference of the shape. Figure A3 in the appendix outlines the components of this reach to grasp task.

In addition to the 90 trials per viewing conditions, 27 “scaling trials” were included. These 27 trials consisted of 3 trials under each reaching condition (3 x 9). During these scaling trials, participants scaled/matched their grasp aperture to the width of the target object. Participants were given the instruction to fixate on the object and not their hand. Adjustments to the grasp aperture were allowed during the 4 seconds of motion tracking. These scaling trials were implemented as a proxy measure of direct sensori-motor transformation of shape perception in absence of reach to grasp movement. This proxy measure will provide a perceptual-kinematic baseline such that inferences can be made on how introducing a reach to grasp movement influence this relationship. With these scaling trials, a total of 234 trials were initially recorded and analyzed using motion tracking during this section of the experiment.

Experimental Setup

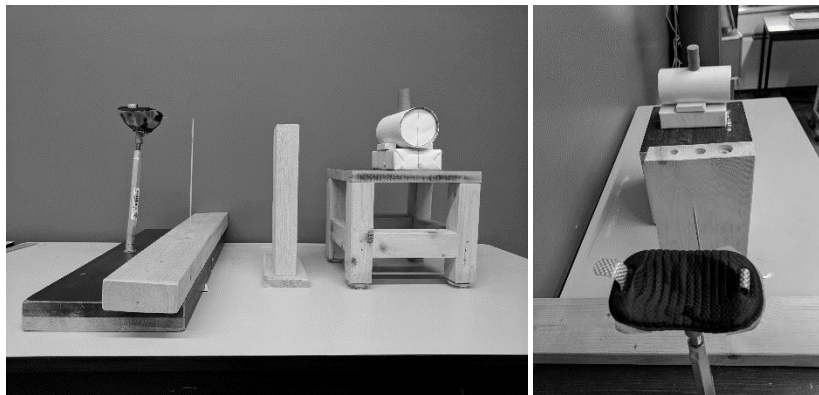


Figure 7. Experimental set up of reach to grasp task

Data reduction

Trials were excluded and repeated when the target object was dropped at any time during the reach to grasp task. In addition, the visibility of the infrared markers for both markers were required to be 100% throughout the reach and grasp portion of the entire task. Data were collected as raw marker position from the calibrated origin. A low pass second order Butterworth filter with a cut-off frequency of 10 Hz was used to process the raw data. All trials

were screened visually for missing data and artefacts. Kinematic calculations such as velocity and maximum grasp aperture were obtained using a custom Matlab script.

Scaling Grasp Aperture (SGA)

Scaling grasp aperture was recorded in place of maximum grasp aperture during “scaling trials”, and was taken as the average of 3 average grasp aperture values between 1200-1300 ms, 1400-1500ms, and 1700-1800ms intervals. Averages of three time intervals in the movement were taken due to the continuous adjustments made on grasp apertures by the participants throughout the 4 seconds of motion tracking. Participants predominantly employed one of two strategies for scaling grasp aperture. One was to begin with a larger aperture to which adjustments are made to decrease its size, and the other was to begin with a smaller aperture followed by adjustments to increase its size. All scaling trials were visually analyzed to ensure that the intervals reflected a stable scaling grasp aperture, one that is at the end of major adjustments. Although there was no official quantitative criterion for a stable scaling grasp aperture, the standard deviation within this interval will be reported in the analysis to provide insight on the degree of adjustments.

Maximum Grasp Aperture (MGA)

Grasp aperture was calculated as the difference of the vector between the finger and thumb marker. During reach to grasp trials, the MGA was determined to be the maximal peak in grip aperture prior to contact with the object during the reach component of the task. This measure has been shown in previous studies to be modulated by viewing condition, such that monocular viewing elicits a greater MGA (Servos, Goodale, and Jakobson, 1991; Jackson et al., 1997; Jackson et al., 2010).

Time in Deceleration (TID)

Time spent in deceleration was calculated as the time between maximum reach velocity and end of the approach phase. The end of the approach phase is typically defined as a velocity <100 mm/s towards the object. This criterion has been used in previous literature as a proxy measure of the end of the reach movement (Gnanaseelan, Gonzalez, and Niechwiej-Szwedo,

2014; Elliot et al., 2006; Glazebrook et al., 2009). Data from the finger was used for this calculation.

Time in Grasping (TIG)

Time spent in grasping was calculated as the time between the end of approach (as defined previously) and the beginning of the object transport phase defined as a velocity of 20 mm/s in the opposite direction (Gnanaseelan, Gonzalez, and Niechwiej-Szwedo, 2014). Without the use of a force transducer on the object, grasping time was estimated as the time in between approach to the object and its subsequent transport. Data from the thumb, instead of the finger were used for this 20 mm/s threshold. While grasping, the finger travels beyond object and then returns in the opposite direction to make contact. This returning movement is in the same direction as object transport and, at times, surpasses the 20 mm/s threshold. This causes the determination of the beginning of object transport to be inaccurately early (prior to even making contact with the object). Using thumb data alleviates this issue as the thumb moves towards the object without any returning movement during grasping.

2.2 Results

The goal of this thesis was to assess the association between perceptual and motor performance. Viewing condition was manipulated to challenge the perceptual and motor systems, and to establish an association in response to the manipulation. It was hypothesized that greater sensitivity to shape perception (threshold and JND) during binocular viewing will be positively correlated with the binocular enhancement in reach to grasp performance, as reflected by the selected kinematic outcome measures (SGA, MGA, TID, TIG). The enhancement in the perceptual and reach to grasp tasks was quantified using a binocular advantage defined by the following formula:

$$\text{Binocular Advantage} = \text{Monocular Measure} / \text{Binocular Measure}$$

A value greater than one suggests enhanced binocular performance, such that larger ratios suggest a larger binocular advantage.

The results are presented in two sections. The first section shows the results for the perceptual and reach to grasp measures, and highlights the binocular advantage obtained in each task separately. With the binocular advantage quantified for both tasks in the first section, the second section shows the correlation analysis between enhancements in the perceptual and reach to grasp tasks. The purpose of the second section is to assess the perceptual-action association, and to ultimately probe the possible interaction between the ventral and dorsal streams of visual processing.

2.2.1 Binocular advantage in perceptual measures

This section presents the binocular advantage for the threshold and JND measures obtained from the RF and MDF tasks. Thresholds and JNDs were calculated from a psychometric function that was fit using a logistic regression. Pearson's χ^2 test confirmed that the logistic model fit the data of all participants (30/30) in the RF task, and 25/30 participants in the MDF task. Three (out of five) excluded participants in the MDF task were due to insufficient responses in the psychophysical test (not being able to reach at least 75% correct in either viewing condition). The other two exclusions were due to insufficient goodness of fit. The individual psychometric functions, as well as results from the χ^2 analysis for both viewing conditions are included in appendices A4/A5 and A6/A7 for the RF and MDF task, respectively.

Radial Frequency (RF)

The psychometric functions for binocular and monocular viewing for a single participant is demonstrated in figure 8. The rightward shift of the monocular function demonstrates a higher threshold, thereby lower sensitivity to object form. Four out of 30 participants did not demonstrate lower sensitivity during monocular viewing. Figure 9 demonstrates the psychometric functions of a participant that did not demonstrate this binocular advantage.

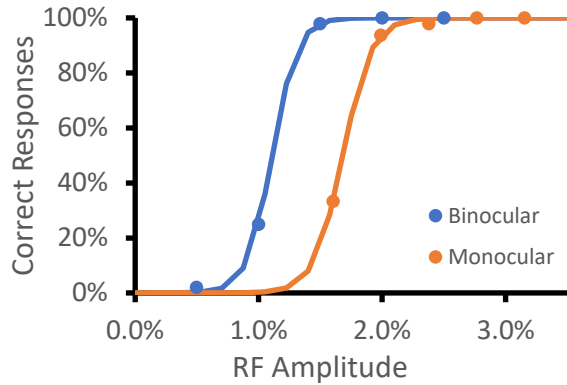


Figure 8. Psychometric functions of participant demonstrating binocular advantage for RF stimulus

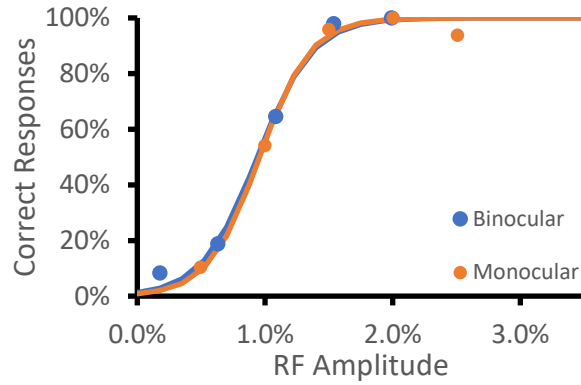


Figure 9. Psychometric functions of participant not demonstrating binocular advantage for RF stimulus

The mean perceptual threshold was 1.16% (SD= 0.35) and 1.34% (SD=0.44) for binocular and monocular viewing, respectively. The mean JND was 0.21% (SD=0.05) and 0.28% (SD=0.12) for binocular and monocular viewing conditions, respectively. For boxplots showing the RF threshold and JND measures within each viewing condition, refer to appendix A8. A one-way repeated measure ANOVA showed that the effect of viewing condition was significant such that a binocular advantage was demonstrated for both measures (threshold: $F(1,29)= 21.22$, $p<0.001$, JND: $F(1,29)=10.9$, $p=0.0026$). The calculated binocular advantage for the threshold and JND was 1.16 (SD= 0.21) and 1.39 (SD= 0.58) respectively. Figure 8 shows the binocular advantage for the RF threshold and JND, with the solid line indicating equal performance in both viewing conditions.

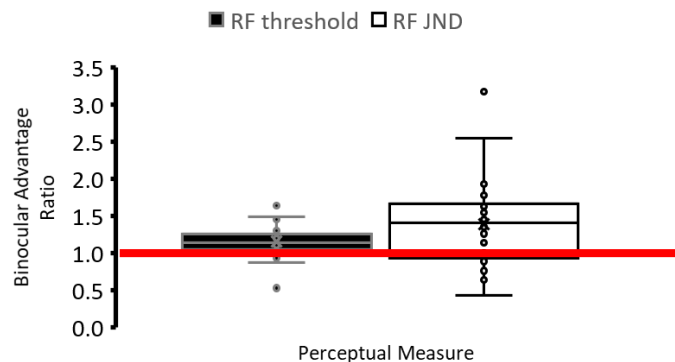


Figure 10. Boxplot outlining RF binocular advantage ratios for threshold and JND

Motion Defined Form (MDF)

The psychometric functions for binocular and monocular viewing for a single participant is demonstrated in figure 11. The rightward shift of the monocular function demonstrates a higher threshold, thereby lower sensitivity to object form. Seven out of 25 participants did not demonstrate lower sensitivity during monocular viewing. Figure 12 demonstrates the psychometric functions of a participant that did not demonstrate this binocular advantage.

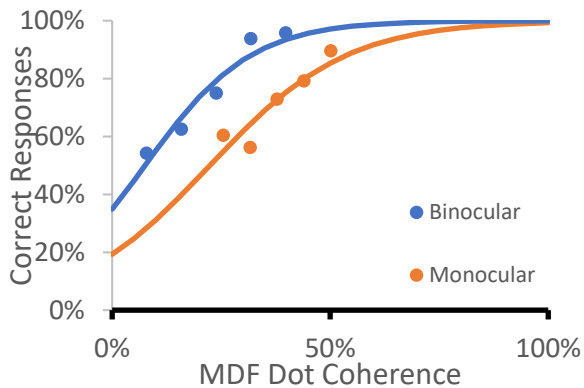


Figure 11. Psychometric functions of participant demonstrating binocular advantage for MDF stimulus

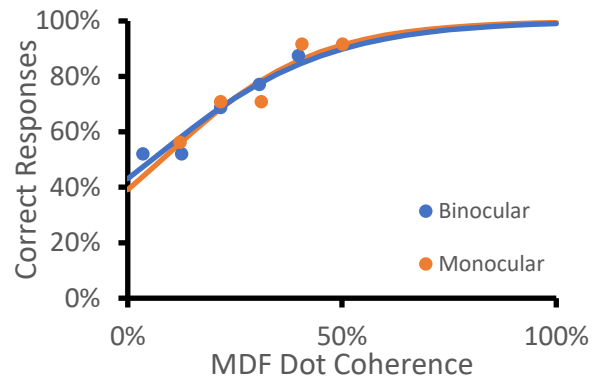


Figure 12. Psychometric functions of participant not demonstrating binocular advantage for MDF stimulus

The mean thresholds for binocular and monocular viewing were 25% (SD=7.6) and 32.1% (SD= 11.95) respectively. The mean JND were 19.5% (SD=7.4) and 22.7% (SD=12.24) for binocular and monocular conditions respectively. For boxplots showing MDF threshold and JND in each viewing condition, refer to appendix A8. A one-way repeated measures ANOVA showed that the effect of viewing condition was significant for both threshold and JND, such that a binocular advantage was demonstrated for both measures (threshold: $F(1,24)=11.05$, $p=0.0026$, JND: $F(1,24) = 4.28$, $p=0.49$). The threshold and JND binocular advantage ratio was 1.36 (SD= 0.52) and 1.22 (SD=0.48), respectively. Figure 9 highlights the binocular advantage in terms of MDF threshold and JND, with the solid line indicating equal performance in both viewing conditions.

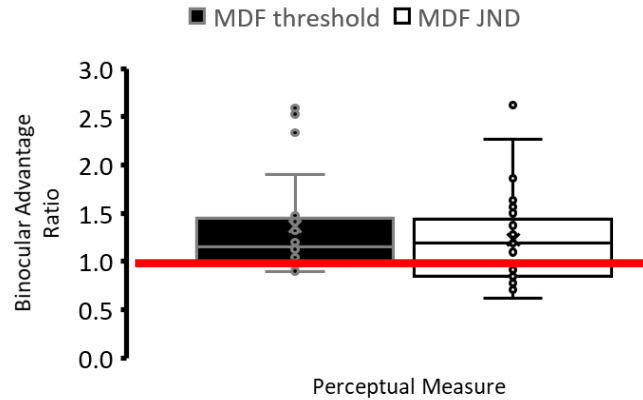


Figure 13. Boxplot outlining MDF binocular advantage ratios for threshold and JND

2.2.2 Binocular advantage for kinematic measures

Kinematic Data Reduction

Data reduction included the removal of reach to grasp trials that were missing kinematic data during the reach to grasp movement. Through visual examination of the velocity profile, a total of 327 (6%) reach to grasp trials were removed due to missing data. More specifically, a total of 91 binocular and 236 monocular trials were removed. The data from 29/30 participants were included in the following analysis as at least 75% of their trials were intact. Data from one participant was excluded as 48% of trials consisted of missing data. A similar data reduction process was implemented for the scaling trials, whereby the scaling grasp aperture was measured. The dataset from one participant was excluded due to inconsistency of marker visibility during motion tracking. As such, data from 29/30 participants were analysed for the scaling trials. Additionally, 100% of the data from these participants were included as there was no missing trials.

Normality of mean kinematic measures (scaling grasp aperture, max. grasp aperture, time in deceleration, and time in grasping) was evaluated using the Shapiro-Wilk test. The distributions were found to be normal for all measures during both viewing conditions. These mean measures were used to calculate the binocular advantage ratio. The distributions of these binocular advantage values were also found to be normal. Refer to appendices A9/A10 for the

normal plots (histogram and probability plot) of mean binocular and monocular kinematic measures and appendix A11 for the normal plots of the binocular advantage ratios.

Sample of Kinematic Data

Displacement, velocity, and grasp aperture measures were plotted throughout the movement for the extraction of the kinematic outcome measures. Figure 14 demonstrates kinematic graphs for a typical reach to grasp trial in terms of displacement (depth axis), velocity (depth axis), and grasp aperture.

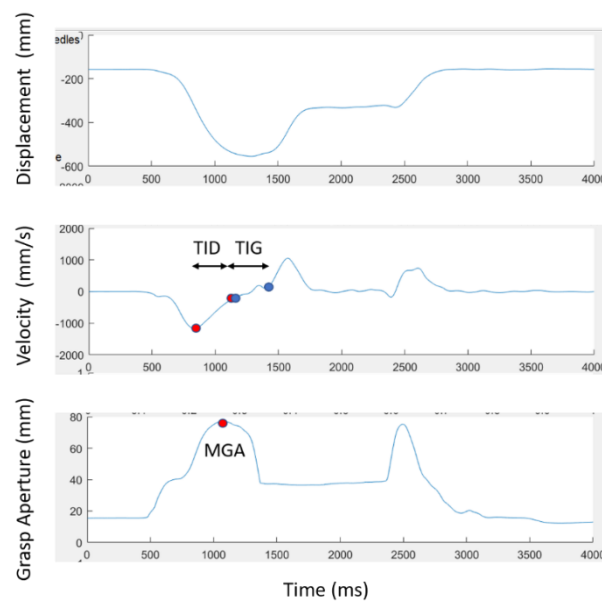


Figure 14. Position, velocity, and grasp aperture graphs for a typical reach to grasp trial

Scaling Grasp Aperture (SGA)

The scaling grasp aperture measure was calculated as the average across three consecutive 100ms intervals in the scaling trials (1200-1500ms). The grasp aperture was visually examined, per trial, to ensure that no significant adjustments were still being made in the span of these intervals. The mean standard deviation within the measured interval was 0.27mm (binocular: 0.29mm; monocular: 0.25mm). This value suggests that no major adjustments to the grasp aperture were made in the span of the 300 ms interval. The mean scaling grasp aperture were 43.3mm (SD=8.07) and 45.67mm (SD=8.55) for binocular and monocular conditions,

respectively. A one-way repeated measure ANOVA analysis showed that the effect of the viewing condition manipulation was significant on mean scaling grasp aperture ($F(1,28)=10.10, p=0.0037$), such that a smaller grasp aperture was found during binocular viewing. A mean binocular advantage ratio of 1.06 ($SD=0.09$) was found for SGA.

Figure 15 demonstrates the distribution of SGA measures across trials of the scaling task during binocular and monocular viewing for a single participant. Figure 16 demonstrates the distribution of mean SGA measures for all participants between the two viewing conditions.

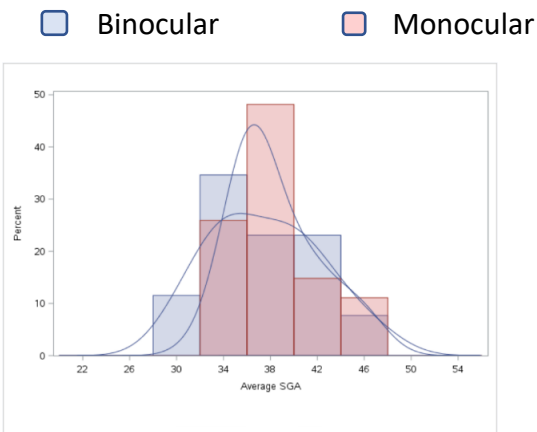


Figure 15. Distribution of binocular and monocular SGA values for single participant

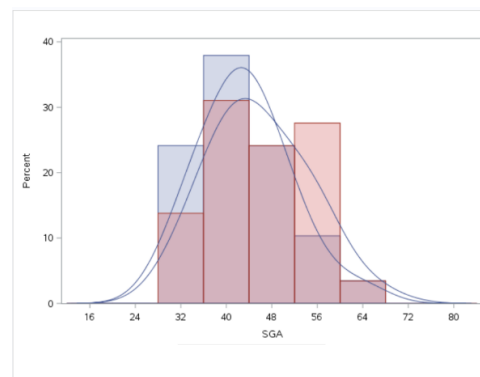


Figure 16. Distribution of binocular and monocular mean SGA values for entire sample

Overall Reach to Grasp Performance

A one-way repeated measures ANOVA analysis showed that reach to grasp movements were performed significantly slower during monocular viewing ($F(1,28)=102.94, p<0.0001$). The mean duration of the reach to grasp movement was 876 ms ($SD=138$) and 1133 ms ($SD=202$) during binocular and monocular viewing respectively. Additionally, χ^2 analysis showed differences in the number of objects dropped during each viewing condition ($\chi^2=174.78, df=29, p<0.0001$). A mean of 0.41 ($SD=0.68$) and 6.5 ($SD=3.4$) object drops were observed respectively. This suggests less effective performance during monocular viewing. Overall reach to grasp performance appears to be enhanced during binocular viewing, as demonstrated through movement duration and number of objects dropped.

Maximum Grasp Aperture (MGA)

A one-way repeated measures ANOVA analysis showed maximum grasp aperture to be smaller during binocular viewing ($F(1,28)=204.75, p<0.001$). The mean MGA was 71 mm (SD=9mm) and 88.4mm (SD=11.22mm) for binocular and monocular viewing, respectively. The binocular advantage was 1.25 (SD=0.10). The results from this study demonstrated that participants tend to employ a larger MGA when approaching an object during monocular viewing.

Figure 17 demonstrates the distribution of MGA across reach to grasp trials during binocular and monocular viewing for a single participant. Figure 18 demonstrates the distribution of mean MGA across all participants between the two viewing conditions.

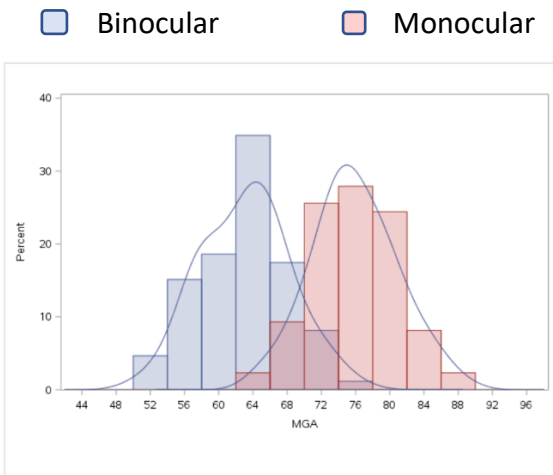


Figure 17. Distribution of binocular and monocular MGA values for single participant

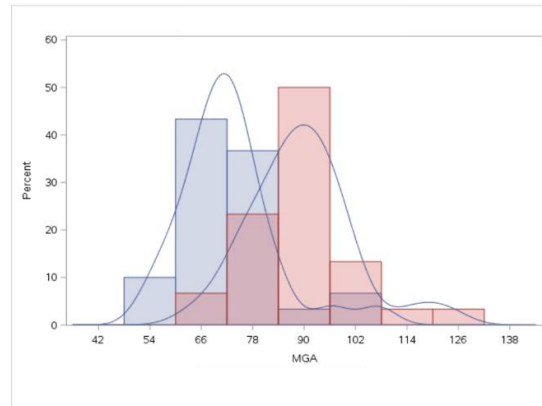


Figure 18. Distribution of binocular and monocular mean MGA values for entire sample

Time in Deceleration (TID)

A one-way repeated measures ANOVA analysis showed that time in deceleration was significantly longer during monocular viewing ($F(1,28)=80.54, p<0.001$). The TID was 331 ms (SD=61.4ms) and 405 ms (SD=68ms) during binocular and monocular viewing, respectively. This suggests that on average, participants spend approximately 74ms longer in deceleration when viewing monocularly. The mean binocular advantage for TID was 1.24 (SD=0.15).

Figure 19 demonstrates the distribution of TID across reach to grasp trials during binocular and monocular viewing for a single participant. Figure 20 demonstrates the distribution of mean TID across all participants between the two viewing conditions.

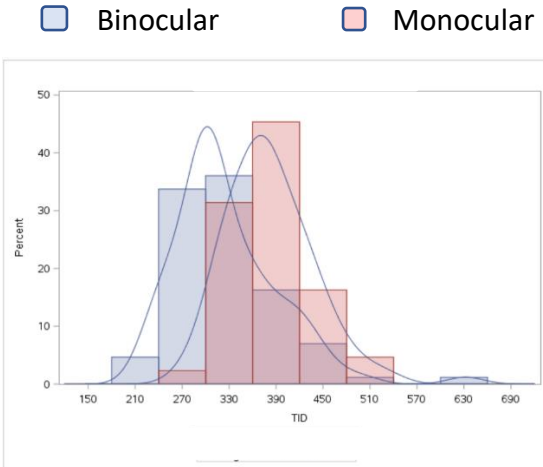


Figure 19. Distribution of binocular and monocular TID values for single participant

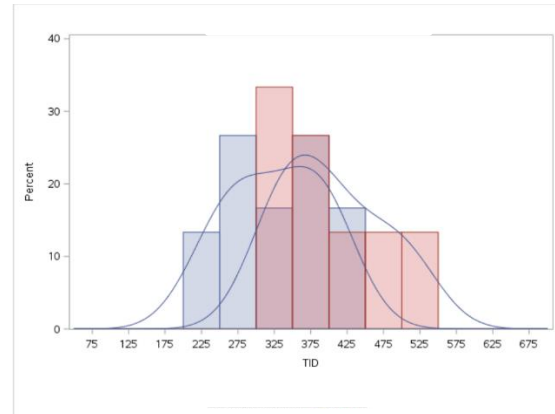


Figure 20. Distribution of binocular and monocular mean TID values for entire sample

Time in Grasping (TIG)

A one-way repeated measures ANOVA analysis showed the effect of viewing condition to be significant, such that longer time in grasping was found during monocular viewing ($F(1,28)= 86.31, p<0.0001$). The mean TIG was 178 ms ($SD=47.3ms$) and 363.8 ms ($SD=111.1ms$) for binocular and monocular viewing, respectively. On average, participants spend approximately 186 ms longer in grasping phase during monocular viewing. The binocular advantage for TIG was 2.12 ($SD=0.68$).

Figure 21 demonstrates the distribution of TIG across reach to grasp trials during binocular and monocular viewing for a single participant. Figure 21 demonstrates the distribution of mean TIG across all participants between the two viewing conditions.

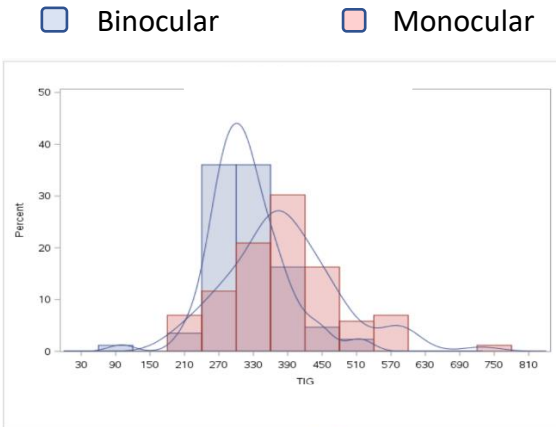


Figure 21. Distribution of binocular and monocular TIG values for single participant

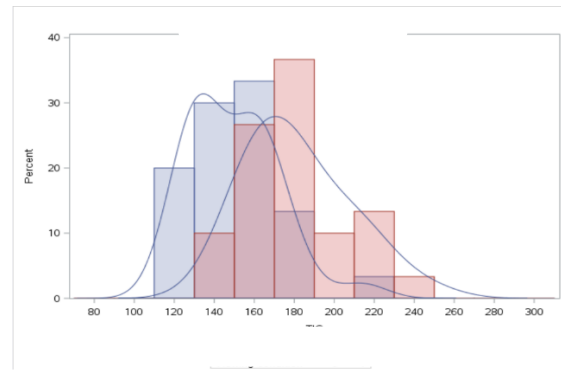


Figure 22. Distribution of binocular and monocular mean TIG values for entire sample

Kinematics – Summary

The 4 kinematic outcome measures (SGA, MGA, TID, and TIG) all demonstrated a binocular advantage. The mean binocular advantage for these measures is shown in Figure 23.

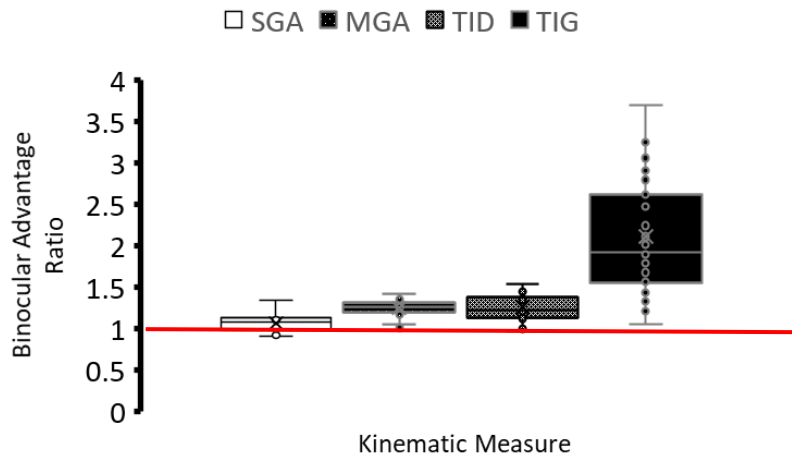


Figure 23. Binocular advantage ratios of kinematic outcome measures

Thus far in the analysis section, a binocular advantage has been demonstrated for both perceptual tasks (RF and MDF) and all 4 kinematic outcome measures in the reach to grasp task (SGA, MGA, TID, TIG). This demonstrates that the tasks and outcome measures used in this study were sensitive to the manipulation of the viewing condition. For boxplots highlighting the actual values of the kinematic measures during binocular and monocular viewing, refer to

appendix A12. The established binocular advantage ratios are important for answering the research question, “is enhanced sensitivity to object shape positively correlated with enhanced reach to grasp performance”. As binocular vision was shown to enhance performance on both tasks, the second section of the analysis will focus on the association of the enhancement in perceptual and reach to grasp task performance.

2.2.3 Perceptual – kinematic correlation

This section presents the results from a correlation analysis between the binocular advantage found for the performance of the perceptual and kinematic tasks. As not all of the correlations are graphically presented, refer to A13 (RF) and A14 (MDF) in the appendices for plots of all perceptual-kinematic binocular advantage correlations. Additionally, the correlation between actual perceptual thresholds/JNDs with the kinematics measures within each viewing condition are reported in appendix A15 (RF) and A16 (MDF).

Radial Frequency (RF) – Kinematic Outcome Measures (SGA, MGA, TID, TIG)

Radial Frequency (RF) – Scaling Grasp Aperture (SGA) correlation

A Pearson correlation demonstrated no significant correlation between the binocular advantage for RF threshold and scaling grasp aperture ($r=-0.21$, $p=0.28$). This suggests that enhancement in RF shape perception was not significantly associated with an enhancement in scaling grasp aperture. No significant association was detected between the RF JND and scaling grasp aperture ($r=-0.07$, $p=0.72$). As such, results show that perceptual precision of shape does not relate to the scaling grasp aperture.

Radial Frequency (RF) – Maximum Grasp Aperture (MGA) Correlation

The binocular advantage in terms of RF threshold was not significantly associated with maximum grasp aperture ($r=-0.36$, $p=0.053$). No significant association was detected between binocular advantages of RF JND and maximum grasp aperture ($r=-0.26$, $p=0.17$). As such, there appears to be no relationship between perceptual precision of object shape with maximum

grasp aperture. Figure 11 and 12 highlights the association between binocular advantage for RF shape perception and maximum grasp aperture in terms of threshold and JND.

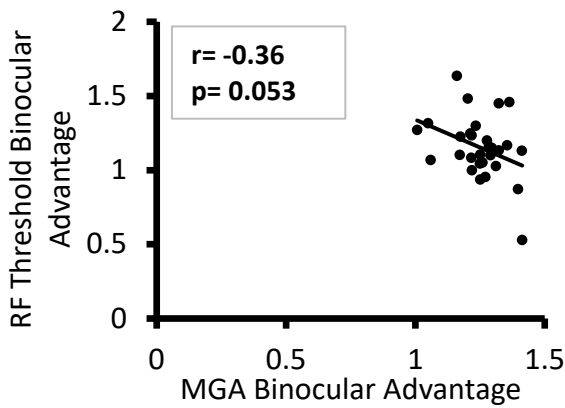


Figure 24. Association between RF Threshold and MGA binocular advantage ratio

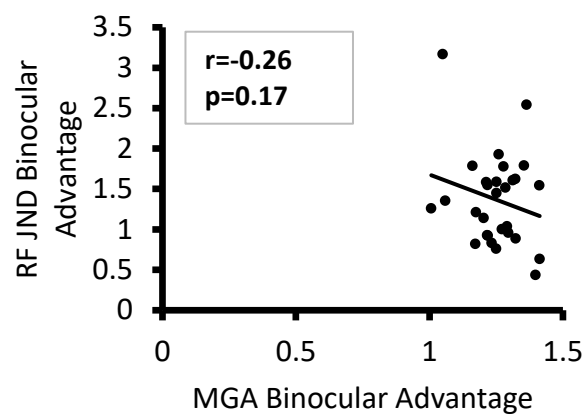


Figure 25. Association between RF JND and MGA binocular advantage ratio

Radial Frequency (RF) – Time in Deceleration (TID) Correlation

No significant correlation was found between the binocular advantages in RF accuracy and precision measures and time in deceleration of the reach to grasp. This finding was consistent for both RF threshold ($r=0.06$, $p=0.76$), and JND ($r=0.22$, $p=0.25$). This suggests that enhanced RF shape perception during binocular viewing is not associated with shorter time in deceleration during the reach to grasp task.

Radial Frequency (RF) – Time in Grasping (TIG) Correlation

No significant correlation was found between the binocular advantages in RF shape perception and time in grasping. This finding was consistent for both RF threshold ($r=0.001$, $p=0.99$), and JND ($r=0.02$, $p=0.92$). The lack of relationships suggests the improvements in performance during binocular viewing are unrelated, such that the enhancement of RF shape perception does not influence the time in grasping of reach to grasp. Table 3 outlines a summary of the correlation coefficients between binocular advantages in RF performance with kinematic measures in reach to grasp.

Table 3. Pearson correlation coefficients of binocular advantage of RF- kinematic measures

	RF Threshold	RF JND
SGA	$r=-0.21, p=0.28$	$r=-0.07, p=0.72$
MGA	$r=-0.36, p=0.053$	$r=-0.26, p=0.17$
TID	$r=0.06, p=0.76$	$r=0.22, p=0.25$
TIG	$r=0.001, p=0.99$	$r=0.02, p=0.92$

Motion Defined Form (MDF) – Kinematic Outcome Measures (SGA, MGA, TID, TIG)

Motion Defined Form (MDF) – Scaling Grasp Aperture (SGA) Correlation

Pearson correlation analyses showed no association between the binocular advantages of MDF shape perception and scaling grasp aperture during scaling trials in terms of accuracy ($r=-0.18, p=0.41$) and precision ($r=-0.37, p=0.07$). The enhancement in object shape perception appears to be unrelated to the enhancements in scaling of the grasp aperture. Figure 13-14 highlights this relationship for both the threshold and JND.

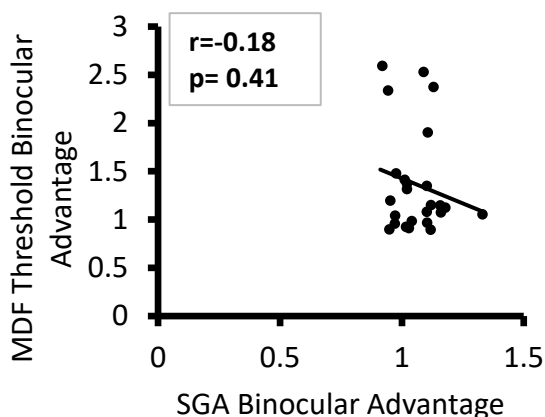


Figure 26. Association between MDF Threshold and SGA binocular advantage ratio

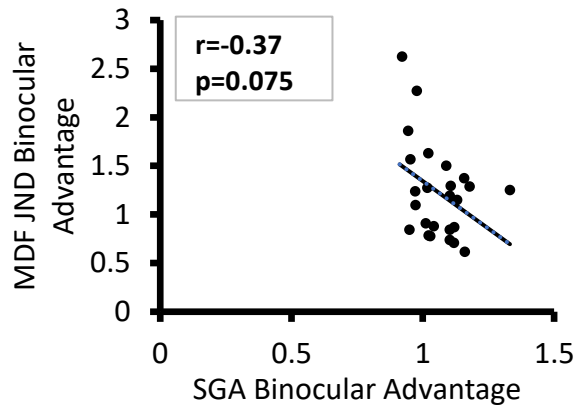


Figure 27. Association between MDF JND and SGA binocular advantage ratio

Motion Defined Form (MDF) – Maximum Grasp Aperture (MGA) Correlation

No significant association was found between binocular advantage of MDF shape perception and maximum grasp aperture. This finding was consistent for both MDF threshold ($r=-0.003, p=0.99$), and JND ($r=-0.1, p=0.63$). The lack of relationship suggests that the

enhancement of MDF shape perception is unrelated to the enhancements of the maximum grasp aperture during reach to grasp.

Motion Defined Form (MDF) – Time in Deceleration (TID) Correlation

Binocular advantages between MDF shape perception did not correlate with time in deceleration during reach to grasp in terms of both threshold ($r=-0.12$, $p=0.57$) and JND ($r=-0.06$, $p=0.77$). This suggests that the enhancement in MDF shape perception is not significantly related to in the duration of the deceleration phase.

Motion Defined Form (MDF) – Time in Grasping (TIG) Correlation

No correlation was found between the binocular advantages of MDF shape perception and time in grasping. This finding was consistent for MDF threshold ($r=0.17$, $p=0.42$) and JND ($r=0.14$, $p=0.50$). The lack of relationships suggests that the enhancement MDF shape perception was not significantly related to more efficient grasping movement. Table 4 summarizes the Pearson correlation coefficient found between binocular advantages in MDF threshold and JND with the reach to grasp kinematic measures.

Table 4. Pearson correlation coefficients of binocular advantage of MDF- kinematic measures

	MDF Threshold	MDF JND
SGA	$r=-0.18$, $p=0.41$	$r=-0.37$, $p=0.075$
MGA	$r=-0.003$, $p= 0.99$	$r=-0.1$, $p=0.63$
TID	$r=-0.12$, $p=0.57$	$r=-0.06$, $p=0.77$
TIG	$r=0.17$, $p=0.42$	$r=0.14$, $p=0.50$

2.3 Discussion

The objective of this study was to assess the association between enhancements in perceptual sensitivity to object form and the kinematic performance of a precision reach to grasp task. The data first demonstrated that binocular viewing was associated with enhanced performance in object shape perception (both RF and MDF stimulus), and reach to grasp kinematics. This finding is in line with previous research which found a binocular advantage during the performance of the RF task (Steeves et al., 2003), and the reach to grasp task (Servos

and Goodale, 1994; Jackson et al., 1997; Read et al., 2012). Previous literature has not explicitly tested the monocular performance in the MDF task, but it has been shown that performance is enhanced in healthy controls compared to observers with abnormal binocular vision (Hayward et al., 2010). The binocular advantage in perceptual and reach to grasp performance provided an opportunity for assessing the association of relative enhancements between the two tasks. This ultimately provided a probe into the interaction between the ventral and dorsal streams of visual processing.

The findings of this study provided no evidence for an association between the magnitude of the binocular advantage found in perceptual and kinematic measures. Specifically, this study demonstrates that enhanced perception of object form is not associated with enhancement in reach to grasp, as the hypotheses remained unsupported. Ultimately, the probe (viewing condition) used in this study was unable to show an interaction between the ventral and dorsal streams of visual processing. As such, the lack of relationship supports the notion that binocular advantage is found independently in the ventral perceptual and dorsal-action pathways.

2.3.1 Methodological considerations – perceptual and reach to grasp tasks

The hypotheses for this study were developed based on a theoretical framework that suggested enhancement of visual perception could be associated with improved reach to grasp performance. After all, numerous separate studies have found the quality and availability of visual input to influence perceptual judgements and reach to grasp performance. However, previous literature did not examine the correlation of performance among the perceptual tasks and the reach to grasp task. The perceptual stimuli used in this study, radial frequency (RF) and motion defined form (MDF), were selected because they rely on different neural substrates, and involve different mechanisms that lead to a binocular advantage. Therefore, using these perceptual tasks could have provided some insight about the mechanisms underlying the binocular advantage.

The RF and MDF stimuli have both been used to elucidate the mechanisms involved in object shape perception; however, they differ in the level of neural processing involved. The RF

stimulus has been shown to elicit neural responses in extrastriate areas V2d, V3d, V3AB, V4 and the intraparietal sulcus area IPS0 (Salmela, Henriksson, Vanni, 2016). The activation of area LO was also found; however, its activation was not specific to the RF stimulus. Additionally, the modulation of RF shape amplitude did not affect responses in the higher areas involved in visual processing (IPS0 and LO) (Salmela, Henriksson, Vanni, 2016). Given these results, early and mid-level visual areas are the neural correlates of RF shape perception.

With regards to the mechanism that is involved in eliciting the binocular advantage, binocular neurons are found in these early-mid areas (V1, V2, V4, MT), as well as the higher processing areas (MST/IPS/IT) in both ventral and dorsal streams (Steinman and Garzia, 2000). It has been proposed that binocular summation is the main mechanism underlying the enhancement of perceptual sensitivity for the RF task (Steeves et al., 2003). Binocular summation refers to the combination of inputs from the two eyes which strengthens the neural signals and the probability of detection, while reducing background noise (Campbell and Green, 1965).

The performance of the MDF task has been shown to require both ventral and dorsal pathways (Regan et al., 1992). Neuroanatomical findings show an interconnected network, including areas V1-V4-IT and V1-MT-MST/7a, activated during discrimination of complex MDF shapes. In addition, patients with damage in either ventral or dorsal stream structures had reduced sensitivity to MDF stimuli (Regan et al., 1992). The processing of MDF stimulus occurs at higher levels of processing, whereby visual cues such as object form and motion detection converge (Regan et al., 1992). The processing of MDF involves a hierarchical process, beginning with 1) direction-specific detection of local motion 2) detection of form defined by equal and opposite speeds 3) spatial discrimination and recognition of MDF (Braddick et al., 1978; Regan, 1982; Regan and Beverly, 1983). For the perception of a simple MDF stimulus (i.e., a single bar), neurons in MT have shown to be largely activated, providing a physiological basis for the detection of MDF (Tanaka et al., 1986). For complex shapes (alphabet letters), increased activation of area TE was detected, suggesting that the ventral stream contributes to the recognition of MDF (Van Essen et al., 1990).

Whereas the binocular advantage found for the RF stimulus was mainly attributed to binocular summation, the binocular advantage in MDF perception additionally relies on binocular disparity. The activated dorsal structures (V3A, V7, MT) during MDF perception have neurons whose responses are modulated by binocular disparity. When comparing the response to disparity of the ventral stream, dorsal stream, and early visual areas, it was found that the activity of dorsal structures (V3A, V7, MT) was significantly greater (Minini, Parker, Bridge, 2010). Additionally, the responses in V7, MT, dorsal intraparietal sulcus anterior (DIPSA) and medial (DIPSM) increase with the degree of disparity (up to 0.7°) (Minini, Parker, Bridge, 2010). Furthermore, all neurons in area MT are binocular and contributes to the integration of motion and disparity signals (Bradley, Qian, and Anderson, 1995). The lack of binocular disparity input during development is associated with reduced sensitivity to motion in MT neurons (Ungerleider and Mishkin, 1979; Tyschen and Lisberger, 1986). To summarize, binocular disparity contributes to the binocular advantage found for the MDF task.

Given the objective of this research was to probe the interaction between ventral and dorsal streams, the reach to grasp task was used in this experiment to probe dorsal performance. The contributions of the ventral and dorsal streams to the reach to grasp task is currently a topic of debate, mainly between two models: the perception-action model suggesting the movement to be strictly a dorsal task, and the planning/control model that suggest ventral involvement during action planning. Despite the differences, both models agree that late movement control, such as target-limb control and grasping depend on processing in the dorsal stream. Target-limb control during reach has been shown to specifically activate the superior parietal occipital cortex (SPOC), while the grasp component was controlled by the anterior parietal sulcus (AIP); both of which are dorsal structures (Culham et al., 2003; Filimon et al., 2009). Evidence of ventral contribution to the early phases of the reach to grasp task was demonstrated by a study which found that the Ebbinghaus illusion influenced grasp formation. The maximum effect of the illusion was found to be approximately at 40% of the movement, with decreasing effect as the movement progressed (Glover and Dixon, 2002). As the ventral perceptual stream was also shown to be sensitive to this illusion, it was suggested that the ventral stream of processing is involved in grasp formation in the early part of the movement

(proxy measure of planning). Therefore, the current study was designed to test the hypothesis that an enhanced perceptual sensitivity to object form would be associated with enhanced grasp formation in a reach to grasp task. The results showed a significant binocular advantage for both the perceptual and reach to grasp kinematic measures; however, the main hypotheses were not supported. Therefore, the lack of association suggests that binocular cues influence each of the pathways separately, supporting independence between the ventral and dorsal streams in this context.

2.3.2 Binocular advantage as a probe for ventral-dorsal interaction

The enhancements were generated by manipulation of viewing condition, such that a binocular advantage was demonstrated for all tasks and measures. This binocular advantage was quantified as a ratio between the monocular and binocular conditions; therefore, the ratio provides information regarding the relative difference in performances between viewing conditions. Using the binocular advantage ratio as a measure of enhancement has many strengths. Firstly, it takes into account the performance under both viewing conditions using a single measure. This is essential, given the research question involves the association between the relative changes in performance during monocular and binocular viewing. Secondly, the ratio controls for individual variability between viewing conditions. Effects such as lapse in attention and learning/familiarization have a smaller influence on a ratio measure as compared to actual measures. Lastly, the ratio is not influenced by the various reach to grasp conditions (3 object size x object distance, no interaction) included in the experiment to increase difficulty and randomization. These manipulations were introduced to increase the difficulty of the task, but they were not the goal of this investigation. Finally, the binocular advantage ratio has been used extensively in previous perceptual studies to describe enhanced binocular performance, under the term *binocular summation ratio*. (Blake and Fox, 1972; Cogan, Silverman, and Sekuler, 1928; Wakayam et al., 2011). For example, visual acuity has been found to have a binocular summation ratio of 1.18 in a young visually healthy population (Gagnon and Kline, 2003), and the binocular summation ratio for contrast sensitivity ranges between 1.3 – 2.7 depending on stimulus presentation parameters (Cogan, Silverman, and Sekuler, 1982; Gagnon and Kline, 2003). To summarize, the ratio takes into account the relative enhancements

in perceptual and reach to grasp performance, and is a suitable measure for probing the ventral-dorsal interaction using the manipulation of viewing condition.

Using binocular advantage, however, does not provide information regarding how the difference in performance came to be. For example, a large ratio could be a result of 1) substantially better binocular performance with normal monocular performance or 2) normal binocular performance with substantially worse monocular performance. This would be a limitation if the aim of this study was to assess the contribution of binocular vision to the perceptual-kinematic relationship; however, this is not the case. Instead, this study uses viewing condition as a manipulation, and assess the correlation between the degree of improvement. As such, the magnitude of enhancement in perceptual and kinematic performance *between* viewing condition is significant, and not the relationship between actual measures *within* each viewing condition.

Although the findings of this study focused only on the correlation between the perceptual and kinematic binocular advantage, correlations of the actual measures within each viewing condition were also analyzed to supplement these findings. In addition to the previous listed strengths of using a binocular advantage, there are several drawbacks of correlating actual measures within each viewing condition. Firstly, the correlations between actual measures would be isolated within each viewing condition, and unable to capture the relative enhancements from the manipulation across the perceptual and kinematic tasks. As the objective of this study was to probe the interaction between ventral-dorsal streams, binocular advantage was selected as the main outcome measure. Additionally, the association of actual perceptual and kinematic measures within each viewing condition would involve 32 correlations. The number of correlations can lead to increased familywise error rate due to a multiple comparison problem, causing false positive results. Using the binocular advantage as the main outcome reduced the number of correlations in half, decreasing the probability of a familywise error rate. Given the reasons above, binocular advantage was selected as the main measure to evaluate the degree of association between ventral-perceptual and dorsal-action tasks.

2.3.3 Behavioural explanations for findings

Greater sensitivity to object form does not appear to enhance reach to grasp performance in terms of grasp aperture, or the time spent in reach deceleration and grasping. This supports the notion of limited ventral contribution in motor control of a reach to grasp task. The lack of relationship found in this study supports the perception-action model outlined by Goodale and Milner, which proposes separate visual pathways for object perception and movement control. Different neural computations are required for perception and action. For example, vision for action requires the computation of intrinsic and extrinsic properties of the object with respect to the intended hand that will be used to execute the reach to grasp movement. Specifically, the dorsal stream computes absolute size and shape of objects as well as its egocentric location for movement planning and execution (Thaler and Goodale, 2010). In contrast, visual information about objects for perceptual tasks is computed in a different way. Specifically, the ventral stream encodes size, orientation, and location of objects relative to each other using a scene-based frame of reference. This provides a perceptual representation irrespective of viewpoint that maintains size, shape, and location constancies over time and in various viewing conditions. To summarize, the dissociation between ventral and dorsal streams may lie within the difference in computations required for the perceptual and action tasks.

In addition to the differences in the type of computations required for perception and action, the method by which information is encoded is also different. Perception of object shape is done in a holistic manner such that individual dimensions cannot be isolated from other dimensions of the object (Ganel and Goodale, 2003). For example, perceptual judgement of object width is affected by its length dimension (Ganel and Goodale, 2003). Conversely, vision for action did not show this tendency as grasping was unaffected by non-relevant dimensions, such as length (Ganel and Goodale, 2003). It has been suggested that visual information processed in the dorsal stream contains only the relevant dimensions for the goal of the movement. As such, the perception in RF and MDF tasks involved the global features of the stimuli, whereas only the relevant feature of the target object (width) were encoded during the reach to grasp task. This dissociation between the features processed in the perceptual and action task may explain the lack of relationship between the binocular advantages.

With ample evidence supporting the idea of two separate visual systems, there is also research that argues against it, with one of the most notable being the planning/control model (Glover, 2004). As the perceptual and kinematic tasks in this study were designed to assess ventral-dorsal interaction, this model is important in supporting the rationale for the study. The planning/control model suggests that action tasks involve multiple stages of processing, beginning with purely perceptual to more dorsal visuomotor control as the movement develops. In this line of thought, ventral contribution would be found early in the movement (planning), and not late stages (movement control). Time in deceleration (TID) is used in this study as a proxy measure for the performance of limb-target control occurring late in the movement (Elliot et al., 2010) and time in grasping (TIG) probes the control of the grasping phase. Both of these measures occur later in the movement and reflect the quality of visually guided movement control. As such, the planning/control model would also suggest time in deceleration and grasping measures to be a function of the dorsal stream. This further provides reason why enhanced object form perception did not correlate with enhanced movement control (TID and TIG). Binocular advantages of reach to grasp planning measures, maximum grasp aperture (MGA) and scaling grasp aperture (SGA), also did not significantly correlate with perceptual binocular advantage, despite the planning/control model suggesting a ventral contribution.

2.3.4 Neurological/physiological explanation of findings

The lack of relationship between the perceptual and kinematic measures can be further explained by considering findings from neuroimaging studies. Beginning with the ventral stream, lateral occipital area (LO) within the ventrolateral part of the occipital cortex has been identified to be selectively responsive to different categories of visual stimuli (Grill-Spector et al., 1998). These categories include shapes that are defined by differences in motion (MDF), texture, or luminance contrast (RF). Additionally, area LO codes for the overall shape of the object, rather than local features (Kourtzi and Kanwisher, 2001) and is insensitive to changes in viewpoints (James et al., 2002; Valyear et al., 2006). Conversely, area LO does not contribute to the programming and online control of reach to grasp movement (Culham, 2004; Cavina-Pratesi, Goodale, and Culham, 2007). Area LO has been found to be activated non-selectively

during reach to grasp tasks, and even during scaling trials (matching grasp aperture to object size without reaching). During perceptual judgements of object size, however, LO was found to be significantly activated (Cavina-Partesi et al., 2007). These neuroimaging studies suggest that the ventral stream contributes to establishing a perceptual representation of the scene and identification of the target object, but is not essential for the planning and online control of the reach to grasp towards that target object.

Neuroimaging studies of the dorsal stream also provide support for the lack of relationship found between perceptual and kinematic enhancements found in this study. Reach to grasp planning and control has been proposed to be a function of complex interaction between the lateral intraparietal sulcus (LIP), anterior intraparietal sulcus (AIP) and superior occipital cortex/parieto-occipital sulcus (SPOC/V6A) (Goodale, 2010). LIP, AIP, and SPOC are involved in the control of voluntary saccadic eye movements, visual control of grasping, and visual control of reaching, respectively (Culham, Cavina-Pratesi, and Singhal, 2006; Filimon et al., 2009; Cavina-Pratesi et al., 2010). Additional research has found AIP to be differentially activated during visually guided reach to grasp, with no selective activation of LO; suggesting AIP and associated dorsal networks are able to program and control grasping movements independently (Cavina-Pratesi et al., 2007). Similar findings of selective activation during reach to grasp movements was found for SPOC (Filimon et al., 2009). Altogether, these findings suggest reach to grasp planning and control to be an independent dorsal process. This notion of independent ventral-perceptual and dorsal-action streams supports the lack of relationships found between the binocular advantages in perceptual and kinematic measures.

2.3.5 Interpretation of unexpected findings

Although statistically insignificant, it is important to note that a moderate strength negative relationship was found between the RF threshold and MGA ($r=-0.36$, $p=0.053$), and MDF JND and SGA ($r=-0.37$, $p=0.075$). These negative correlations go against the hypotheses, and were unexpected as they suggest greater enhancements in perceptual sensitivity to be associated with smaller enhancements in reach to grasp planning. On one hand, these findings could be a result of performing multiple correlation tests, as the significance decreases when

controlling for the familywise-error rate using the Holm-Bonferroni method (Holm, 1979). The inclusion of participants who did not demonstrate a binocular advantage in the perceptual tasks for the correlation could have added noise, contributing to the lack of association. On the other hand, there could be an underlining mechanism to offer a logical explanation. To provide clarity for these questions, the following section will delve into the neural mechanisms involved with the RF, MDF, and grasp formation to highlight possible areas of interaction.

fMRI evidence suggests the control of grasping is mediated by the dorsal stream under binocular vision without any additional activity from ventral stream areas during binocular viewing (Verhagen et al., 2008). Conversely, ventral stream (V4, LO) contributes to the control of grasping during monocular viewing due to the increased reliance on pictorial cues (Verhagen et al., 2008). As both shape perception and monocular grasping elicit activation of ventral stream structures V4 and LO, the common neural structures provide a physiological basis for a possible association between the two tasks during monocular viewing.

Formation of grasp during monocular viewing is reliant on perception of pictorial cues through ventral stream structures; therefore, it is possible that the formation of grasp to be more optimal (more scaled to the size of the object) for those with greater sensitivity (lower threshold) during monocular viewing. Better monocular performance in grasp formation would decrease the difference in the maximum grasp aperture measures between the two viewing conditions, subsequently decreasing the binocular advantage ratio. In essence, the finding that enhanced perception is associated with decreased enhancement in maximum/scaling grasp aperture could be a result of better monocular grasp formation causing a smaller binocular advantage ratio. Support for this explanation would be require a positive association between monocular threshold and maximum/scaling grasp aperture. In contrast to this prediction, experimental results did not show a significant positive association between perceptual sensitivity and grasp scaling in the monocular condition.

An alternative explanation for the peculiar findings could be that there is an optimal perceptual sensitivity for the control of grasp formation. Deviations from this optimal condition would elicit detriments to the control of grasp formation. This idea is purely a speculation

based on a “tele-assistance” model developed by Goodale and Humphrey (1998) to explain ventral-dorsal interaction. According to this model, the ventral stream processes detailed representation of the visual scene to identify the target object and decide on how to interact with it, resembling an attention-like process (Goodale and Humphrey, 1998). Once the target object has been flagged, visuomotor networks in the dorsal stream are engaged to transform the visual information into appropriate coordinates for motor action (Goodale and Humphrey, 1998). These processes ultimately occur in parallel, each using visual information for different purposes. In the context of this model, higher perceptual sensitivity to object shape may cause information that is more detailed than required to be encoded, which may complicate the transformation of the visual information to the appropriate coordinates for action. Conversely, lower perceptual sensitivity may cause a lack of detail in the encoded information, which will also negatively influence the transformation into action. As such, an optimal perceptual sensitivity may exist that encodes the visual scene with just the right level of detail. It is important to note that no evidence of this computational mechanism exists in previous literature, as this is strictly speculation to perhaps explore with future research.

2.3.6 Alternative conclusions for lack of perceptual-reach to grasp association

The lack of association between the perceptual and reach to grasp performance does not provide definitive evidence of independence between the ventral and dorsal stream of processing. Alternative explanations for this lack of association can be that the methods were not sensitive enough to detect an interaction due to limitations in the binocular advantage ratio measure and data analysis. Binocular advantage ratios result from multiple levels of data processing; therefore, do not capture a detailed representation of the raw data. This provides an opportunity for certain aspects of the data to be unreported. For example, a binocular advantage ratio above 1 were not demonstrated by four participants on the RF and seven participants on MDF tasks. These ratios do not provide insight on the reasons why certain participants did not demonstrate a binocular advantage. Moreover, correlating participants that did not demonstrate a perceptual binocular advantage with binocular advantages in reach to grasp creates noise in the data, which can potentially mask possible associations.

Categorizing participants into two groups: one for those that demonstrate binocular advantage in both tasks and one for those who do not would ensure that enhancements in perceptual performance is indeed being associated with enhancement in reach to grasp performance. As such, the lack of relationship between the perceptual and reach to grasp performance can be attributed to the limitations of the study instead of being evidence for independent ventral and dorsal streams of processing.

2.3.7 Auxiliary finding

When analyzing the association between perceptual and kinematic measures within each viewing condition, a statistically significant association was found between the performance on the MDF task and maximum grasp aperture (appendix 16). This indicates that greater perceptual sensitivity to object form is associated with a more accurate and precise scaling of maximum grasp aperture, and that this is consistent across viewing conditions. It is important to note this finding is auxiliary, given the objective of this study was to probe the association between enhancements in perceptual and reach to grasp performance during binocular viewing. It was not the objective of the study to establish the differences in the perceptual-kinematic relationship within each viewing condition. As no association was found between the binocular advantages of the MDF and reach to grasp task, the enhancements in the two tasks appear to be independent. Although out of the scope of this study, the positive relationship between perceptual sensitivity and maximum grasp aperture provide some insight and indication of a ventral-dorsal interaction.

2.3.8 Limitations

There are several limitations to this study with the main one being the discrepancy between the shapes used as the target stimuli in the perceptual task and the target object used in the reach to grasp task. Although the RF has been used as a measure for shape perception, it more specifically tests for curvature perception. MDF specifically tests for shape perception through the perception of moving dots. As neither curvature or moving dots were involved during the performance of the reach to grasp task, it becomes a limitation when an association is to be made between the performance on the different tasks. Despite this, it is important to

note that there are limited methods in measuring perceptual sensitivity to 3D object shape. Both RF and MDF stimuli were selected based on the extensive literature suggesting that performance on both tasks provides a measure of shape perception (Giaschi et al., 1997; Wilkinson et al., 1998). Additionally, both of these tests have shown to be sensitive to viewing condition manipulation, which is essential given that the study design was to associate binocular advantages in perception and reach to grasp.

Additional limitations of this study may be the effect of practice and lapse in attention. The experimental design required a total of 234 kinematic trials, and 480 perceptual trials across the two viewing conditions. Randomization of object size and distance was implemented to control for practice effect in the reach to grasp and scaling trials. The random insertion of scaling trials among the reach to grasp trials was implemented to maintain participant attention. Additionally, the implementation of an unstable target object surface increased task difficulty and novelty, which also served as a method of maintaining participant attention. The only control for maintaining participant attention during the psychophysical testing was verbal motivation and monitoring for attentiveness performed by the researcher. The conversion of measures into binocular advantages provided some control for practice and attentional affects, assuming they influence performance in either viewing conditions equally.

As mentioned in previous sections, the use of binocular ratio is an oversimplification of the quantification of enhancement in performance. It does not provide information as to how the enhancement was generated; it simply highlights the difference in performance between binocular and monocular viewing conditions. This drawback, however, can be controlled for by investigating the perceptual-kinematic correlation within each viewing condition. Doing so provides background information on how the binocular advantage was achieved.

2.3.9 Future research direction

The correlation of performance between perceptual and reach to grasp performance is a novel approach to probe the interaction between the ventral and dorsal streams of visual processing. Future research should incorporate perceptual measurements of 3D objects that are more similar to the target object in the reach to grasp task. This will facilitate a more direct

comparison of perceptual and kinematic performance. Virtual reality can be used to measure sensitivity to 3D shapes to facilitate a more direct comparison. Alternatively, an experimental design that includes an amalgamation of both perceptual and reach to grasp task can also decrease the gap between the perceptual reach to grasp tasks. For example, a task where participants are presented with two slightly different sized objects and asked to reach to grasp the smaller one includes both a perceptual and action component. Additionally, the results of this study identified several participants who did not demonstrate a binocular advantage in the perceptual tasks. Further investigation on reasons why this occurred can potentially provide guidance for future studies using these techniques, as well as identify factors that influence sensitivity to object form. The implementation of force transducers on the target object will allow a more direct measure of time in grasping than the method used in this study. Information regarding the forces and points of contact during the grasp will allow insight into the contribution of the ventral perceptual system on grasping. Together, more translatable perceptual stimuli, information on movement corrective strategies, and direct measurement of the grasping component can provide a deeper understanding of perceptual influence at various components of the reach to grasp task. Doing so will further the understanding of the ventral-dorsal relationship.

2.4 Conclusion

This study was able to replicate the binocular advantages in the perceptual RF and MDF tasks, as well as in the selected kinematic measures of the reach to grasp task. No significant associations were found between the binocular advantages found in the perceptual and reach to grasp tasks. This potentially supports the notion of separate ventral stream for perception and dorsal stream for action, suggesting independent processing of binocular information to guide perception and action. An alternative explanation for this lack of relationship could be the limitations in the binocular advantage ratio measure and data analysis approach used in this study. It is possible that the probe utilized in this study was not sensitive enough to investigate the ventral-dorsal interaction entirely. As such, it is important to note the limitations when discussing its support for independent ventral and dorsal streams. Despite this, the potential finding not only benefits our current understanding of visuomotor planning and control, but

also provides insight towards the debated topic of ventral-dorsal interaction. Furthermore, knowledge about ventral and dorsal processing streams has implications for clinical and ergonomics applications. For instance, patients with abnormal binocular vision often have concurrent deficits in perception and goal directed action. The notion of independent binocular processing in the ventral and dorsal streams suggests that the deficits in perception and action should be assessed and treated separately. Results from the current study may also have implications in the field of ergonomics. Specifically, improved understanding of ventral-dorsal interaction can provide guidance in workstation and tool designs. For example, the notion that enhanced perceptual performance does not associate with enhanced reach to grasp performance suggests that separate design principles for perceptual and action tasks are needed. In conclusion, the lack of association in a binocular advantage between perceptual sensitivity to object shape and the performance kinematics of a reach to grasp task provides insight into the extent of ventral-dorsal interactions, and may inform future research directions, as well as clinical and occupational applications.

References

- Ahissar, E., Arieli, A., Fried, M., & Bonneh, Y. (2016). On the possible roles of microsaccades and drifts in visual perception. *Vision Research*, *118*, 25–30. <https://doi.org/10.1016/j.visres.2014.12.004>
- Altman DG, Bland JM. Statistics notes: the normal distribution. *BMJ*. 1995;310(6975):298.
- Andersen, R. A., & Buneo, C. A. (2003). Sensorimotor integration in posterior parietal cortex. *Advances in Neurology*, *93*, 159–177.
- Bae, S., Choi, J., & Armstrong, T. J. (2008). Influence of object properties on reaching and grasping tasks. In *Digital Human Modeling for Design and Engineering Conference and Exhibition* DOI: 10.4271/2008-01-1905
- Bédard, P., Wu, M., & Sanes, J. N. (2011). Brain activation related to combinations of gaze position, visual input, and goal-directed hand movements. *Cerebral Cortex*, *21*(6), 1273–1282. <https://doi.org/10.1093/cercor/bhq205>
- Bell, J., Badcock, D. R., Wilson, H., & Wilkinson, F. (2007). Detection of shape in radial frequency contours: Independence of local and global form information. *Vision Research*, *47*(11), 1518–1522. <https://doi.org/10.1016/j.visres.2007.01.006>
- Binsted, G., Chua, R., Helsen, W., & Elliott, D. (2001). Eye -hand coordination in goal-directed aiming. *Human Movement Science*, *20*, 563–585.
- Blake, R., & Fox, R. (1973). The psychophysical inquiry into binocular summation. *Perception & Psychophysics*, *14*(1), 161–185. <https://doi.org/10.3758/BF03198631>
- Blake, R., & Sekuler, R. (2006) *Perception* (5th ed.). New York, NY: McGraw-Hill.
- Bootsma, R. J., Marteniuk, R. G., MacKenzie, C. L., & Zaal, F. T. J. M. (1994). The speed-accuracy trade-off in manual prehension: effects of movement amplitude, object size and object width on kinematic characteristics. *Experimental Brain Research*, *98*(3), 535–541. <https://doi.org/10.1007/BF00233990>
- Borghia, A. M., & Riggio, L. (2015). Stable and variable affordances are both automatic and flexible. *Frontiers in Human Neuroscience*, *9*(June), 1–16. <https://doi.org/10.3389/fnhum.2015.00351>
- Borra, E., Ichinohe, N., Sato, T., Tanifuji, M., & Rockland, K. S. (2010). Cortical connections to area TE in monkey: Hybrid modular and distributed organization. *Cerebral Cortex*, *20*(2), 257–270. <https://doi.org/10.1093/cercor/bhp096>

- Bozzacchi, C., Giusti, M. A., Pitzalis, S., Spinelli, D., & Di Russo, F. (2012). Awareness affects motor planning for goal-oriented actions. *Biological Psychology*, *89*(2), 503–514. <https://doi.org/10.1016/j.biopsycho.2011.12.020>
- Brochier, T., Spinks, R. L., Umiltà, M. A., & Lemon, R. N. (2004). Patterns of muscle activity underlying object-specific grasp by the macaque monkey. *Journal of Neurophysiology*, *92*(3), 1770–82. <https://doi.org/10.1152/jn.00976.2003>
- Braddick O., Campbell F.W., Atkinson J. (1978) Channels in Vision: Basic Aspects. In: Held R., Leibowitz H.W., Teuber HL. (eds) Perception. Handbook of Sensory Physiology, vol 8. Springer, Berlin, Heidelberg
- Campbell, F. W. & Green, D. G. (1965). Monocular versus binocular visual acuity. *Nature*, *208*, 191-192.
- Cant, J. S., Large, M. E., McCall, L., & Goodale, M. A. (2008). Independent processing of form, colour, and texture in object perception. *Perception*, *37*(1), 57–78. <https://doi.org/10.1068/p5727>
- Castiello, U., Bennett, K. M. B., & Paulignan, Y. (1992). Does the type of prehension influence the kinematics of reaching. *Behavioural Brain Research*, *50*(1–2), 7–15. [https://doi.org/10.1016/S0166-4328\(05\)80283-9](https://doi.org/10.1016/S0166-4328(05)80283-9)
- Cavina-Pratesi, C., Goodale, M. A., & Culham, J. C. (2007). fMRI reveals a dissociation between grasping and perceiving the size of real 3D objects. *PLOS One*, *2*, e424.
- Cavina-Pratesi, C., Letswaart, M., Humphreys, G. W., Lestou, V., & Milner, A. D. (2010). Impaired grasping in a patient with optic ataxia: Primary visuomotor deficit or secondary consequence of misreaching. *Neuropsychologia*, *48*, 226–234.
- Churchill, A., Hopkins, B., Rönqvist, L., & Vogt, S. (2000). Vision of the hand and environmental context in human prehension. *Experimental Brain Research*, *134*(1), 81–89. <https://doi.org/10.1007/s002210000444>
- Cloutman, L. L. (2013). Interaction between dorsal and ventral processing streams: Where, when and how? *Brain and Language*, *127*(2), 251–263. <https://doi.org/10.1016/j.bandl.2012.08.003>
- Cogan, A. I., Silverman, G., & Sekuler, R. (1982). Binocular summation in detection of contrast flashes. *Perception & Psychophysics*, *31*(4), 330–338. <https://doi.org/10.3758/BF03202656>
- Cohen, R., & Rosenbaum, D. (2004). Where grasps are made reveals how grasps are planned: generation and recall of motor plans. *Experimental Brain Research*, *157*(2004), 486–495. <https://doi.org/10.1007/s00221-004-1862-9>

- Culham, J. C. (2004). Human brain imaging reveals a parietal area specialized for grasping. In N. Kanwisher & J. Duncan (Eds.), *Attention and performance XX: Functional brain imaging of human cognition*. Oxford: Oxford University Press (pp. 417–438).
- Culham, J. C., Cavina-Pratesi, C., & Singhal, A. (2006). The role of parietal cortex in visuomotor control: What have we learned from neuroimaging?. *Neuropsychologia*, 44, 2668–2684.
- Culham, J. C., Danckert, S. L., DeSouza, J. F. X., Gati, J. S., Menon, R. S., & Goodale, M. A. (2003). Visually guided grasping produces fMRI activation in dorsal but not ventral stream brain areas. *Experimental Brain Research*, 153(2), 180–189. <https://doi.org/10.1007/s00221-003-1591-5>
- Doll, R. J., Buitenweg, J. R., Meijer, H. G. E., & Veltink, P. H. (2014). Tracking of nociceptive thresholds using adaptive psychophysical methods. *Behavior Research Methods*, 46(1), 55–66. <https://doi.org/10.3758/s13428-013-0368-4>
- Elliott, D., Hansen, S., Grierson, L. E. M., Lyons, J., Bennett, S. J., & Hayes, S. J. (2010). Goal-directed aiming: two components but multiple processes. *Psychological Bulletin*, 136(6), 1023–1044. <https://doi.org/10.1037/a0020958>
- Elliott, D., Welsh, T. N., Lyons, J., Hansen, S., and Wu, M. (2006). The visual regulation of goal-directed reaching movements in adults with Williams syndrome, Down syndrome, and other developmental delays. *Motor Control*, 10, 34–54.
- Elliott AC, Woodward WA. *Statistical analysis quick reference guidebook with SPSS examples*. 1st ed. London: Sage Publications; 2007
- Feix, T., Bullock, I. M., & Dollar, A. M. (2014). Analysis of human grasping behavior: Correlating tasks, objects and grasps. *IEEE Transactions on Haptics*, 7(4), 430–441. <https://doi.org/10.1109/TOH.2014.2326867>
- Field A. *Discovering statistics using SPSS*. 3 ed. London: SAGE publications Ltd; 2009. p. 822.
- Filimon, F., Nelson, J. D., Huang, R. S., & Sereno, M. I. (2009). Multiple parietal reach regions in humans: Cortical representations for visual and proprioceptive feedback during on-line reaching. *Journal of Neuroscience*, 29, 2961–2971.
- Fisk, J. D., & Goodale, M. A. (1985). The organization of eye and limb movements during unrestricted reaching to targets in contralateral and ipsilateral visual space. *Experimental Brain Research*, 60(1), 159–178. <https://doi.org/10.1007/BF00237028>

- Flatters, I. J., Otten, L., Witvliet, A., Henson, B., Holt, R. J., Culmer, P., Mon-Williams, M. (2012). Predicting the effect of surface texture on the qualitative form of prehension. *PLOS ONE*, 7(3). <https://doi.org/10.1371/journal.pone.0032770>
- Foley, R. T., Whitwell, R. L., & Goodale, M. A. (2015). The two-visual-systems hypothesis and the perspectival features of visual experience. *Consciousness and Cognition*, 35, 225–233. <https://doi.org/10.1016/j.concog.2015.03.005>
- Fourkas, A. D., Marteniuk, R. G., & Khan, M. A. (2003). Guiding movements with internal representations: a reach-and-grasp task. *Research Quarterly for Exercise and Sport*, 74(2), 165–172. <https://doi.org/10.1080/02701367.2003.10609078>
- Freud, E., Plaut, D. C., & Behrmann, M. (2016). “What” Is Happening in the Dorsal Visual Pathway. *Trends in Cognitive Sciences*, 20(10), 773–784. <https://doi.org/10.1016/j.tics.2016.08.003>
- Frings, C., & Spence, C. (2013). Gestalt grouping effects on tactile information processing: when touching hands override spatial proximity. *Attention, Perception & Psychophysics*, 75(3), 468–80. <https://doi.org/10.3758/s13414-012-0417-6>
- Fukui, T., & Inui, T. (2013). Utilization of visual feedback of the hand according to target view availability in the online control of prehension movements. *Human Movement Science*, 32(4), 580–595. <https://doi.org/10.1016/j.humov.2013.03.004>
- Fukui, T., & Inui, T. (2015). Use of early phase online vision for grip configuration is modulated according to movement duration in prehension. *Experimental Brain Research*, 233(8), 2257–2268. <https://doi.org/10.1007/s00221-015-4295-8>
- Gagnon, R. W. C., & Kline, D. W. (2003). Senescent effects on binocular summation for contrast sensitivity and spatial interval acuity. *Current Eye Research*, 27(5), 315–21. <https://doi.org/10.1076/ceyr.27.5.315.17225>
- Gallivan, J.P. et al. (2013) Activity patterns in the category selective occipitotemporal cortex predict upcoming motor actions. *European Journal Neuroscience*. 38, 2408–242423
- Ganel, T., & Goodale, M. A. (2003). Visual control of action but not perception requires analytical processing of object shape. *Nature*, 426, 664–667.
- Giaschi, D. E., Regan, D., Kraft, S. P., & Hong, X. H. (1992). Defective processing of motion-defined form in the fellow eye of patients with unilateral amblyopia. *Investigative Ophthalmology and Visual Science*, 33(8), 2483–2489.
- Gillebert, C.R. et al. (2015) 3D shape perception in posterior cortical atrophy: a visual neuroscience perspective. *Journal of Neuroscience*. 35, 12673–12692

- Glazebrook, C., Gonzalez, D. A., Hansen, S., and Elliot, D. (2009). The role of vision for online control of manual aiming movements in persons with autism spectrum disorders. *Autism*, 13, 411–433. doi: 10.1177/1362361309105659
- Glover, S., & Dixon, P. (2002). Dynamic effects of the Ebbinghaus illusion in grasping: Support for a planning/control model of action. *Perception & Psychophysics*, 64, 266–278.
- Glover, S. (2004). Separate visual representations in the planning and control of action. *Behavioural and Brain Sciences*, 27, 3–24.
- Gnanaseelan, R., Gonzalez, D. a., & Niechwiej-Szwedo, E. (2014). Binocular advantage for prehension movements performed in visually enriched environments requiring visual search. *Frontiers in Human Neuroscience*, 8(November), 1–11. <https://doi.org/10.3389/fnhum.2014.00959>
- Gogel, W. C. (1961). Convergence as a cue to the perceived distance of objects in a binocular configuration. *The Journal of Psychology*, 52, 303–315. <https://doi.org/10.1080/00223980.1961.9916530>
- Goodale, M. A. (2011). Transforming vision into action. *Vision Research*, 51(13), 1567–1587. <https://doi.org/10.1016/j.visres.2010.07.027>
- Goodale, M. A., & Haffenden, A. M. (2003). Interactions between dorsal and ventral streams of visual processing. In A. Siegel, R. Andersen, H.-J. Freund, & D. Spencer (Eds.), *Advances in neurology: The parietal lobe* (Vol. 93, pp. 249–267). Philadelphia: Lippincott-Raven.
- Goodale, M. A., & Humphrey, G. K. (1998). The objects of action and perception. *Cognition*, 67, 179–205.
- Goodale, A., & Jakobson, S. (1992). The Role of Binocular a Kinematic Analysis. *Vision Research*, 32(8), 1513–1521.
- Goodale, M. A., & Milner, A. D. (1992). Separate visual pathways for perception and action. *Trends in Neurosciences*, 15(1), 20–25. [https://doi.org/https://doi.org/10.1016/0166-2236\(92\)90344-8](https://doi.org/https://doi.org/10.1016/0166-2236(92)90344-8)
- Goodale, M. a, Meenan, J. P., Heinrich, H., Nicolle, D. A., Murphy, K. J., & Racicot, C. I. (1994). Separate neural pathways for the visual analysis of object shape in perception and prehension. *Current Biology*, 4(7), 604–610.
- Gorbet, D. J., Wilkinson, F., & Wilson, H. R. (2014). Neural correlates of radial frequency trajectory perception in the human brain. *Journal of Vision*, 14(1), 1–19. <https://doi.org/10.1167/14.1.11>

- Grafton, S. T. (2010). The cognitive neuroscience of prehension: Recent developments. *Experimental Brain Research*, 204(4), 475–491. <https://doi.org/10.1007/s00221-010-2315-2>
- Grierson, L. E. M., & Elliott, D. (2008). Kinematic analysis of goal-directed aims made against early and late perturbations: An investigation of the relative influence of two online control processes. *Human Movement Science*, 27(6), 839–856. <https://doi.org/10.1016/j.humov.2008.06.001>
- Grill-Spector, K. (2003). The neural basis of object perception. *Current Opinion in Neurobiology*, 13, 159-166
- Grill-Spector K., Kushnir T., Edelman S., Avidan G., Itzchak Y., & Malach R. (1999). Differential processing of objects under various viewing conditions in the human lateral occipital complex. *Neuron*, 24, 187-203
- Hayward, J., Truong, G., Partanen, M., & Giaschi, D. (2011). Effects of speed, age, and amblyopia on the perception of motion-defined form. *Vision Research*, 51(20), 2216–2223. <https://doi.org/10.1016/j.visres.2011.08.023>
- Holm S. (1979). A simple sequentially rejective multiple test procedure. *Scandinavian Journal of Statistics*, 6 (2): 65-70. JSTOR 4615733 MR 538597
- Intraub, H., Morelli, F., & Gagnier, K. M. (2015). Visual, haptic and bimodal scene perception: Evidence for a unitary representation. *Cognition*, 138, 132–147. <https://doi.org/10.1016/j.cognition.2015.01.010>
- James, T.W. et al. (2003) Ventral occipital lesions impair object recognition but not object-directed grasping: an fMRI study. *Brain*, 126, 2463–2475
- Jackson, S. R., Jones, C. a., Newport, R., & Pritchard, C. (1997). A Kinematic Analysis of Goal-directed Prehension Movements Executed under Binocular, Monocular, and Memory-guided Viewing Conditions. *Visual Cognition*, 4(2), 113–142. <https://doi.org/10.1080/713756755>
- Johnson-Frey, S. H., McCarty, M., & Keen, R. (2004). Reaching beyond spatial perception: Effects of intended future actions on visually guided prehension. *Visual Cognition*, 11(2–3), 371–399. <https://doi.org/10.1080/13506280344000329>
- Frey, S., Rotte, M., Kanowski, M., Gazzaniga, M., & Heinze, H.-J. (2000). Temporal relationships among areas involved in planning prehension of visual objects: An event-related fMRI experiment. *Neuroimage*, 11. [https://doi.org/10.1016/S1053-8119\(00\)91832-9](https://doi.org/10.1016/S1053-8119(00)91832-9)

- Kable, J. W., Kan, I. P., Wilson, A., Thompson-Schill, S. L., & Chatterjee, A. (2005). Conceptual representations of action in the lateral temporal cortex. *Journal of Cognitive Neuroscience*, 17, 1855–1870. <https://doi.org/10.1162/089892905775008625>
- Karl, J. M., Schneider, L. R., & Whishaw, I. Q. (2013). Nonvisual learning of intrinsic object properties in a reaching task dissociates grasp from reach. *Experimental Brain Research*, 225(4), 465–477. <https://doi.org/10.1007/s00221-012-3386-z>
- Kawato, M. (1999). Internal models for motor control and trajectory planning. *Current Opinion in Neurobiology*, 9(6), 718–727. [https://doi.org/10.1016/S0959-4388\(99\)00028-8](https://doi.org/10.1016/S0959-4388(99)00028-8)
- Keefe, B. D., Hibbard, P. B., & Watt, S. J. (2011). Depth-cue integration in grasp programming: No evidence for a binocular specialism. *Neuropsychologia*, 49(5), 1246–1257. <https://doi.org/10.1016/j.neuropsychologia.2011.02.047>
- Klein, S. A. (2001). Measuring, estimating, and understanding the psychometric function: a commentary. *Perception & Psychophysics*, 63(8), 1421–55. <https://doi.org/10.3758/BF03194552>
- Kopecz, K., & Schöner, G. (1995). Saccadic motor planning by integrating visual information and pre-information on neural dynamic fields. *Biological Cybernetics*, 73(1), 49–60. <https://doi.org/10.1007/BF00199055>
- Korneev, A. A., & Kurganskii, A. V. (2014). Internal representation of movement sequences on reproduction of static drawings and the trajectories of moving objects. *Neuroscience and Behavioral Physiology*, 44(8), 892–901. <https://doi.org/10.1007/s11055-014-9998-y>
- Kourtzi Z., & Kanwisher N. (2001). Representation of perceived object shape by human lateral occipital complex. *Science*, 293, 1506-1509
- Krakauer, J. W., Latash, M. L., & Zatsiorsky, V. M. (2009). Progress in Motor Control. *Learning*, 629(585), 597–618. <https://doi.org/10.1007/978-0-387-77064-2>
- Kravitz, D.J. et al. (2011) A new neural framework for visuospatial processing. *Nature Reviews Neuroscience*. 12, 217–230
- Kudoh, N., Hattori, M., Numata, N., & Maruyama, K. (1997). An analysis of spatiotemporal variability during prehension movements: Effects of object size and distance. *Experimental Brain Research*, 117(3), 457–464. <https://doi.org/10.1007/s002210050241>
- Lestou, V. et al. (2014) A dorsal visual route necessary for global form perception: evidence from neuropsychological fMRI. *J. Cogn. Neurosci.* 26, 621–634

- Loftus, A., Servos, P., Goodale, M. A., Mendarozqueta, N., & Mon-Williams, M. (2004). When two eyes are better than one in prehension: Monocular viewing and end-point variance. *Experimental Brain Research*, 158(3), 317–327. <https://doi.org/10.1007/s00221-004-1905-2>
- Mahon, B. Z., Milleville, S. C., Negri, G. A. L., Rumiati, R. I., Caramazza, A., & Martin, A. (2007). Action-related properties shape object representations in the ventral stream. *Neuron*, 55(3), 507–520. <https://doi.org/10.1016/j.neuron.2007.07.011>
- Marotta, J. J., Kruyer, A., & Goodale, M. A. (1998). The role of head movements in the control of manual prehension. *Experimental Brain Research*, 120, 134–138.
- Martinez-Conde, S., Macknik, S. L., & Hubel, D. H. (2004). The role of fixational eye movements in visual perception. *Nature Reviews Neuroscience*, 5(3), 229–240
- Marteniuk, R. G., Leavitt, J. L., MacKenzie, C. L., & Athenes, S. (1990). Functional relationships between grasp and transport components in a prehension task. *Human Movement Science*, 9(2), 149–176. [https://doi.org/10.1016/0167-9457\(90\)90025-9](https://doi.org/10.1016/0167-9457(90)90025-9)
- Maule, A. J. (1985). The importance of an updating internal representation of the environment in the control of visual sampling. *The Quarterly Journal of Experimental Psychology. A, Human Experimental Psychology*, 37(4), 533–551. <https://doi.org/10.1080/14640748508400918>
- Melmoth, D. R., & Grant, S. (2006). Advantages of binocular vision for the control of reaching and grasping. *Experimental Brain Research*, 171(3), 371–388. <https://doi.org/10.1007/s00221-005-0273-x>
- Melmoth, D. R., Storoni, M., Todd, G., Finlay, A. L., & Grant, S. (2007). Dissociation between vergence and binocular disparity cues in the control of prehension. *Experimental Brain Research*, 183, 283–298.
- Miller, R.G. (1981). *Simultaneous statistical inference* (2nd Ed). New York: Springer Verla. ISBN 0-387-90548-0
- Monaco, S., Sedda, A., Cavina-Pratesi, C., & Culham, J. C. (2015). Neural correlates of object size and object location during grasping actions. *European Journal of Neuroscience*, 41(4), 454–465. <https://doi.org/10.1111/ejn.12786>
- Mon-Williams, M., & Dijkerman, H. C. (1999). The use of vergence information in the programming of prehension. *Experimental Brain Research*, 128(4), 578–582. <https://doi.org/10.1007/s002210050885>

- Movshon, J. A., Adelson, E. H., Gizzi, M. S., & Newsome, W. T. (1985). The analysis of moving visual patterns. *Pattern Recognition Mechanisms*, 117–151.
<https://doi.org/10.1098/rstb.1998.0333>
- Murphy, A. P., Leopold, D. A., Humphreys, G. W., & Welchman, A. E. (2016). Lesions to right posterior parietal cortex impair visual depth perception from disparity but not motion cues. *Philosophical Transactions of the Royal Society B: Biological Sciences*, 371(1697), 20150263. <https://doi.org/10.1098/rstb.2015.0263>
- Olweny, E. O., Mir, S. A., Best, S. L., Park, S. K., Donnally, C., Cadeddu, J. A., & Tracy, C. R. (2012). Importance of cosmesis to patients undergoing renal surgery: A comparison of laparoendoscopic single-site (LESS), laparoscopic and open surgery. *BJU International*, 110(2), 268–272. <https://doi.org/10.1111/j.1464-410X.2011.10784.x>
- Oztuna D, Elhan AH, Tuccar E. Investigation of four different normality tests in terms of type 1 error rate and power under different distributions. *Turkish Journal of Medical Sciences*. 2006;36(3):171–6.
- Pallant, J. (2007). *SPSS survival manual: a step by step guide to data analysis using SPSS for Windows*. Maidenhead: Open University Press.
- Paulignan, Y., Frak, V. G., Toni, I., & Jeannerod, M. (1997). Influence of object position and size on human prehension movements. *Experimental Brain Research*, 114(2), 226–34.
<https://doi.org/10.1007/PL00005631>
- Rainville, S. J. M., & Wilson, H. R. (2004). The influence of motion-defined form on the perception of spatially-defined form. *Vision Research*, 44(11), 1065–1077.
<https://doi.org/10.1016/j.visres.2004.01.003>
- Read, J. C. A., Begum, S. F., McDonald, A., & Trowbridge, J. (2013). The binocular advantage in visuomotor tasks involving tools. *I-Perception*, 4(2), 101–110.
<https://doi.org/10.1068/i0565>
- Regan D, Beverley KI (1983) Spatial frequency detection and discrimination: comparison of post-adaption thresholds. *Journal of Optical Society*, 73, 1684-1690.
- Regan, D., Giaschi, D., Sharpe, J. a, & Hong, X. H. (1992). Visual processing of motion-defined form: selective failure in patients with parietotemporal lesions. *The Journal of Neuroscience*, 12(6), 2198–2210.
- Rosenbaum, D. A., Chapman, K. M., Weigelt, M., Weiss, D. J., & van der Wel, R. (2012). Cognition, action, and object manipulation. *Psychological Bulletin*, 138(5), 924–946.
<https://doi.org/10.1037/a0027839>

- Roth, Z.N. and Zohary, E. (2015) Position and identity information available in fMRI patterns of activity in human visual cortex. *Journal of Neuroscience*. 35, 11559–11571
- Ruddock, K. H. (1975). Visual form perception. *Contemporary Physics*, 16(4), 317–348.
<https://doi.org/10.1080/00107517508210817>
- Sakata, H., Saltzman, H., & Zachar (2003). The role of the parietal cortex in grasping. *Advances in Neurology*, 93, 121–139.
- Salmela, V. R., Henriksson, L., & Vanni, S. (2016). Radial Frequency Analysis of Contour Shapes in the Visual Cortex. *PLOS Computational Biology*, 12(2), 1–18.
<https://doi.org/10.1371/journal.pcbi.1004719>
- Saunders, J. a., & Knill, D. C. (2005). Humans use continuous visual feedback from the hand to control both the direction and distance of pointing movements. *Experimental Brain Research*, 162(4), 458–473. <https://doi.org/10.1007/s00221-004-2064-1>
- Saxena, A., Schulte, J., & Andrew, Y. (2007). Depth estimation using monocular and stereo cues. *Proceedings of the 20th International Joint Conference on Artificial Intelligence*, 2197–2203.
- Schall, J. D., & Thompson, K. G. (1999). Neural selection and control of visually guided eye movements [In Process Citation]. *Annual Review of Neuroscience*, 22:241-59, 241–259.
<https://doi.org/10.1146/annurev.neuro.22.1.241>
- Scott, S.H. (2012) The computational and neural basis of voluntary motor control and planning. *Trends in Cognitive Science*, 16, 541-549.
[doi:10.1016/j.tics.2012.09.008](https://doi.org/10.1016/j.tics.2012.09.008), [pmid:23031541](https://pubmed.ncbi.nlm.nih.gov/23031541/)
- Seegelke, C., & Hughes, C. M. L. (2015). The influence of action possibility and end-state comfort on motor imagery of manual action sequences. *Brain and Cognition*, 101, 12–16.
<https://doi.org/10.1016/j.bandc.2015.10.006>
- Servos, P., & Goodale, M. a. (1994). Binocular vision and the on-line control of human prehension. *Experimental Brain Research*. 98(1), 119–27.
- Smeets, J. B., & Brenner, E. (1999). A new view on grasping. *Motor Control*, 3(3), 237–271.
- Snyder, A. N., Bockbrader, M. a, Hoffa, A. M., Dziedzic, M. a, Talavage, T. M., Wong, D., Shekhar, A. (2011). Psychometrically matched tasks evaluating differential fMRI activation during form and motion processing. *Neuropsychology*, 25(5), 622–633.
<https://doi.org/10.1037/a0022984>

- Sober, S. J., & Sabes, P. N. (2003). Multisensory integration during motor planning. *Journal of Neuroscience*, 23(18), 6982–6992. <https://doi.org/citeulike-article-id:409345>
- Steeves, J. K. E., Wilkinson, F., González, E. G., Wilson, H. R., & Steinbach, M. J. (2004). Global shape discrimination at reduced contrast in enucleated observers. *Vision Research*, 44(9), 943–949. <https://doi.org/10.1016/j.visres.2003.11.015>
- Steinman SB., Steinman BA., & Garzia RP. (2000). *Foundations of binocular vision: a clinical perspective*. New York: McGraw-Hill. 153-160 ISBN 0-8385-2670-5
- Stepniewska, I. et al. (2016) Cortical connections of the caudal portion of posterior parietal cortex in prosimian galagos. *Cerebral Cortex*, 26, 2753–2777
- Strasburger, H. (2001). Converting between measures of slope of the psychometric function. *Perception & Psychophysics*, 63(8), 1348–1355. <https://doi.org/10.3758/BF03194547>
- Tanaka K, Hikosaka K, Saito Y (1986) Analysis of local and widefield movements in the superior temporal visual areas of the macaque monkey. *Journal of Neuroscience*, 6, 134-144.
- Thaler, L., & Goodale, M. A. (2010). Beyond distance and direction: The brain represents target locations non-metrically. *Journal of Vision*, 10, 1–27.
- Tremblay, L., Crainic, V. A., de Grosbois, J., Bhattacharjee, A., Kennedy, A., Hansen, S., & Welsh, T. N. (2016). An optimal velocity for online limb-target regulation processes. *Experimental Brain Research*, 1–12. <https://doi.org/10.1007/s00221-016-4770-x>
- Treutwein, B., & Strasburger, H. (1999). Fitting the psychometric function. *Perception & Psychophysics*, 61(1), 87–106. <https://doi.org/10.3758/BF03211951>
- Tychsen, L., & Lisberger, S. G. (1986). Maldevelopment of visual motion processing in humans who had strabismus with onset in infancy. *The Journal of Neuroscience*, 6(9), 2495–508. Retrieved from <http://www.ncbi.nlm.nih.gov/pubmed/3746419>
- Ungerleider, L.G., and Mishkin, M. (1982). Two cortical visual systems. In *Analysis of Visual Behavior*, D.J. Ingle, M.A. Goodale, and R.J.W. Mansfield, eds. (Cambridge, MA: The MIT Press), pp. 549–586.
- Van Essen DC, Felleman DJ, De Yoe EA, Olavania J, Knierim J (1990) Modular and hierarchical organization of extrastriate visual cortex in the macaque. *Brain*, 15, pp 679-696.
- Verhagen, L., Dijkerman, H. C., Grol, M. J., & Toni, I. (2008). Perceptuo-motor interactions during prehension movements. *Journal of Neuroscience*, 28, 4726–4735.

- Vienne, C., Sorin, L., Blondé, L., Huynh-Thu, Q., & Mamassian, P. (2014). Effect of the accommodation-vergence conflict on vergence eye movements. *Vision Research*, *100*, 124–133. <https://doi.org/10.1016/j.visres.2014.04.017>
- Wakayama, A., Matsumoto, C., Ohmure, K., Inase, M., & Shimomura, Y. (2011). Influence of target size and eccentricity on binocular summation of reaction time in kinetic perimetry. *Vision Research*, *51*(1), 174–178. <https://doi.org/10.1016/j.visres.2010.11.002>
- Wang, J., Zhou, T., Qiu, M., Du, A., Cai, K., Wang, Z., ... Chen, L. (1999). Relationship between ventral stream for object vision and dorsal stream for spatial vision: An fMRI + ERP study. *Human Brain Mapping*, *8*(4), 170–181. [https://doi.org/10.1002/\(SICI\)1097-0193\(1999\)8:4<170::AID-HBM2>3.0.CO;2-W](https://doi.org/10.1002/(SICI)1097-0193(1999)8:4<170::AID-HBM2>3.0.CO;2-W)
- Watt, S. J., & Bradshaw, M. F. (2000). Temporal delay affects the reach but not the grasp in natural prehension movements. *Experimental Psychology Society*, *38*, 1473–1481.
- Whitwell, R. L., Milner, A. D., & Goodale, M. A. (2014). The two visual systems hypothesis: New challenges and insights from visual form agnostic patient DF. *Frontiers in Neurology*, *5*(DEC), 1–8. <https://doi.org/10.3389/fneur.2014.00255>
- Wichmann, F. A., & Hill, N. J. (2001). The psychometric function: I. Fitting, sampling, and goodness of fit. *Perception and Psychophysics*, *63*(8), 1293–1313. <https://doi.org/10.3758/BF03194544>
- Wilkinson, F., Wilson, H. R., & Habak, C. (1998). Detection and recognition of radial frequency patterns. *Vision Research*, *38*(22), 3555–3568. [https://doi.org/10.1016/S0042-6989\(98\)00039-X](https://doi.org/10.1016/S0042-6989(98)00039-X)
- Wilson, H. R., & Propp, R. (2015). Detection and recognition of angular frequency patterns. *Vision Research*, *38*(Part A), 51–56. <https://doi.org/10.1016/j.visres.2015.02.022>

Appendices

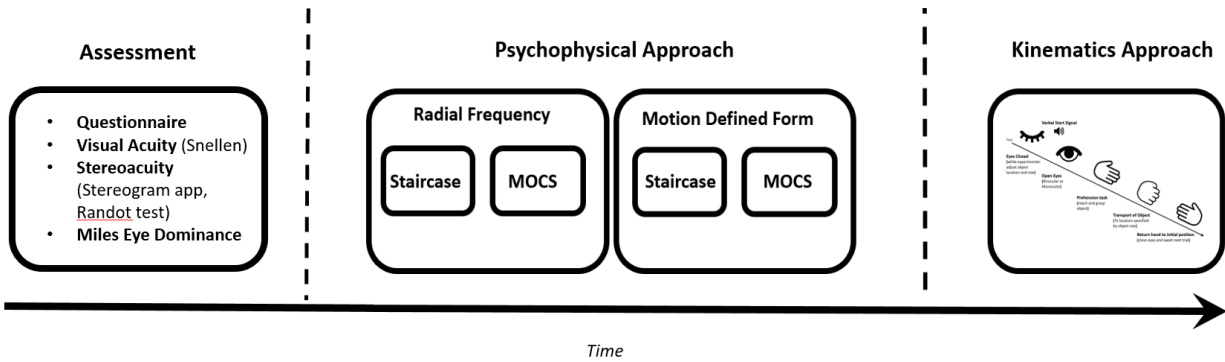


Figure A1. Experimental design of proposed study

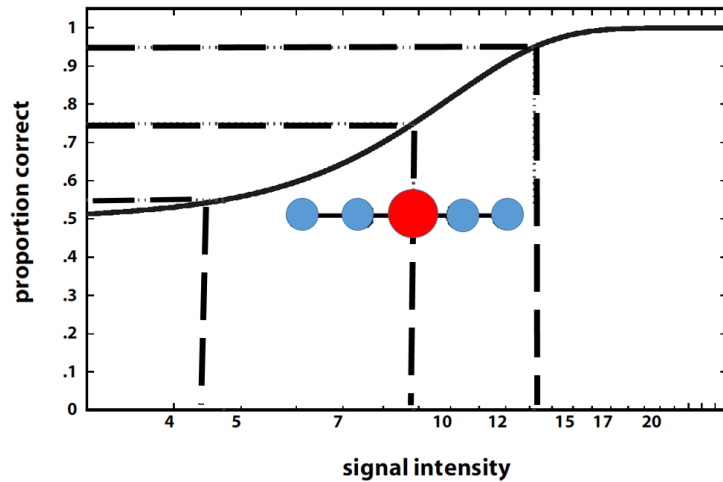


Figure A2. The sampling scheme outlining the test values and the portion of the psychometric function they may be testing. Highlighted are the staircase threshold (red) and calculated test values (blue)

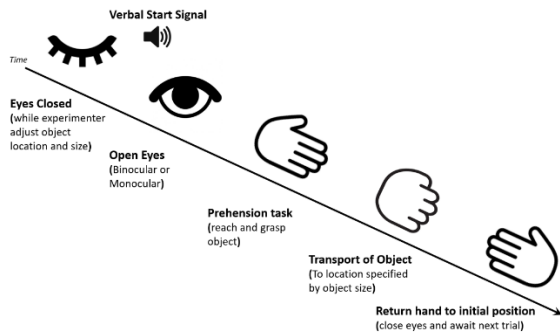
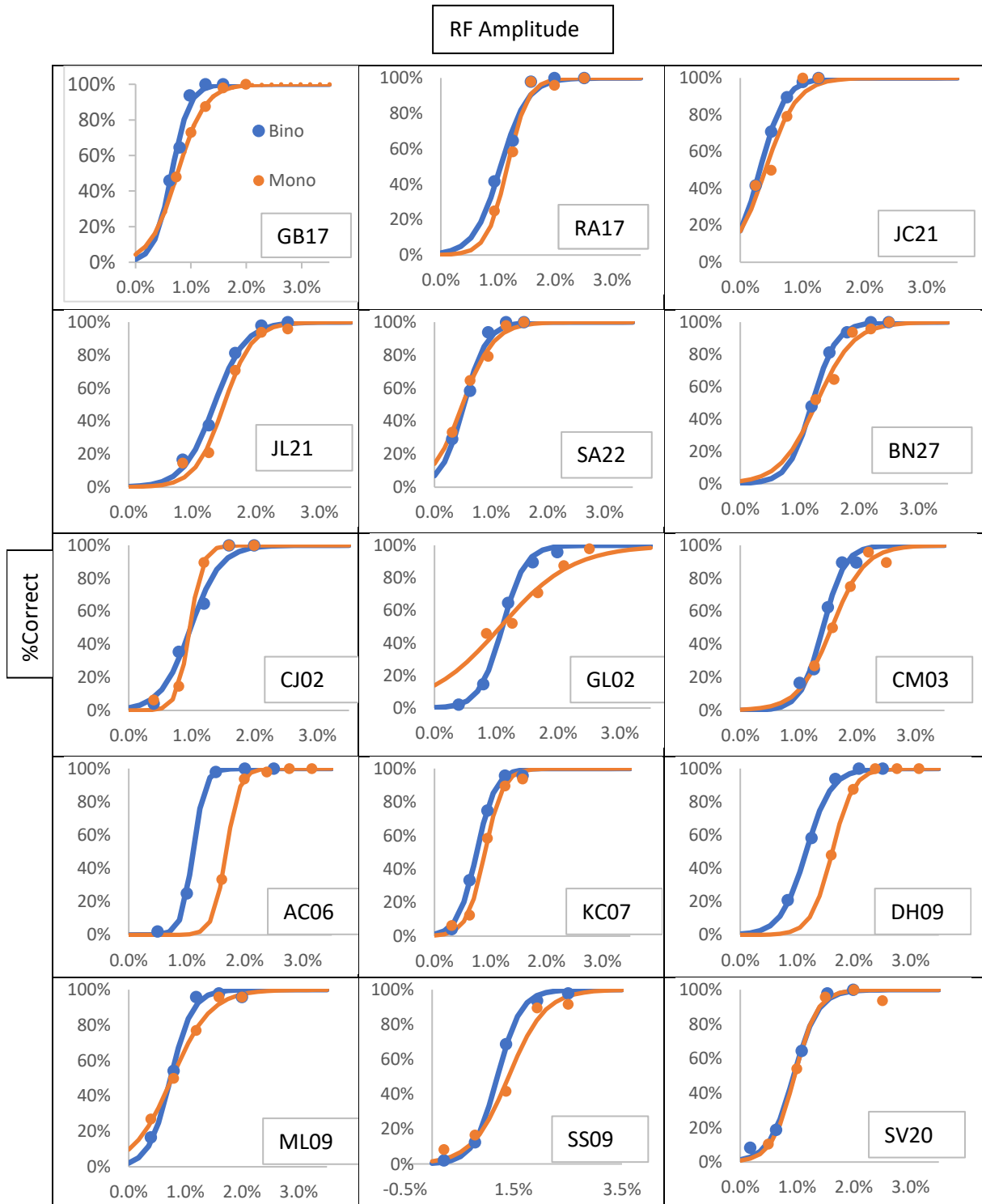
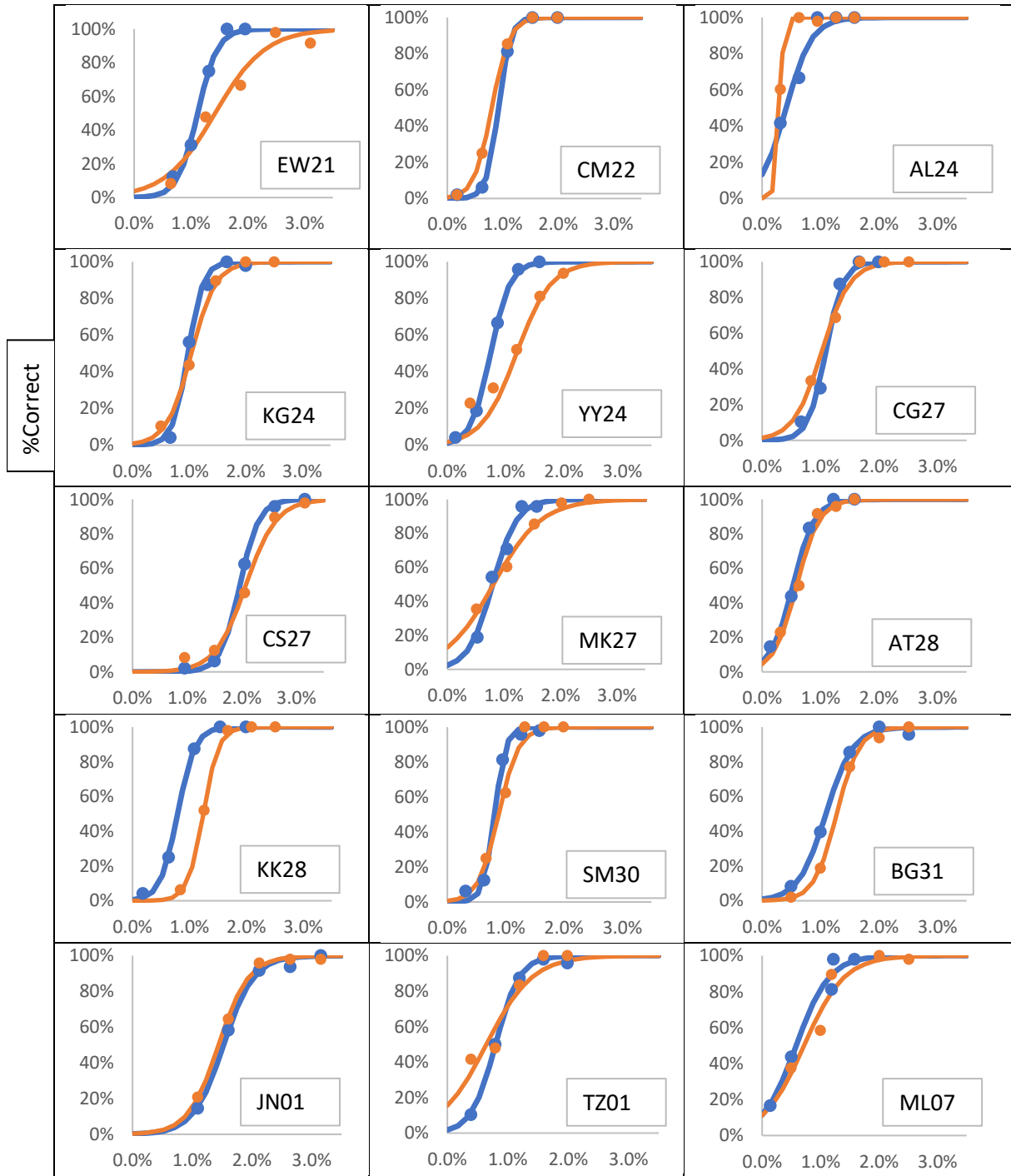


Figure A3. Sequence of actions during reach to grasp task

A4. RF Psychometric functions for all participants during binocular (blue) and monocular (orange) viewing. The x and y axis reflect RF amplitude and % correct responses, respectively

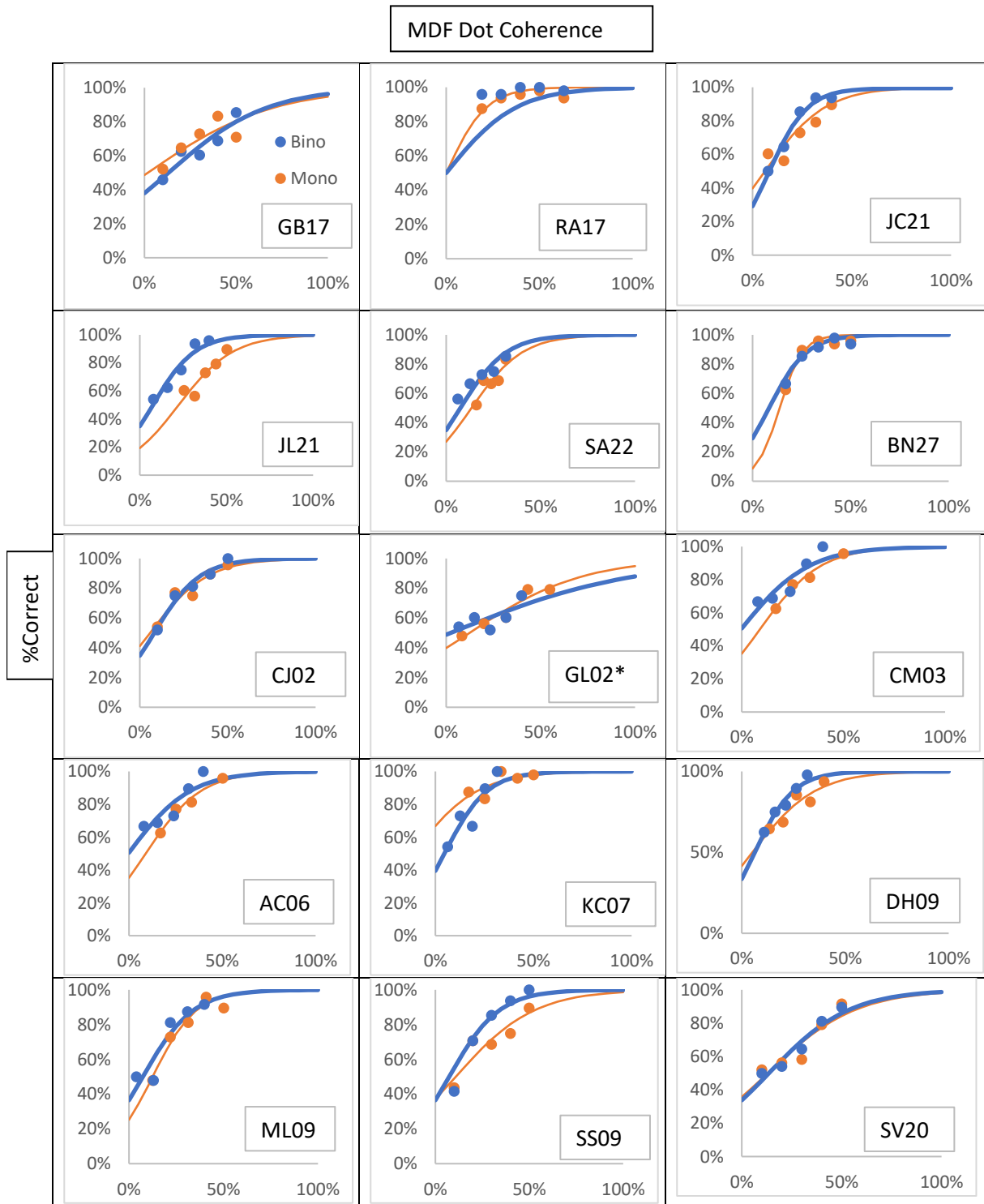


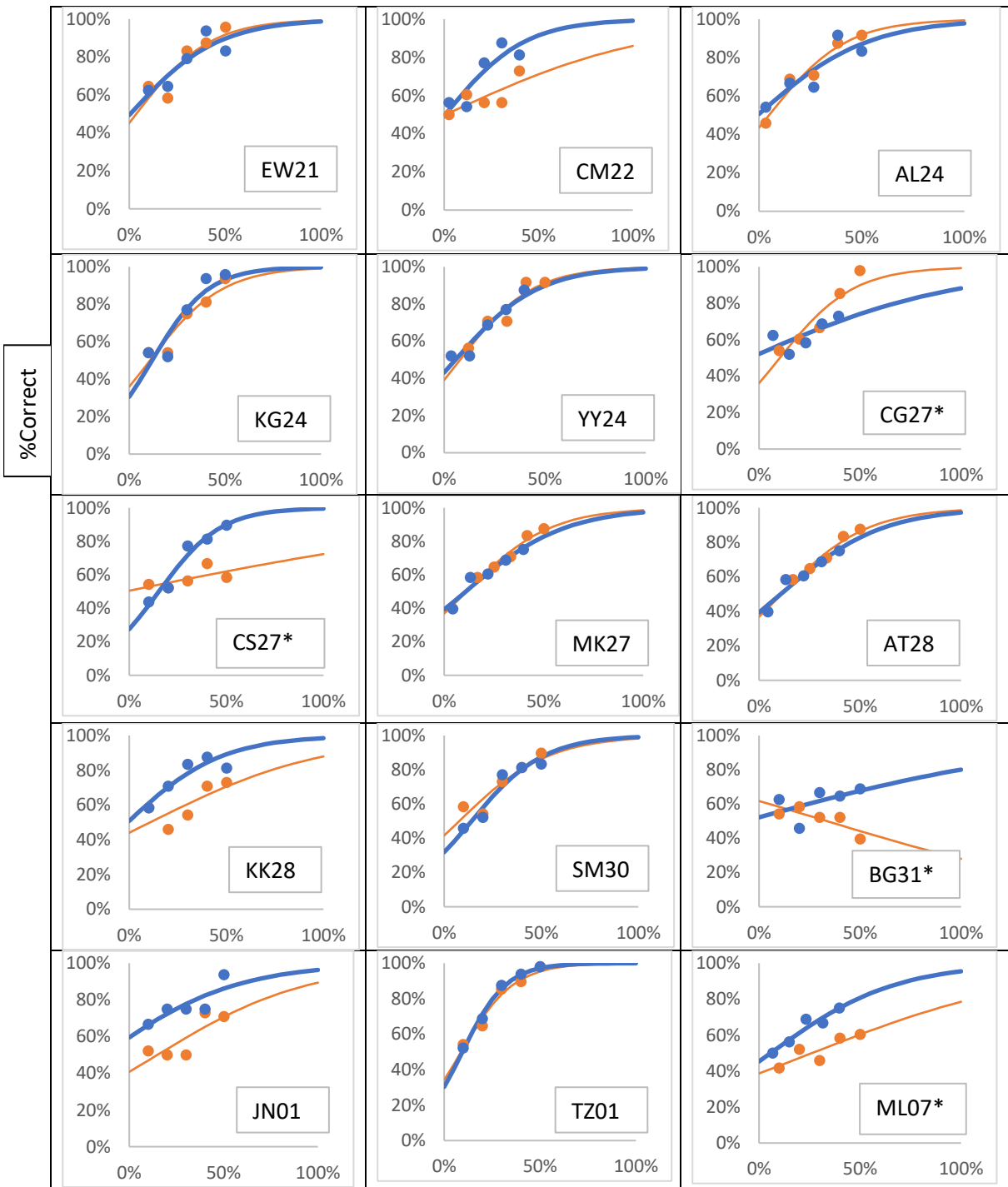


A5. RF Psychometric Function Chi Squared Goodness of Fit Values

Participant	Binocular RF X ²	p value	Monocular RF X ²	p value
GB17	1.07	0.899	0.04	0.999
RA17	1.46	0.834	1.28	0.865
JC21	0.02	0.999	3.66	0.454
JL21	2.15	0.708	7.31	0.120
SA22	0.98	0.913	0.56	0.967
BN27	0.03	0.999	1.55	0.818
CJ07	4.52	0.340	5.55	0.235
GL02	0.51	0.973	1.85	0.763
CM03	3.91	0.418	0.93	0.920
AC06	1.65	0.800	0.04	0.999
KC07	1.68	0.794	3.25	0.517
DH09	0.35	0.986	0.03	0.999
ML09	0.92	0.922	0.41	0.982
SS09	0.66	0.956	5.46	0.243
SV20	3.83	0.430	0.66	0.956
EW21	2.48	0.648	7.21	0.125
CM22	1.88	0.758	0.036	0.999
AL24	1.49	0.828	0.044	0.999
KG24	5.42	0.247	0.84	0.933
YY24	0.62	0.961	5.55	0.235
CG27	3.75	0.441	0.70	0.951
CS27	1.56	0.816	5.37	0.251
MK27	1.72	0.787	0.49	0.974
AT28	1.07	0.899	1.46	0.834
KK28	1.52	0.823	0.40	0.982
SM30	5.40	0.249	1.02	0.907
BG31	0.36	0.986	0.27	0.992
JN01	0.31	0.989	0.15	0.997
TZ01	0.27	0.992	4.97	0.290
ML07	1.46	0.833	3.47	0.482

A6. MDF Psychometric functions for all participants during binocular (blue) and monocular (orange) viewing. The x and y axis reflect MDF dot coherence and % correct responses, respectively. Functions with an asterisk (*) represent data that was excluded from the analysis

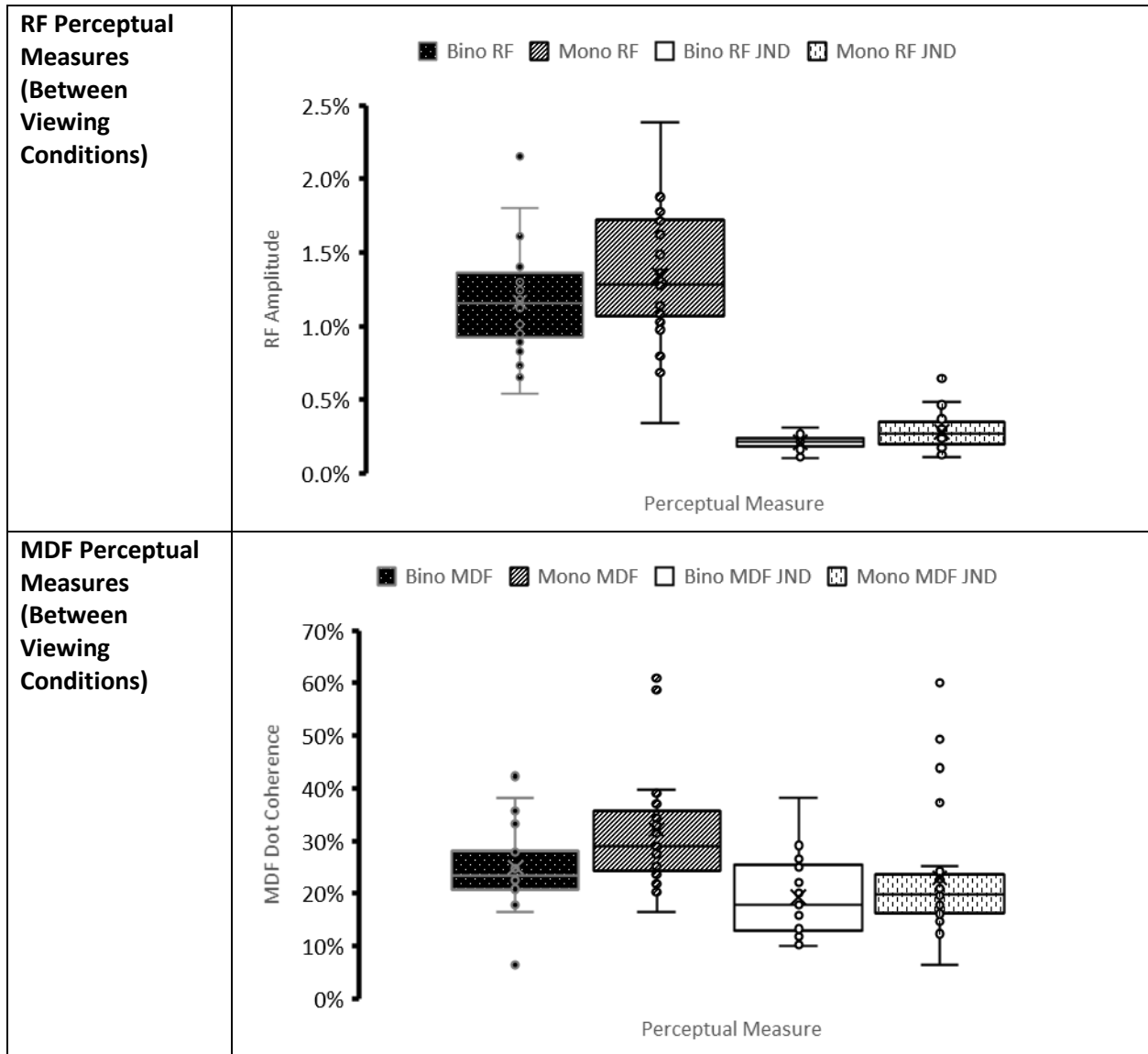




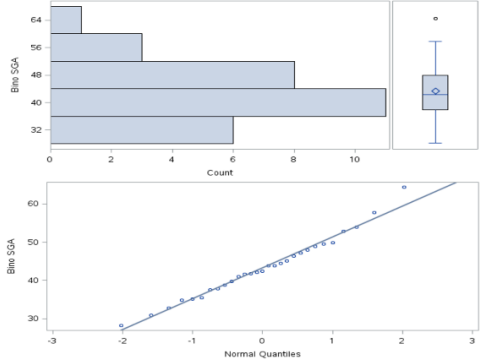
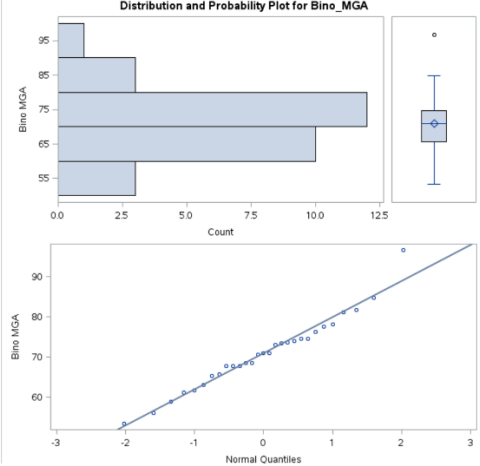
A7. MDF Psychometric Function Chi Squared Goodness of Fit Values

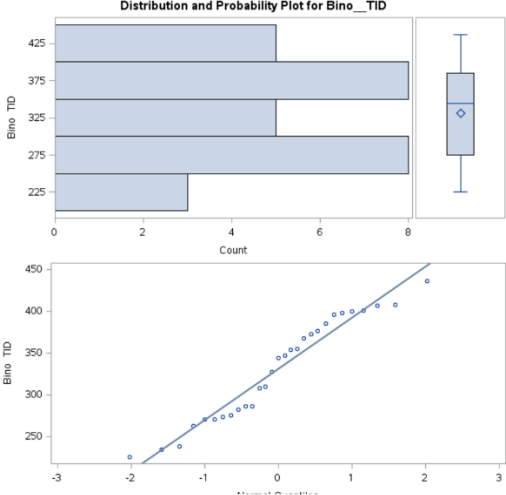
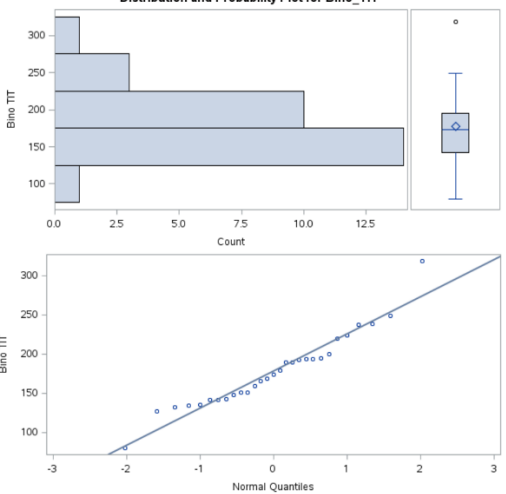
Participant	Binocular MDF X ²	p value	Monocular MDF X ²	p value
GB17	1.67	0.796	2.54	0.637
RA17	8.2	0.085	0.46	0.977
JC21	0.43	0.980	1.03	0.905
JL21	1.13	0.889	1.86	0.761
SA22	0.26	0.992	1.52	0.823
BN27	0.59	0.964	0.54	0.969
CJ07	0.55	0.968	1.27	0.866
GL02*	2.58	0.630	0.87	0.929
CM03	2.08	0.721	4.51	0.341
AC06	0.95	0.917	0.18	0.996
KC07	3.31	0.507	1.04	0.904
DH09	0.40	0.982	0.96	0.916
ML09	4.58	0.333	0.99	0.911
SS09	0.15	0.997	2.60	0.627
SV20	1.23	0.873	3.00	0.558
EW21	1.89	0.756	3.34	0.503
CM22	2.91	0.573	1.98	0.739
AL24	2.71	0.607	0.99	0.911
KG24	4.06	0.398	1.93	0.749
YY24	1.32	0.858	1.27	0.866
CG27*	2.35	0.672	2.17	0.705
CS27*	1.04	0.904	10.19	0.037
MK27	1.03	0.905	0.32	0.988
AT28	0.50	0.973	0.64	0.959
KK28	1.32	0.858	4.40	0.355
SM30	1.51	0.825	2.18	0.703
BG31*	9.75	0.045	11.44	0.022
JN01	1.53	0.821	3.27	0.514
TZ01	0.17	0.997	0.62	0.961
ML07*	0.53	0.971	1.32	0.858

A8. Boxplot demonstrating difference in perceptual threshold between viewing conditions for RF and MDF tasks

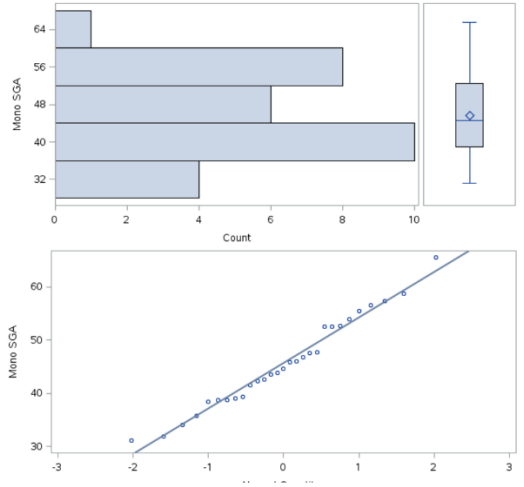
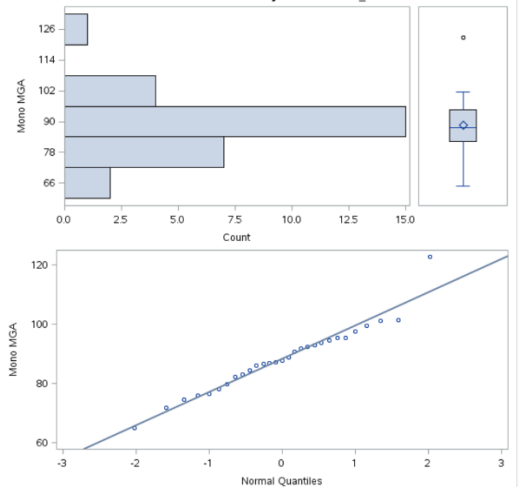


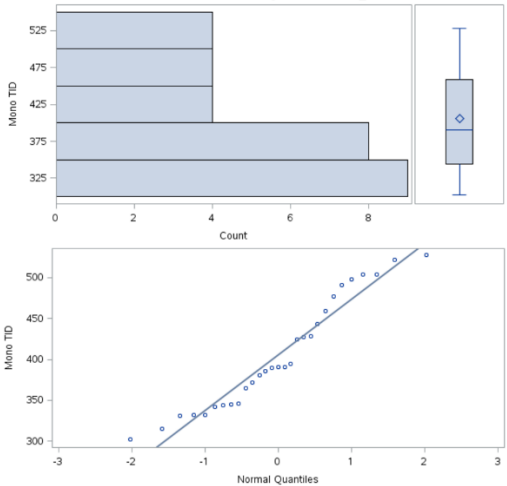
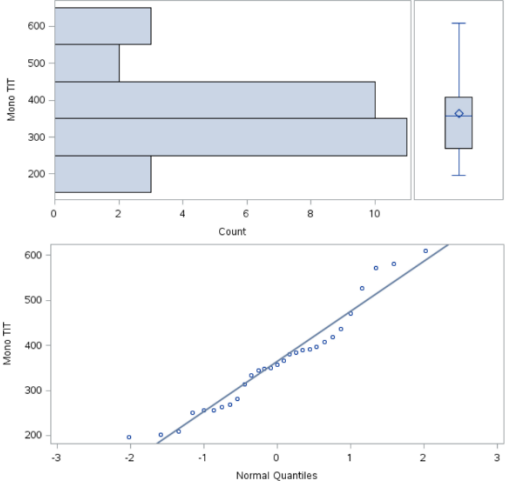
A9. Normal plots (histogram and probability plot) along with Shapiro-Wilk statistic for binocular kinematic measures

Measure	Shapiro-Wilk Statistic	Plot																												
Scaling Grasp Aperture	$W=0.9836$ $p=0.9187$	<div style="text-align: center;"> <p>Distribution and Probability Plot for Bino_SGA</p>  </div> <table border="1" data-bbox="711 726 1265 940"> <thead> <tr> <th colspan="4">Moments</th> </tr> </thead> <tbody> <tr> <td>N</td> <td>29</td> <td>Sum Weights</td> <td>29</td> </tr> <tr> <td>Mean</td> <td>43.3021865</td> <td>Sum Observations</td> <td>1255.76341</td> </tr> <tr> <td>Std Deviation</td> <td>8.07720636</td> <td>Variance</td> <td>65.2412626</td> </tr> <tr> <td>Skewness</td> <td>0.48494479</td> <td>Kurtosis</td> <td>0.53341981</td> </tr> <tr> <td>Uncorrected SS</td> <td>56204.0568</td> <td>Corrected SS</td> <td>1826.75535</td> </tr> <tr> <td>Coeff Variation</td> <td>18.6531143</td> <td>Std Error Mean</td> <td>1.49989957</td> </tr> </tbody> </table>	Moments				N	29	Sum Weights	29	Mean	43.3021865	Sum Observations	1255.76341	Std Deviation	8.07720636	Variance	65.2412626	Skewness	0.48494479	Kurtosis	0.53341981	Uncorrected SS	56204.0568	Corrected SS	1826.75535	Coeff Variation	18.6531143	Std Error Mean	1.49989957
Moments																														
N	29	Sum Weights	29																											
Mean	43.3021865	Sum Observations	1255.76341																											
Std Deviation	8.07720636	Variance	65.2412626																											
Skewness	0.48494479	Kurtosis	0.53341981																											
Uncorrected SS	56204.0568	Corrected SS	1826.75535																											
Coeff Variation	18.6531143	Std Error Mean	1.49989957																											
Maximum Grasp Aperture	$W=0.9735$ $p=0.6591$	<div style="text-align: center;"> <p>Distribution and Probability Plot for Bino_MGA</p>  </div> <table border="1" data-bbox="711 1453 1265 1667"> <thead> <tr> <th colspan="4">Moments</th> </tr> </thead> <tbody> <tr> <td>N</td> <td>29</td> <td>Sum Weights</td> <td>29</td> </tr> <tr> <td>Mean</td> <td>70.9598722</td> <td>Sum Observations</td> <td>2057.83629</td> </tr> <tr> <td>Std Deviation</td> <td>8.98609515</td> <td>Variance</td> <td>80.749906</td> </tr> <tr> <td>Skewness</td> <td>0.51217394</td> <td>Kurtosis</td> <td>1.31111896</td> </tr> <tr> <td>Uncorrected SS</td> <td>148284.798</td> <td>Corrected SS</td> <td>2260.99737</td> </tr> <tr> <td>Coeff Variation</td> <td>12.6636293</td> <td>Std Error Mean</td> <td>1.66867598</td> </tr> </tbody> </table>	Moments				N	29	Sum Weights	29	Mean	70.9598722	Sum Observations	2057.83629	Std Deviation	8.98609515	Variance	80.749906	Skewness	0.51217394	Kurtosis	1.31111896	Uncorrected SS	148284.798	Corrected SS	2260.99737	Coeff Variation	12.6636293	Std Error Mean	1.66867598
Moments																														
N	29	Sum Weights	29																											
Mean	70.9598722	Sum Observations	2057.83629																											
Std Deviation	8.98609515	Variance	80.749906																											
Skewness	0.51217394	Kurtosis	1.31111896																											
Uncorrected SS	148284.798	Corrected SS	2260.99737																											
Coeff Variation	12.6636293	Std Error Mean	1.66867598																											

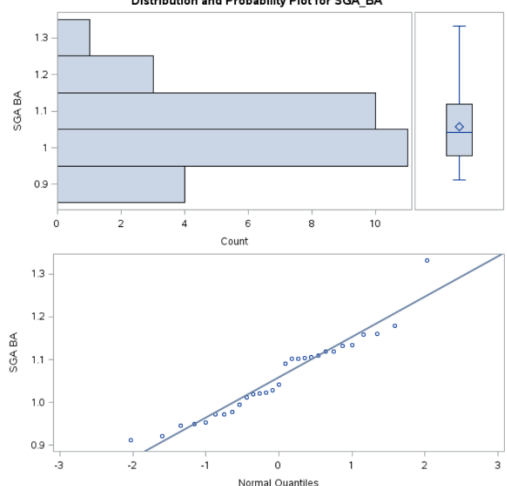
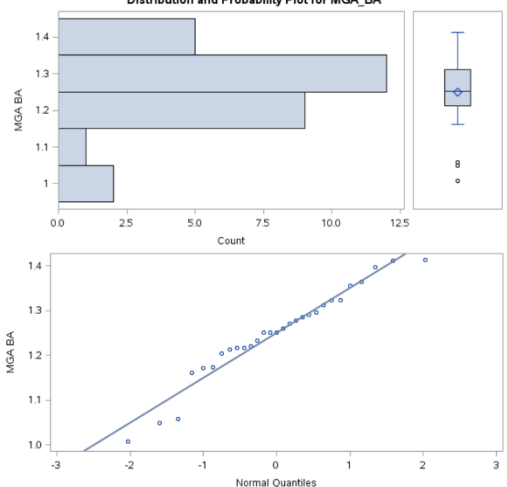
<p>Time in Deceleration</p>	<p>W=0.9408 p=0.1054</p>																														
		<table border="1"> <thead> <tr> <th colspan="4">Moments</th> </tr> </thead> <tbody> <tr> <td>N</td> <td>29</td> <td>Sum Weights</td> <td>29</td> </tr> <tr> <td>Mean</td> <td>331.012054</td> <td>Sum Observations</td> <td>9599.34955</td> </tr> <tr> <td>Std Deviation</td> <td>61.4206126</td> <td>Variance</td> <td>3772.49165</td> </tr> <tr> <td>Skewness</td> <td>-0.101481</td> <td>Kurtosis</td> <td>-1.28623</td> </tr> <tr> <td>Uncorrected SS</td> <td>3283130.17</td> <td>Corrected SS</td> <td>105629.766</td> </tr> <tr> <td>Coeff Variation</td> <td>18.5554006</td> <td>Std Error Mean</td> <td>11.4055214</td> </tr> </tbody> </table>	Moments				N	29	Sum Weights	29	Mean	331.012054	Sum Observations	9599.34955	Std Deviation	61.4206126	Variance	3772.49165	Skewness	-0.101481	Kurtosis	-1.28623	Uncorrected SS	3283130.17	Corrected SS	105629.766	Coeff Variation	18.5554006	Std Error Mean	11.4055214	
Moments																															
N	29	Sum Weights	29																												
Mean	331.012054	Sum Observations	9599.34955																												
Std Deviation	61.4206126	Variance	3772.49165																												
Skewness	-0.101481	Kurtosis	-1.28623																												
Uncorrected SS	3283130.17	Corrected SS	105629.766																												
Coeff Variation	18.5554006	Std Error Mean	11.4055214																												
<p>Time in Grasping</p>	<p>W= 0.9494 p=0.1766</p>																														
		<table border="1"> <thead> <tr> <th colspan="4">Moments</th> </tr> </thead> <tbody> <tr> <td>N</td> <td>29</td> <td>Sum Weights</td> <td>29</td> </tr> <tr> <td>Mean</td> <td>178.001715</td> <td>Sum Observations</td> <td>5162.04972</td> </tr> <tr> <td>Std Deviation</td> <td>47.2735717</td> <td>Variance</td> <td>2234.79058</td> </tr> <tr> <td>Skewness</td> <td>0.78390609</td> <td>Kurtosis</td> <td>1.6587467</td> </tr> <tr> <td>Uncorrected SS</td> <td>981427.838</td> <td>Corrected SS</td> <td>62574.1362</td> </tr> <tr> <td>Coeff Variation</td> <td>26.5579305</td> <td>Std Error Mean</td> <td>8.77848187</td> </tr> </tbody> </table>	Moments				N	29	Sum Weights	29	Mean	178.001715	Sum Observations	5162.04972	Std Deviation	47.2735717	Variance	2234.79058	Skewness	0.78390609	Kurtosis	1.6587467	Uncorrected SS	981427.838	Corrected SS	62574.1362	Coeff Variation	26.5579305	Std Error Mean	8.77848187	
Moments																															
N	29	Sum Weights	29																												
Mean	178.001715	Sum Observations	5162.04972																												
Std Deviation	47.2735717	Variance	2234.79058																												
Skewness	0.78390609	Kurtosis	1.6587467																												
Uncorrected SS	981427.838	Corrected SS	62574.1362																												
Coeff Variation	26.5579305	Std Error Mean	8.77848187																												

A10. Normal plots (histogram and probability plot) along with Shapiro-Wilk statistic for monocular kinematic measures

Measure	Shapiro-Wilk Statistic	Plot																												
Scaling Grasp Aperture	W= 0.975649 p= 0.7193	<div style="text-align: center;"> <p>Distribution and Probability Plot for Mono_SGA</p>  </div> <table border="1" style="width: 100%; border-collapse: collapse;"> <thead> <tr> <th colspan="4" style="text-align: center;">Moments</th> </tr> </thead> <tbody> <tr> <td>N</td> <td style="text-align: center;">29</td> <td>Sum Weights</td> <td style="text-align: center;">29</td> </tr> <tr> <td>Mean</td> <td style="text-align: center;">45.6646052</td> <td>Sum Observations</td> <td style="text-align: center;">1324.27355</td> </tr> <tr> <td>Std Deviation</td> <td style="text-align: center;">8.55353175</td> <td>Variance</td> <td style="text-align: center;">73.1629053</td> </tr> <tr> <td>Skewness</td> <td style="text-align: center;">0.33078456</td> <td>Kurtosis</td> <td style="text-align: center;">-0.3951046</td> </tr> <tr> <td>Uncorrected SS</td> <td style="text-align: center;">62520.9901</td> <td>Corrected SS</td> <td style="text-align: center;">2048.56135</td> </tr> <tr> <td>Coeff Variation</td> <td style="text-align: center;">18.7312071</td> <td>Std Error Mean</td> <td style="text-align: center;">1.58835097</td> </tr> </tbody> </table>	Moments				N	29	Sum Weights	29	Mean	45.6646052	Sum Observations	1324.27355	Std Deviation	8.55353175	Variance	73.1629053	Skewness	0.33078456	Kurtosis	-0.3951046	Uncorrected SS	62520.9901	Corrected SS	2048.56135	Coeff Variation	18.7312071	Std Error Mean	1.58835097
Moments																														
N	29	Sum Weights	29																											
Mean	45.6646052	Sum Observations	1324.27355																											
Std Deviation	8.55353175	Variance	73.1629053																											
Skewness	0.33078456	Kurtosis	-0.3951046																											
Uncorrected SS	62520.9901	Corrected SS	2048.56135																											
Coeff Variation	18.7312071	Std Error Mean	1.58835097																											
Maximum Grasp Aperture	W= 0.958427 p= 0.3005	<div style="text-align: center;"> <p>Distribution and Probability Plot for Mono_MGA</p>  </div> <table border="1" style="width: 100%; border-collapse: collapse;"> <thead> <tr> <th colspan="4" style="text-align: center;">Moments</th> </tr> </thead> <tbody> <tr> <td>N</td> <td style="text-align: center;">29</td> <td>Sum Weights</td> <td style="text-align: center;">29</td> </tr> <tr> <td>Mean</td> <td style="text-align: center;">88.4261311</td> <td>Sum Observations</td> <td style="text-align: center;">2564.3578</td> </tr> <tr> <td>Std Deviation</td> <td style="text-align: center;">11.2289811</td> <td>Variance</td> <td style="text-align: center;">126.090017</td> </tr> <tr> <td>Skewness</td> <td style="text-align: center;">0.60061409</td> <td>Kurtosis</td> <td style="text-align: center;">2.12160241</td> </tr> <tr> <td>Uncorrected SS</td> <td style="text-align: center;">230286.759</td> <td>Corrected SS</td> <td style="text-align: center;">3530.52046</td> </tr> <tr> <td>Coeff Variation</td> <td style="text-align: center;">12.6987136</td> <td>Std Error Mean</td> <td style="text-align: center;">2.08516944</td> </tr> </tbody> </table>	Moments				N	29	Sum Weights	29	Mean	88.4261311	Sum Observations	2564.3578	Std Deviation	11.2289811	Variance	126.090017	Skewness	0.60061409	Kurtosis	2.12160241	Uncorrected SS	230286.759	Corrected SS	3530.52046	Coeff Variation	12.6987136	Std Error Mean	2.08516944
Moments																														
N	29	Sum Weights	29																											
Mean	88.4261311	Sum Observations	2564.3578																											
Std Deviation	11.2289811	Variance	126.090017																											
Skewness	0.60061409	Kurtosis	2.12160241																											
Uncorrected SS	230286.759	Corrected SS	3530.52046																											
Coeff Variation	12.6987136	Std Error Mean	2.08516944																											

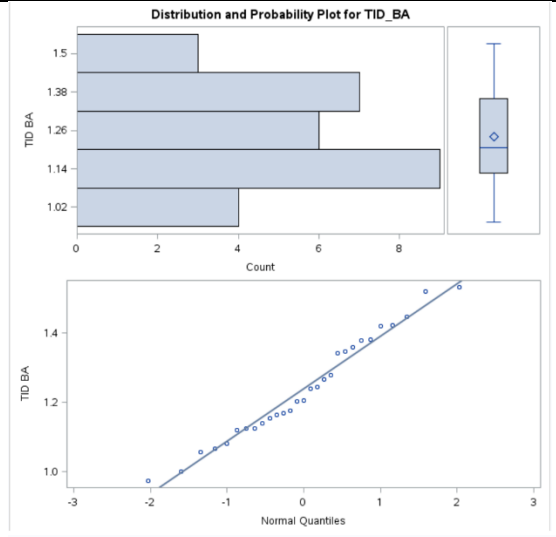
<p>Time in Deceleration</p>	<p>W= 0.931725 <p>ρ= 0.0610</p> </p>	<div style="text-align: center;"> <p>Distribution and Probability Plot for Mono_TID</p>  </div> <table border="1" style="width: 100%; border-collapse: collapse;"> <thead> <tr> <th colspan="4" style="text-align: center;">Moments</th> </tr> </thead> <tbody> <tr> <td>N</td> <td style="text-align: center;">29</td> <td>Sum Weights</td> <td style="text-align: center;">29</td> </tr> <tr> <td>Mean</td> <td style="text-align: center;">405.605774</td> <td>Sum Observations</td> <td style="text-align: center;">11762.5675</td> </tr> <tr> <td>Std Deviation</td> <td style="text-align: center;">67.9895894</td> <td>Variance</td> <td style="text-align: center;">4622.58426</td> </tr> <tr> <td>Skewness</td> <td style="text-align: center;">0.38892097</td> <td>Kurtosis</td> <td style="text-align: center;">-1.0959485</td> </tr> <tr> <td>Uncorrected SS</td> <td style="text-align: center;">4900397.64</td> <td>Corrected SS</td> <td style="text-align: center;">129432.359</td> </tr> <tr> <td>Coeff Variation</td> <td style="text-align: center;">16.7624806</td> <td>Std Error Mean</td> <td style="text-align: center;">12.6253498</td> </tr> </tbody> </table>	Moments				N	29	Sum Weights	29	Mean	405.605774	Sum Observations	11762.5675	Std Deviation	67.9895894	Variance	4622.58426	Skewness	0.38892097	Kurtosis	-1.0959485	Uncorrected SS	4900397.64	Corrected SS	129432.359	Coeff Variation	16.7624806	Std Error Mean	12.6253498
Moments																														
N	29	Sum Weights	29																											
Mean	405.605774	Sum Observations	11762.5675																											
Std Deviation	67.9895894	Variance	4622.58426																											
Skewness	0.38892097	Kurtosis	-1.0959485																											
Uncorrected SS	4900397.64	Corrected SS	129432.359																											
Coeff Variation	16.7624806	Std Error Mean	12.6253498																											
<p>Time in Grasping</p>	<p>W= 0.946398 <p>ρ= 0.1475</p> </p>	<div style="text-align: center;"> <p>Distribution and Probability Plot for Mono_TIT</p>  </div> <table border="1" style="width: 100%; border-collapse: collapse;"> <thead> <tr> <th colspan="4" style="text-align: center;">Moments</th> </tr> </thead> <tbody> <tr> <td>N</td> <td style="text-align: center;">29</td> <td>Sum Weights</td> <td style="text-align: center;">29</td> </tr> <tr> <td>Mean</td> <td style="text-align: center;">363.826108</td> <td>Sum Observations</td> <td style="text-align: center;">10550.9571</td> </tr> <tr> <td>Std Deviation</td> <td style="text-align: center;">111.138076</td> <td>Variance</td> <td style="text-align: center;">12351.672</td> </tr> <tr> <td>Skewness</td> <td style="text-align: center;">0.58180463</td> <td>Kurtosis</td> <td style="text-align: center;">-0.0791616</td> </tr> <tr> <td>Uncorrected SS</td> <td style="text-align: center;">4184560.49</td> <td>Corrected SS</td> <td style="text-align: center;">345846.817</td> </tr> <tr> <td>Coeff Variation</td> <td style="text-align: center;">30.5470317</td> <td>Std Error Mean</td> <td style="text-align: center;">20.6378227</td> </tr> </tbody> </table>	Moments				N	29	Sum Weights	29	Mean	363.826108	Sum Observations	10550.9571	Std Deviation	111.138076	Variance	12351.672	Skewness	0.58180463	Kurtosis	-0.0791616	Uncorrected SS	4184560.49	Corrected SS	345846.817	Coeff Variation	30.5470317	Std Error Mean	20.6378227
Moments																														
N	29	Sum Weights	29																											
Mean	363.826108	Sum Observations	10550.9571																											
Std Deviation	111.138076	Variance	12351.672																											
Skewness	0.58180463	Kurtosis	-0.0791616																											
Uncorrected SS	4184560.49	Corrected SS	345846.817																											
Coeff Variation	30.5470317	Std Error Mean	20.6378227																											

A11. Normal plots (histogram and probability plot) along with Shapiro-Wilk statistic for binocular advantage ratios of the kinematic measures

Measure	Shapiro-Wilk Statistic	Plot																												
Scaling Grasp Aperture Binocular Advantage	W= 0.941702 p= 0.1111	<div style="text-align: center;"> <p>Distribution and Probability Plot for SGA_BA</p>  </div> <table border="1" data-bbox="706 850 1226 1050"> <thead> <tr> <th colspan="4">Moments</th> </tr> </thead> <tbody> <tr> <td>N</td> <td>29</td> <td>Sum Weights</td> <td>29</td> </tr> <tr> <td>Mean</td> <td>1.05822408</td> <td>Sum Observations</td> <td>30.6884984</td> </tr> <tr> <td>Std Deviation</td> <td>0.09434685</td> <td>Variance</td> <td>0.00890133</td> </tr> <tr> <td>Skewness</td> <td>0.6459764</td> <td>Kurtosis</td> <td>0.8719204</td> </tr> <tr> <td>Uncorrected SS</td> <td>32.7245453</td> <td>Corrected SS</td> <td>0.24923718</td> </tr> <tr> <td>Coeff Variation</td> <td>8.91558323</td> <td>Std Error Mean</td> <td>0.01751977</td> </tr> </tbody> </table>	Moments				N	29	Sum Weights	29	Mean	1.05822408	Sum Observations	30.6884984	Std Deviation	0.09434685	Variance	0.00890133	Skewness	0.6459764	Kurtosis	0.8719204	Uncorrected SS	32.7245453	Corrected SS	0.24923718	Coeff Variation	8.91558323	Std Error Mean	0.01751977
Moments																														
N	29	Sum Weights	29																											
Mean	1.05822408	Sum Observations	30.6884984																											
Std Deviation	0.09434685	Variance	0.00890133																											
Skewness	0.6459764	Kurtosis	0.8719204																											
Uncorrected SS	32.7245453	Corrected SS	0.24923718																											
Coeff Variation	8.91558323	Std Error Mean	0.01751977																											
Maximum Grasp Aperture Binocular Advantage	W= 0.953451 p= 0.2248	<div style="text-align: center;"> <p>Distribution and Probability Plot for MGA_BA</p>  </div> <table border="1" data-bbox="706 1585 1226 1774"> <thead> <tr> <th colspan="4">Moments</th> </tr> </thead> <tbody> <tr> <td>N</td> <td>29</td> <td>Sum Weights</td> <td>29</td> </tr> <tr> <td>Mean</td> <td>1.25015067</td> <td>Sum Observations</td> <td>36.2543695</td> </tr> <tr> <td>Std Deviation</td> <td>0.10024334</td> <td>Variance</td> <td>0.01004873</td> </tr> <tr> <td>Skewness</td> <td>-0.6003128</td> <td>Kurtosis</td> <td>0.51110393</td> </tr> <tr> <td>Uncorrected SS</td> <td>45.6047888</td> <td>Corrected SS</td> <td>0.28136438</td> </tr> <tr> <td>Coeff Variation</td> <td>8.01850088</td> <td>Std Error Mean</td> <td>0.01861472</td> </tr> </tbody> </table>	Moments				N	29	Sum Weights	29	Mean	1.25015067	Sum Observations	36.2543695	Std Deviation	0.10024334	Variance	0.01004873	Skewness	-0.6003128	Kurtosis	0.51110393	Uncorrected SS	45.6047888	Corrected SS	0.28136438	Coeff Variation	8.01850088	Std Error Mean	0.01861472
Moments																														
N	29	Sum Weights	29																											
Mean	1.25015067	Sum Observations	36.2543695																											
Std Deviation	0.10024334	Variance	0.01004873																											
Skewness	-0.6003128	Kurtosis	0.51110393																											
Uncorrected SS	45.6047888	Corrected SS	0.28136438																											
Coeff Variation	8.01850088	Std Error Mean	0.01861472																											

Time in Deceleration Binocular Advantage

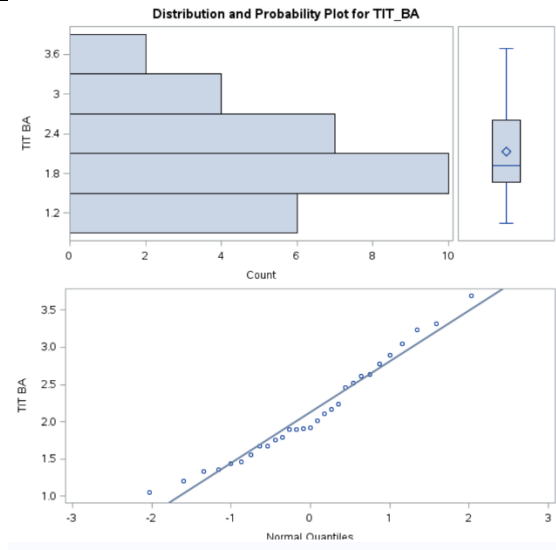
W= 0.969242
 ρ= 0.5393



Moments			
N	29	Sum Weights	29
Mean	1.2391053	Sum Observations	35.9340536
Std Deviation	0.15133434	Variance	0.02290208
Skewness	0.25304971	Kurtosis	-0.7853767
Uncorrected SS	45.1673346	Corrected SS	0.64125835
Coeff Variation	12.2131949	Std Error Mean	0.02810208

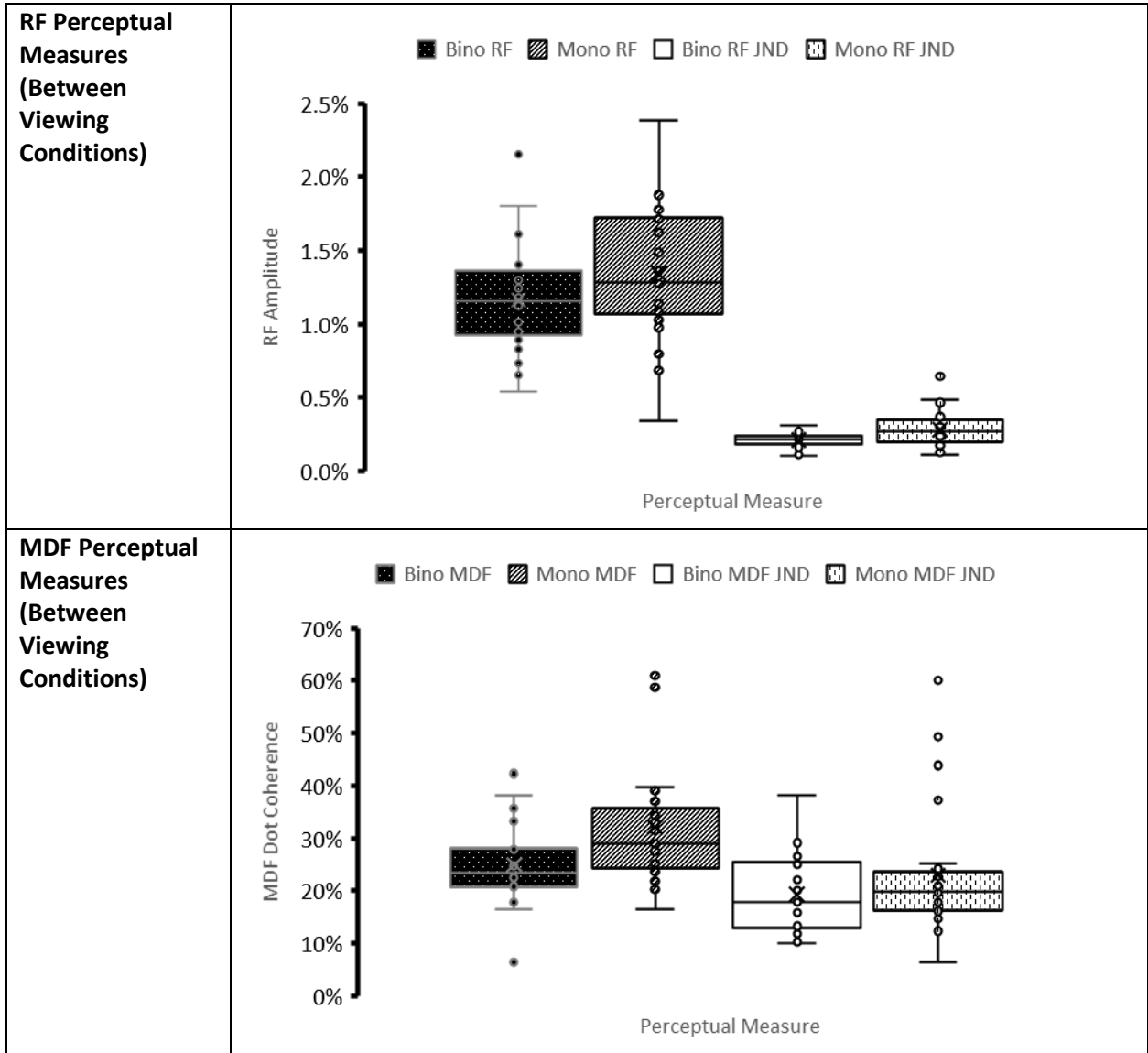
Time in Grasping Binocular Advantage

W= 0.959614
 ρ= 0.3216

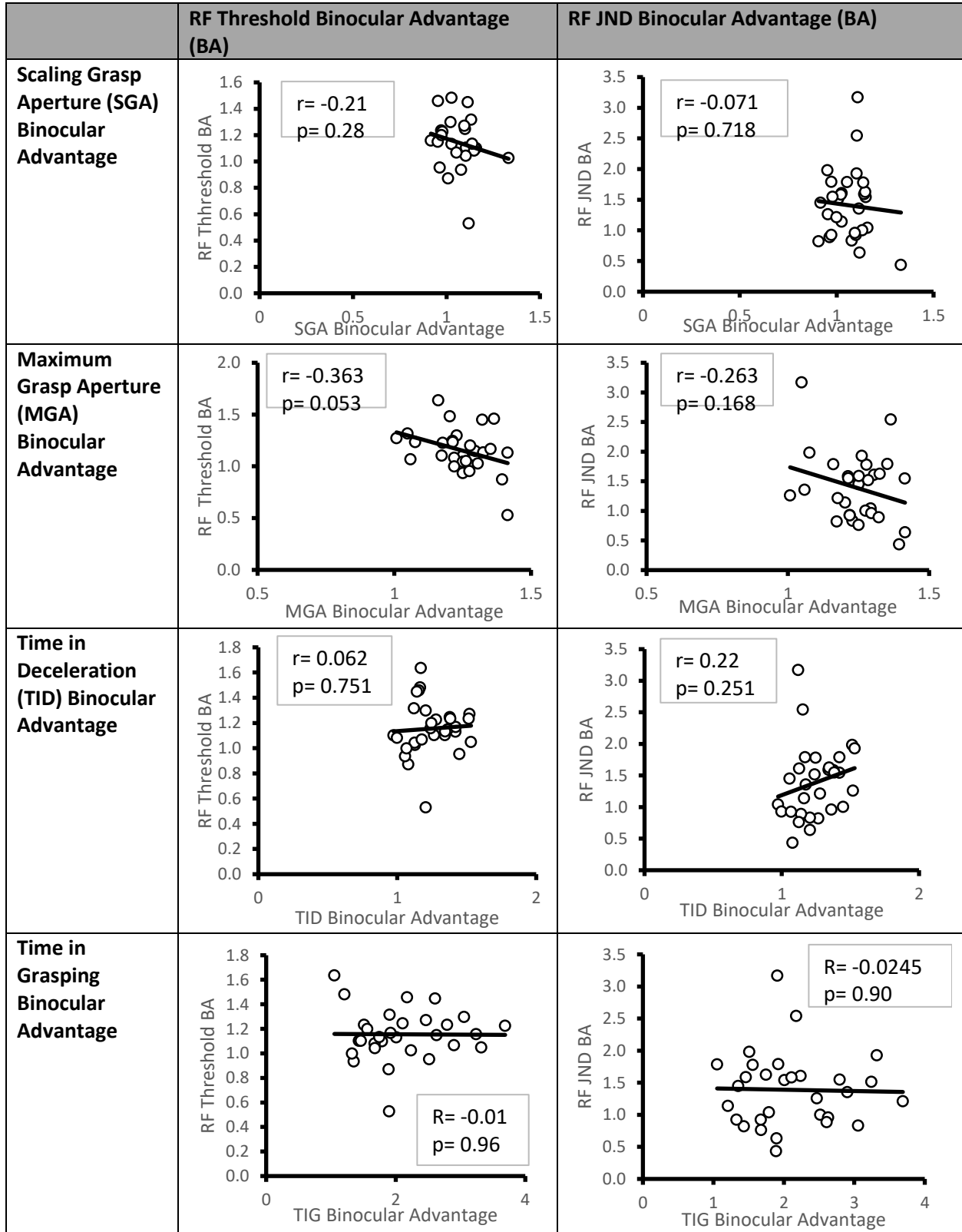


Moments			
N	29	Sum Weights	29
Mean	2.12452311	Sum Observations	61.6111703
Std Deviation	0.68408882	Variance	0.46797751
Skewness	0.56660159	Kurtosis	-0.42035
Uncorrected SS	143.997726	Corrected SS	13.1033703
Coeff Variation	32.1996411	Std Error Mean	0.1270321

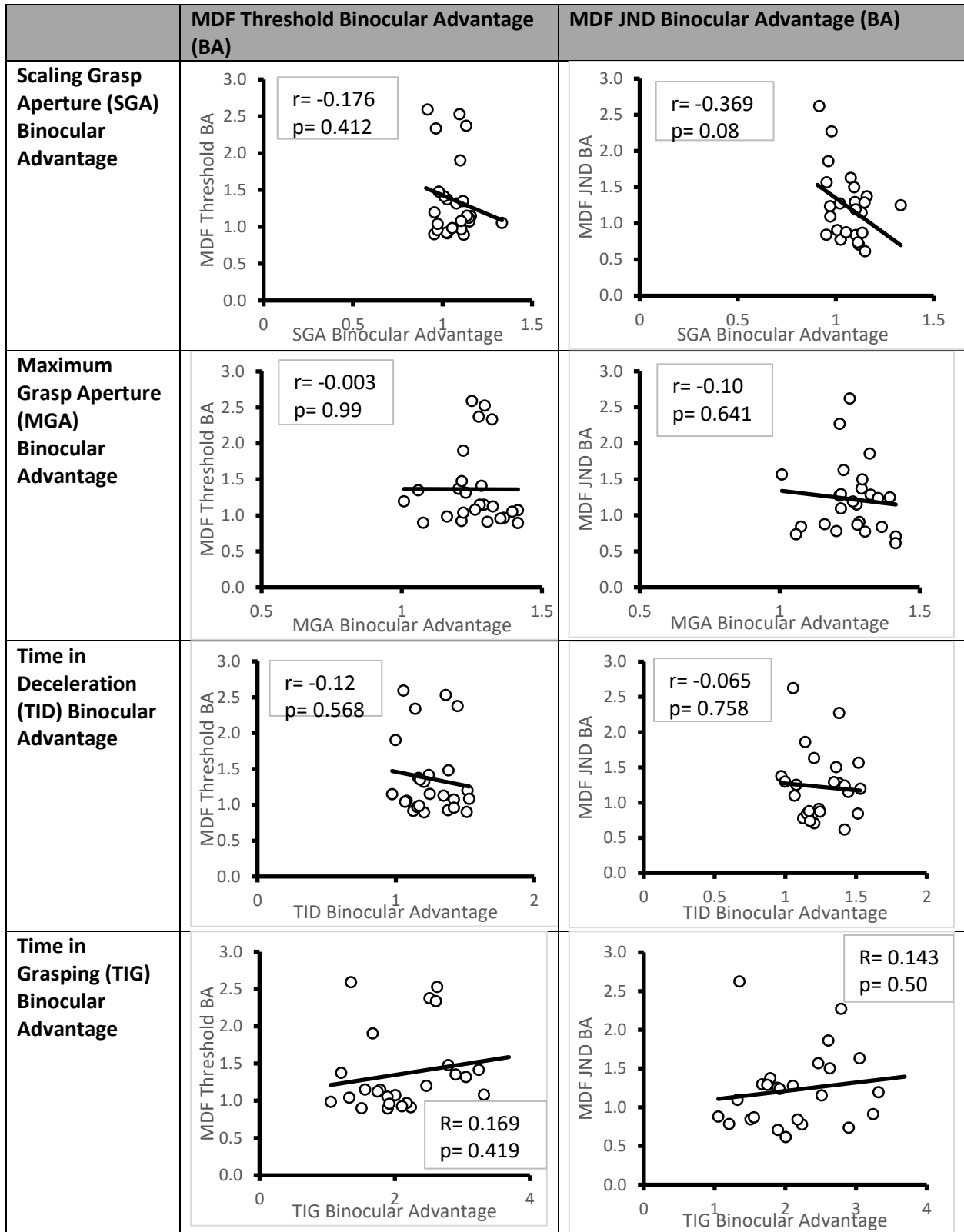
A12. Boxplots highlighting the differences in kinematic performance during binocular and monocular viewing



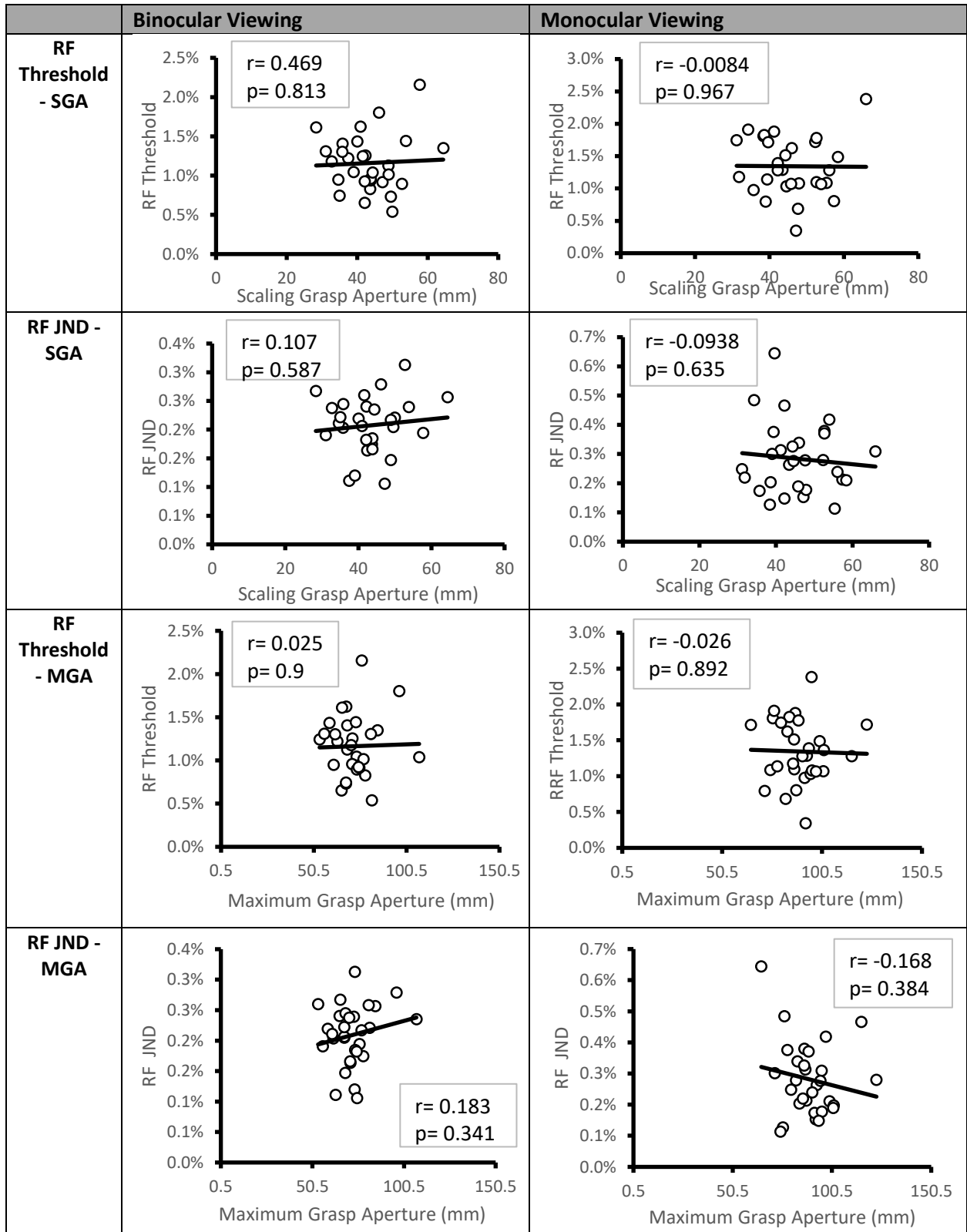
A13. Correlations between binocular advantages in RF perceptual (Threshold/JND) and kinematic performance

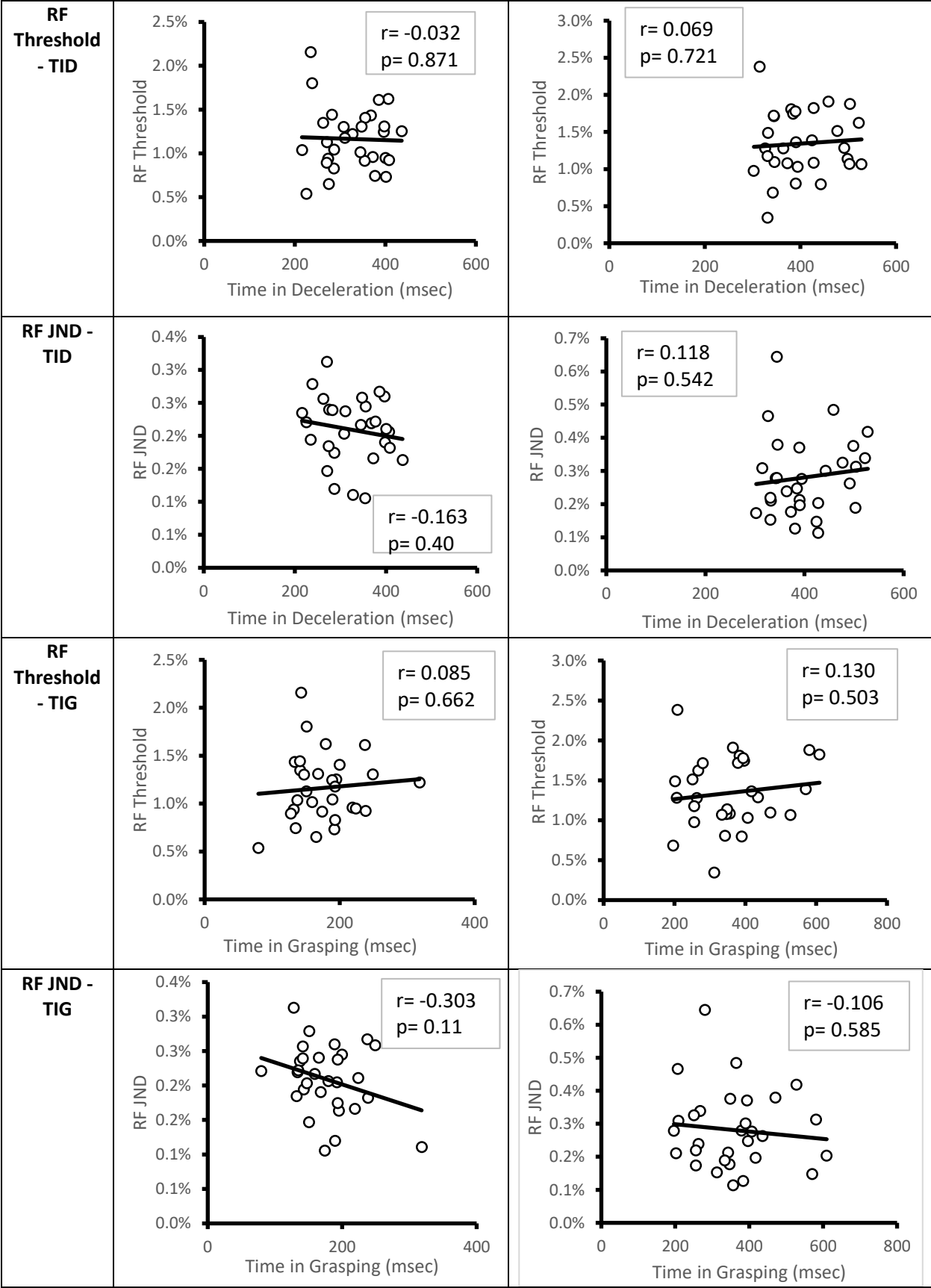


A14. Correlations between binocular advantages in MDF perceptual (Threshold/JND) and kinematic performance



A15. Correlation between actual RF perceptual (Threshold/JND) and kinematic measures for binocular and monocular viewing conditions





A16. Correlation between actual MDF perceptual (Threshold/JND) and kinematic measures for binocular and monocular viewing conditions

